The history of the density of Active Galactic Nuclei and Super-Massive Black Holes

Fabio La Franca

and the HELLAS, ELAIS and SWIRE collaborations

Dipartimento di Fisica

Universita` degli Studi ROMA TRE

The Astrophysical Journal, 635:864–879, 2005 December 20

THE HELLAS2XMM SURVEY. VII. THE HARD X-RAY LUMINOSITY FUNCTION OF AGNs UP TO $z = 4$: MORE ABSORBED AGNs AT LOW LUMINOSITIES AND HIGH REDSHIFTS

F. La Franca,[1] F. Fiore,[2] A. Comastri,[3] G. C. Perola,[1] N. Sacchi,[1] M. Brusa,[4] F. Cocchia,[2] C. Feruglio,[2] G. Matt,[1] C. Vignali,[5] N. Carangelo,[6] P. Ciliegi,[3] A. Lamastra,[1] R. Maiolino,[7] M. Mignoli,[3] S. Molendi,[8] and S. Puccetti[2]
Received 2005 May 16; accepted 2005 August 15

[1] Dipartimento di Fisica, Università degli Studi "Roma Tre," Via della Vasca Navale 84, I-00146 Roma, Italy; lafranca@fis.uniroma3.it.
[2] INAF, Osservatorio Astronomico di Roma, Via Frascati 33, I-00100 Monteporzio, Italy.
[3] INAF, Osservatorio Astronomico di Bologna, Via Ranzani 1, I-40127 Bologna, Italy.
[4] Max Planck Institut für Extraterrestrische Physik (MPE), Giessenbachstrasse, Postfach 1312, 85741 Garching, Germany.
[5] Dipartimento di Astronomia, Università di Bologna, Via Ranzani 1, I-40127 Bologna, Italy.
[6] Università di Milano-Bicocca, Piazza della Scienza 3, I-20126 Milano, Italy.
[7] INAF, Osservatorio Astrofisico di Arcetri, Largo Fermi 5, I-50125 Firenze, Italy.
[8] INAF, IASF, Via Bassini 15, I-20133, Milano, Italy.

The Cosmic Energy Density Spectrum

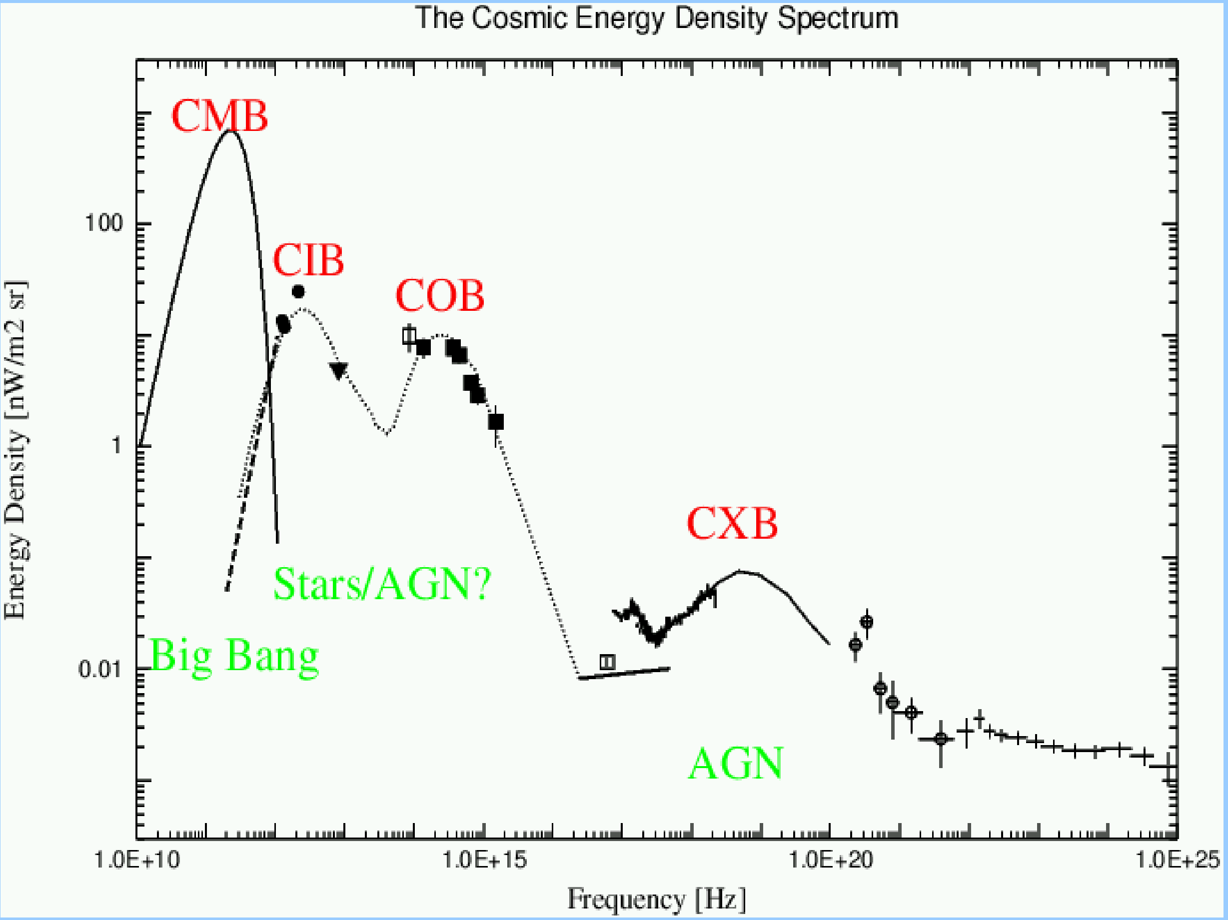

OPTICAL

X-RAYS

AGN1

optical lines: broad + narrow

un-absorbed in the X-rays

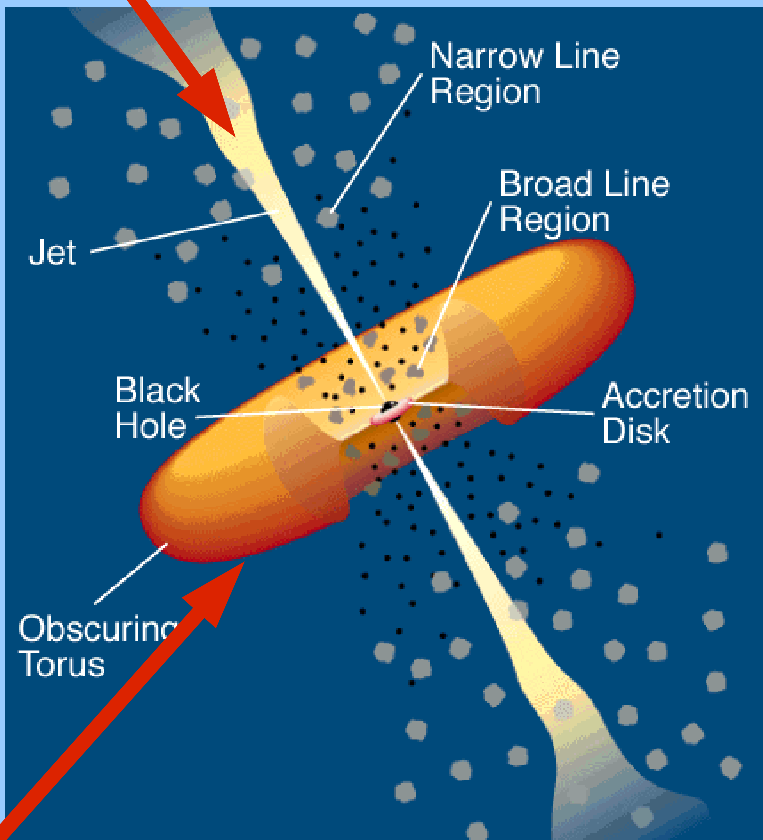

AGN2

optical lines: narrow

absorbed in the X-rays

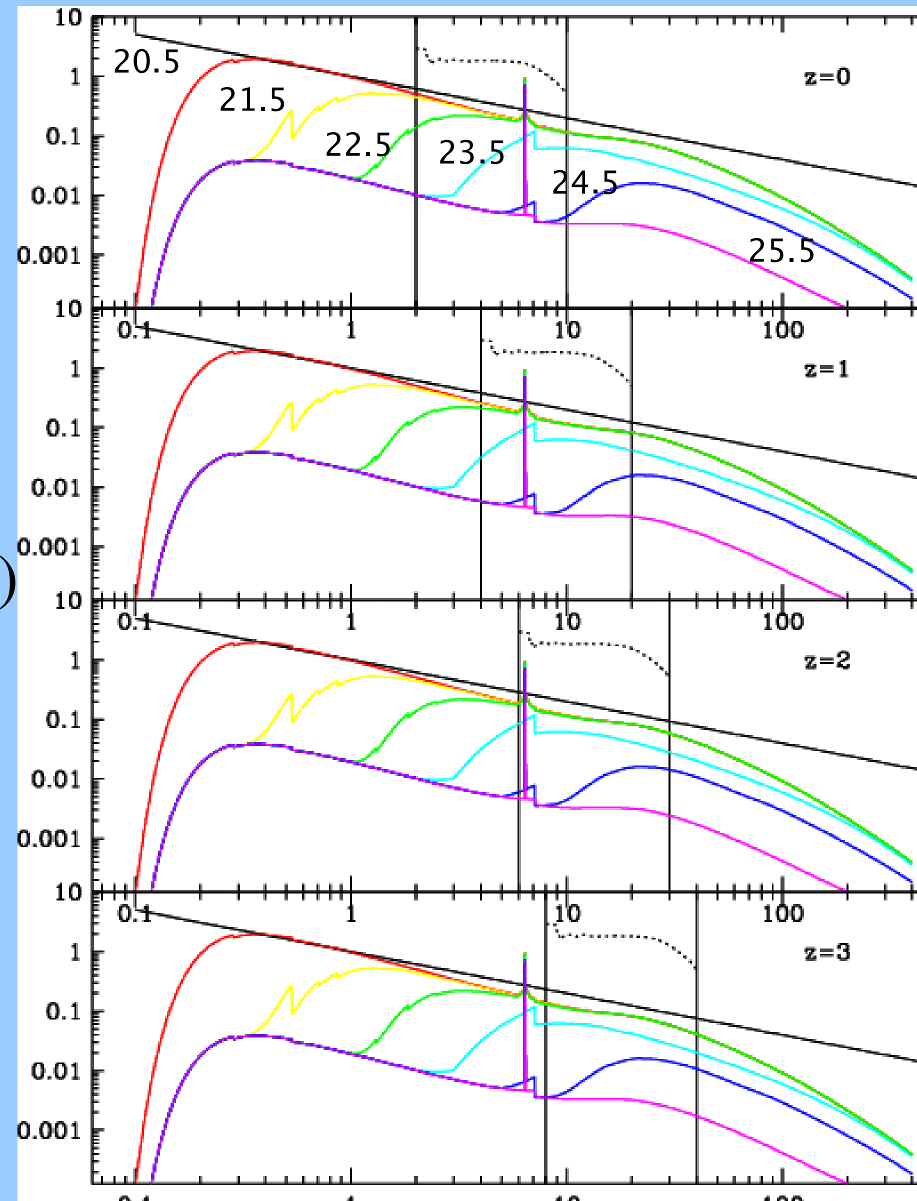

Optical AGN classification

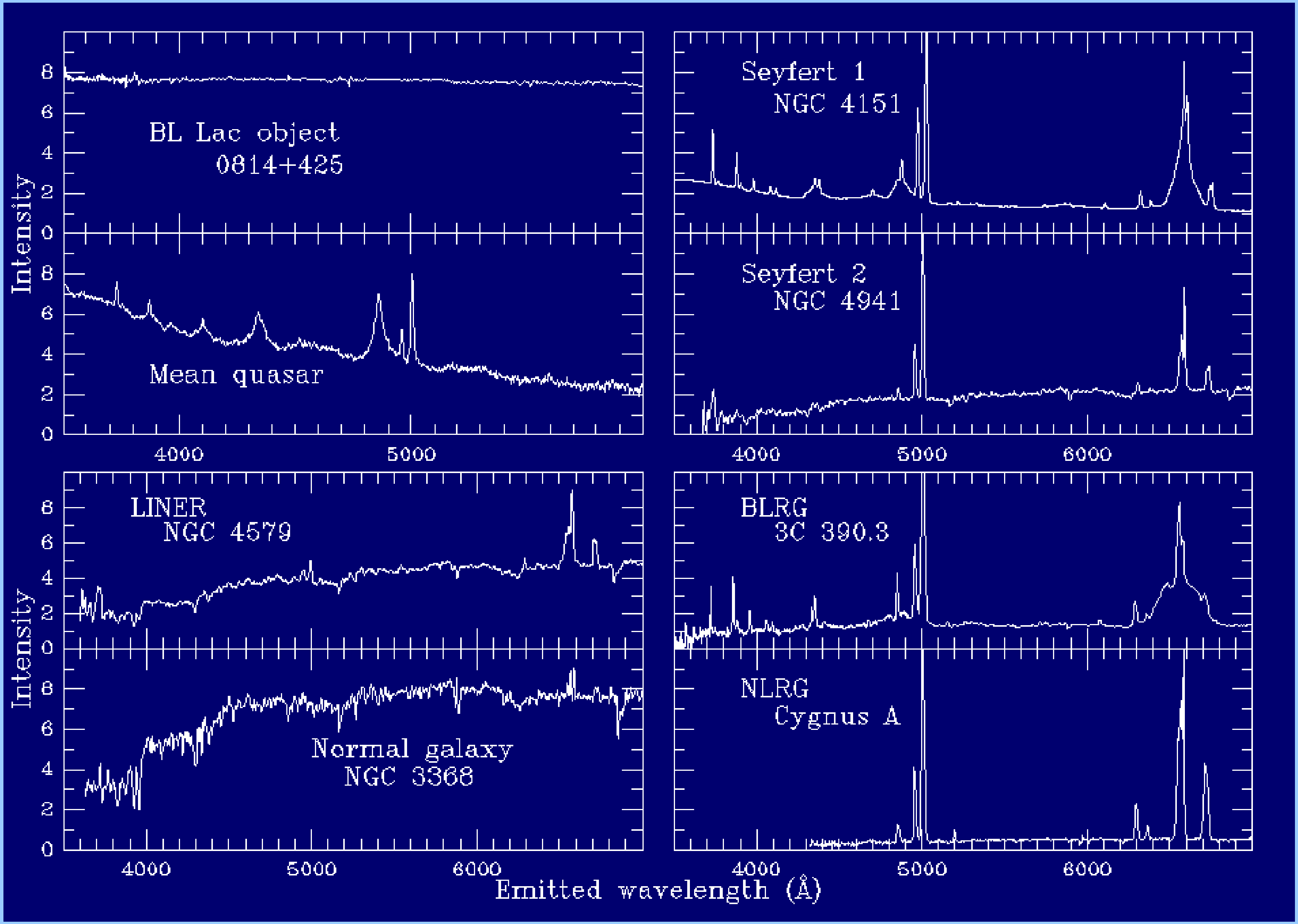

First Spectroscopic identification of Chandra sources

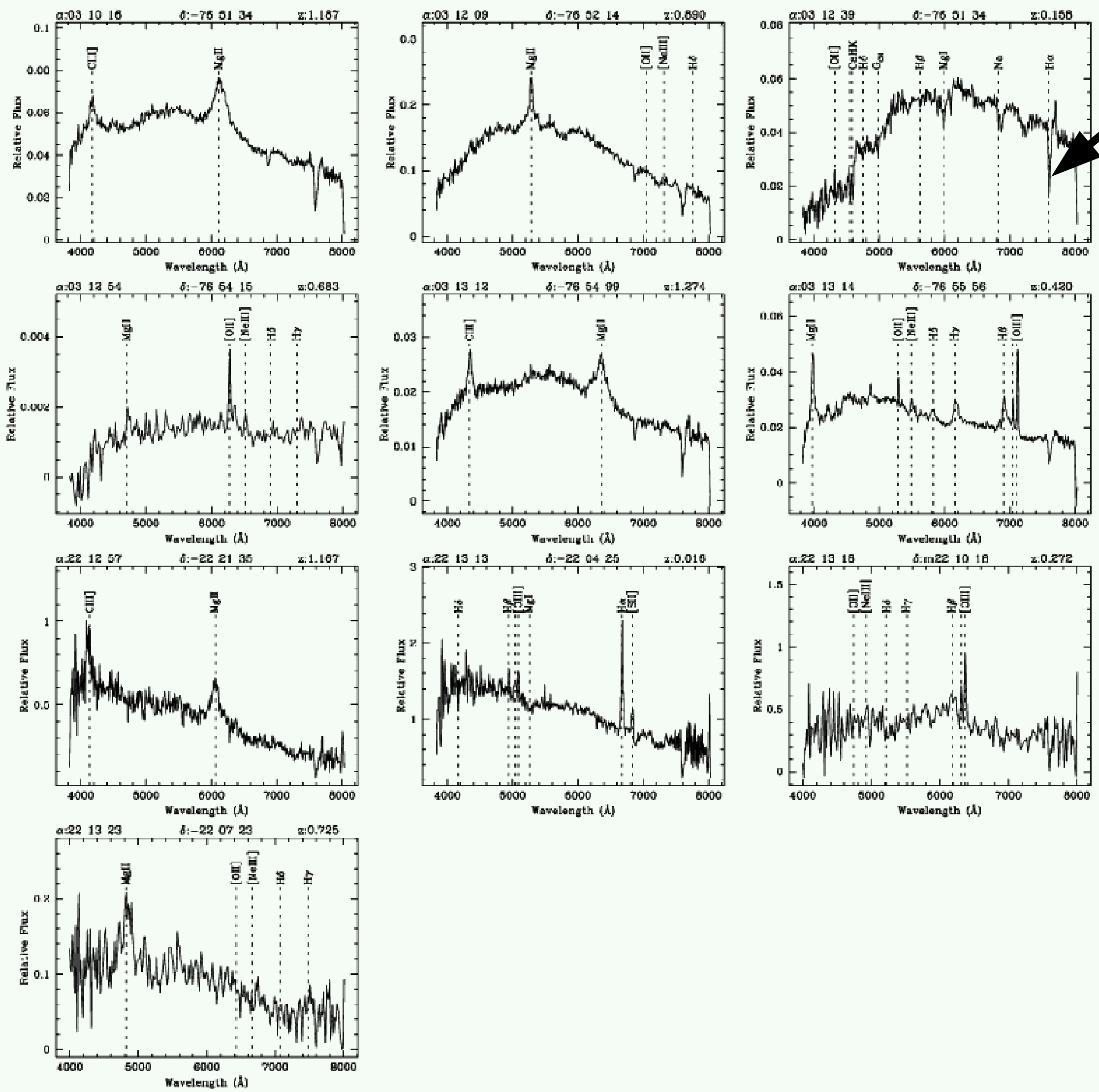

Fig. 1. The EFOSC2 spectra of the ten spectroscopically identified *Chandra* hard X-ray selected sources. Vertical dashed lines are the most important expected atomic transitions, and are reported only for reference.

XBONG

(X-ray Bright Optically Normal Galaxy)

Fiore, LF, Vignali et al. (2000)

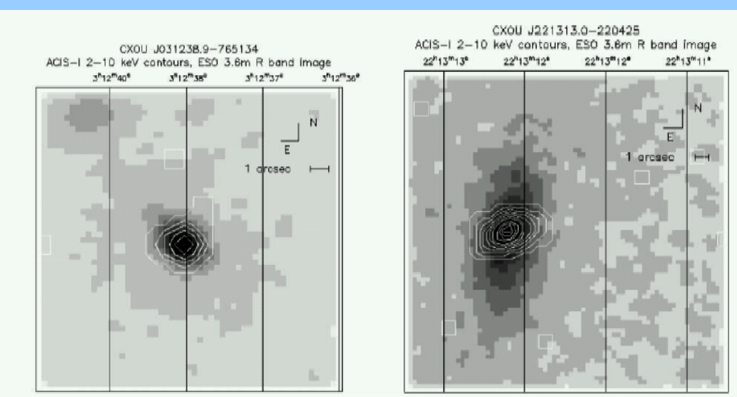

Fig. 2. *Chandra* ACIS-I (contours) and R band images (grayscale) of CXOUJ031238.9-7651, P3 (a), and CXOUJ221313.0-220425, LAR5 (b). The second source was observed by ACIS-I at an off-axis angle of 6 arcmin leading to contours slightly elongated in the East-West direction.

The N_H distribution of AGN2

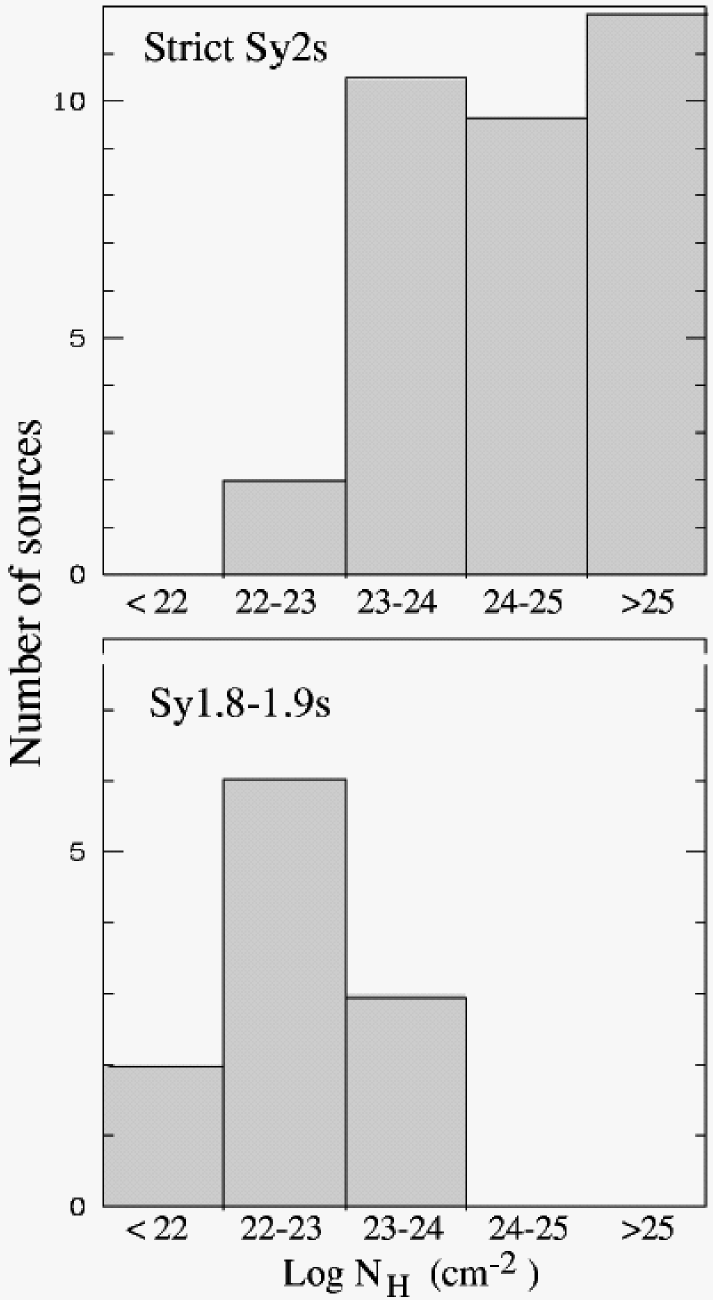

FIG. 5.—Separate contribution to the N_H distribution from "strict" type 2 Seyfert galaxies (*top*) and from intermediate type 1.8–1.9 Seyfert galaxies (*bottom*).

Risaliti et al. (1999)

·The measure of the evolution of the density of AGN provides fundamental constraints to the physical models of the growth of supermassive black holes in galaxies within the context of hierarchical collapse of structures in the universe.

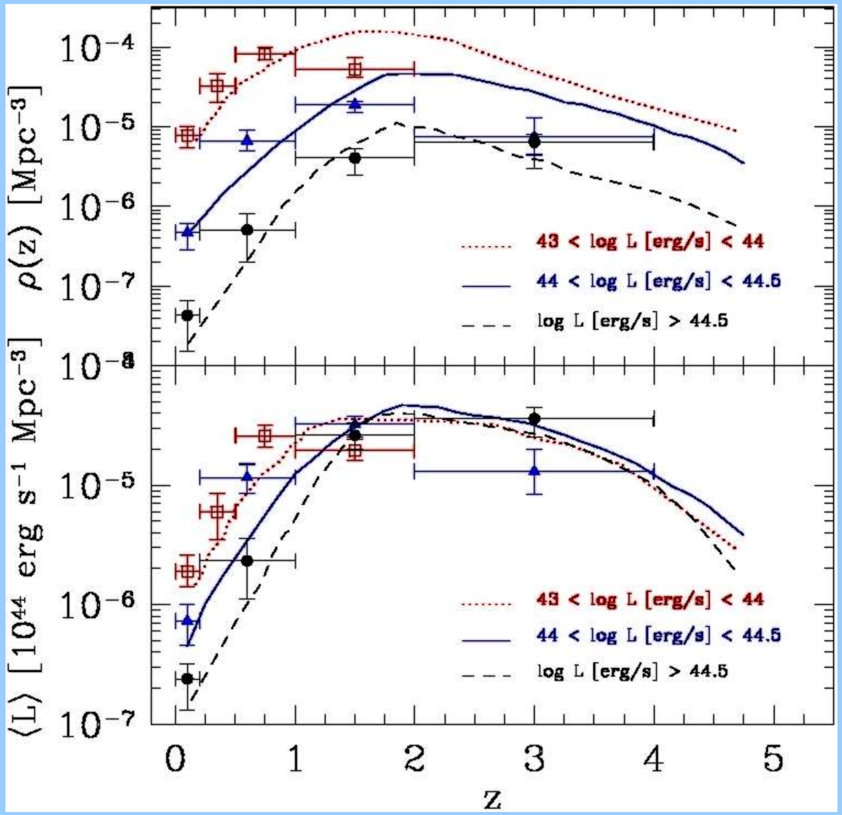

Menci et al. (2004)

See:

- Kauffmann & Haehnelt (2000)
- Monaco, Salucci & Danese (2000)
- Cavaliere & Vittorini (2000, 2002)
- Cattaneo et al. (2001, 2005)
- Granato et al. (2001, 2004)
- Mahmood et al. (2004)
- Bromley et al. (2004)
- Menci et al. (2003, 2004, 2006)
- Vittorini et al. (2005)
- Bower et al. (2006)
- Croton et al. (2006)
- Hopkins et al. (2006)
- Malbon et al. (2006)
- Fontanot, Monaco, Cristiani & Tozzi (2006)

BH-bulge-DMH relations

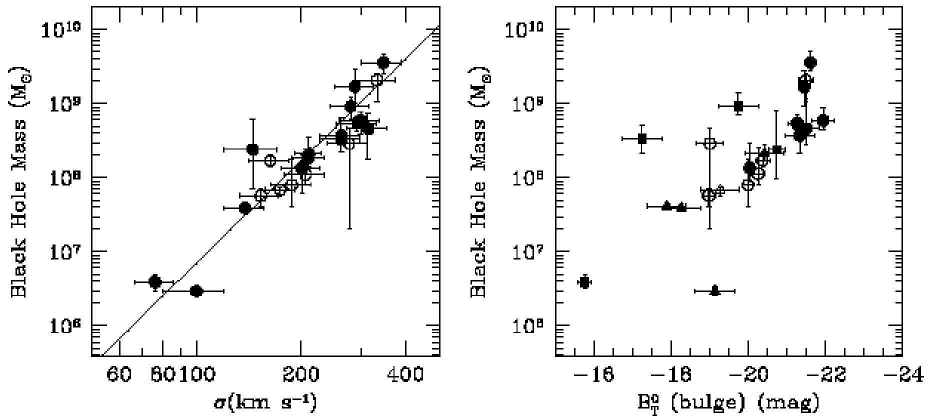

Figure 2: (left) Correlation between central velocity dispersion and black hole mass for all secure SBH detections. Published data are shown as solid symbols, data based on unpublished analyses as open symbols.
Figure 3: (right) Correlation between bulge B—band magnitude and black hole mass for the same sample shown in Fig. 2. Elliptical galaxies are shown as circles, lenticulars and compact ellipticals as squares, and spirals as triangles.

$$M_\bullet = (1.66 \pm 0.32) \times 10^8 \ M_\odot \left(\frac{\sigma}{200 \ \mathrm{km \ s^{-1}}} \right)^{4.58 \pm 0.52} .$$

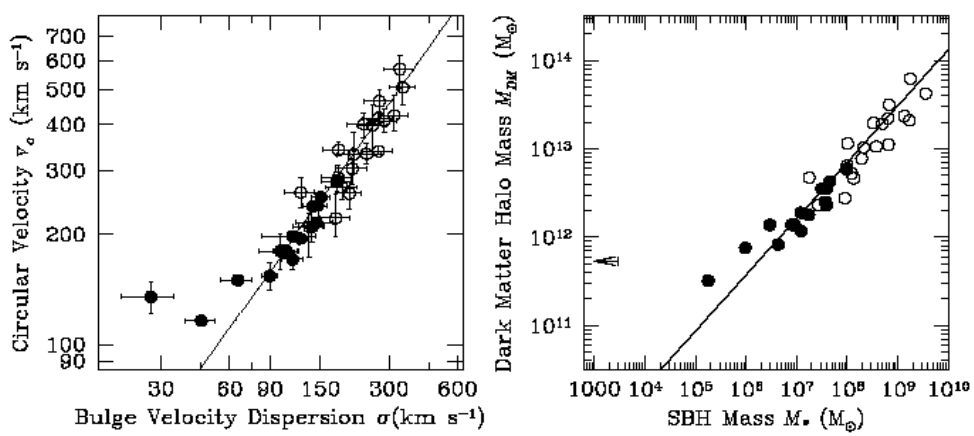

Figure 5: (left) Correlation between the rotational velocity and bulge velocity dispersion for a sample of 16 spiral galaxies (solid circles) and 21 ellipticals (open circles; plot adapted from Ferrarese 2002).
Figure 6: (right) Same as Fig. 5, but with v_c and σ converted to halo mass and black hole mass respectively (see text for further details). The upper limit on the SBH mass in M33 (Merritt *et al.* 2001) is shown by the arrow.

Ferrarese (2002)

$$\frac{M_\bullet}{10^8 \ M_\odot} \sim 0.046 \left(\frac{M_{DM}}{10^{12} \ M_\odot} \right)^{1.6}$$

·The measure of the evolution of the density of AGN provides fundamental constraints to the physical models of the growth of supermassive black holes in galaxies within the context of hierarchical collapse of structures in the universe.

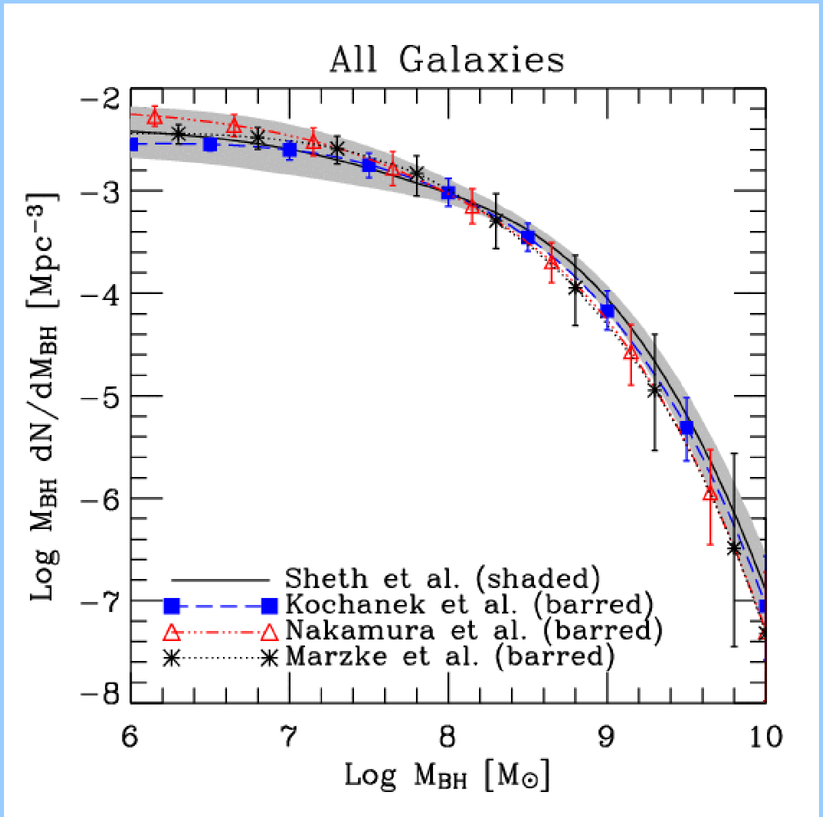

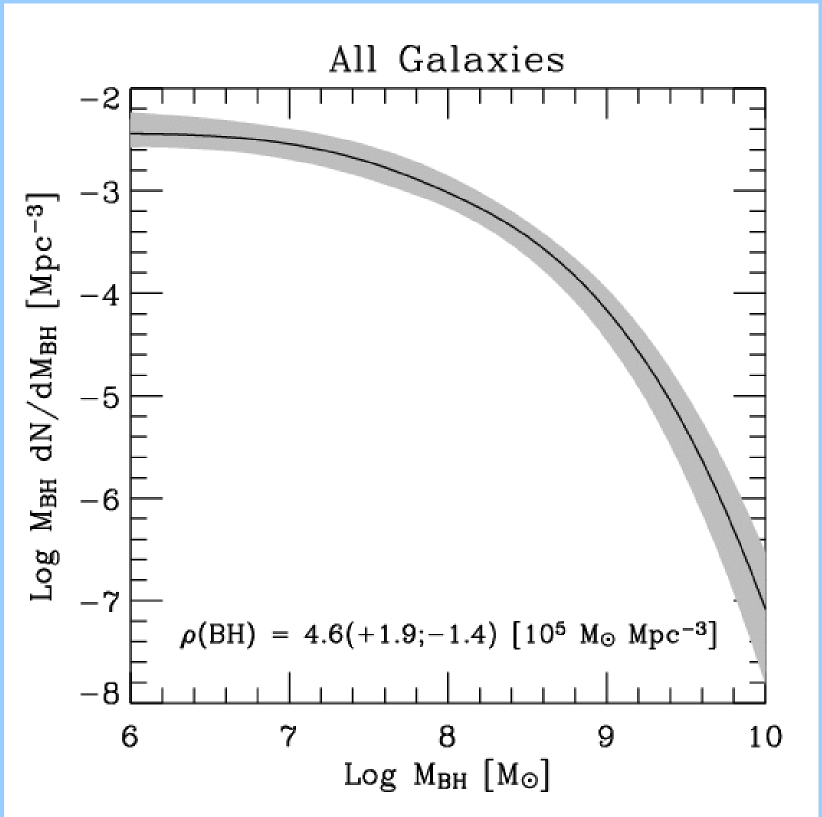

Marconi et al. (2004)

Interpretazioni

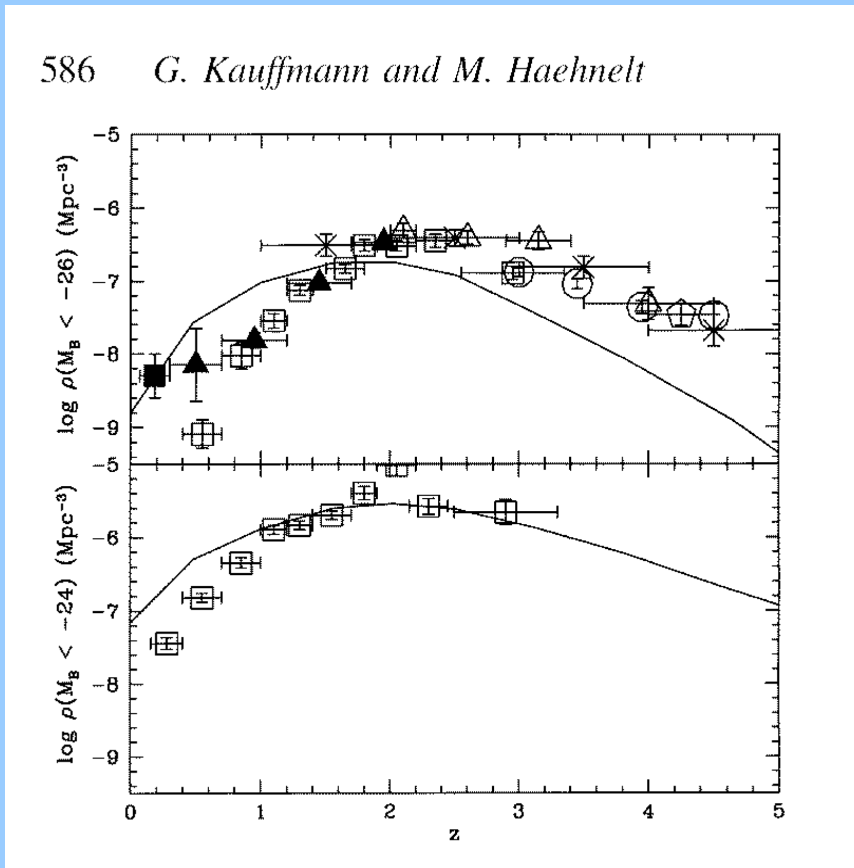

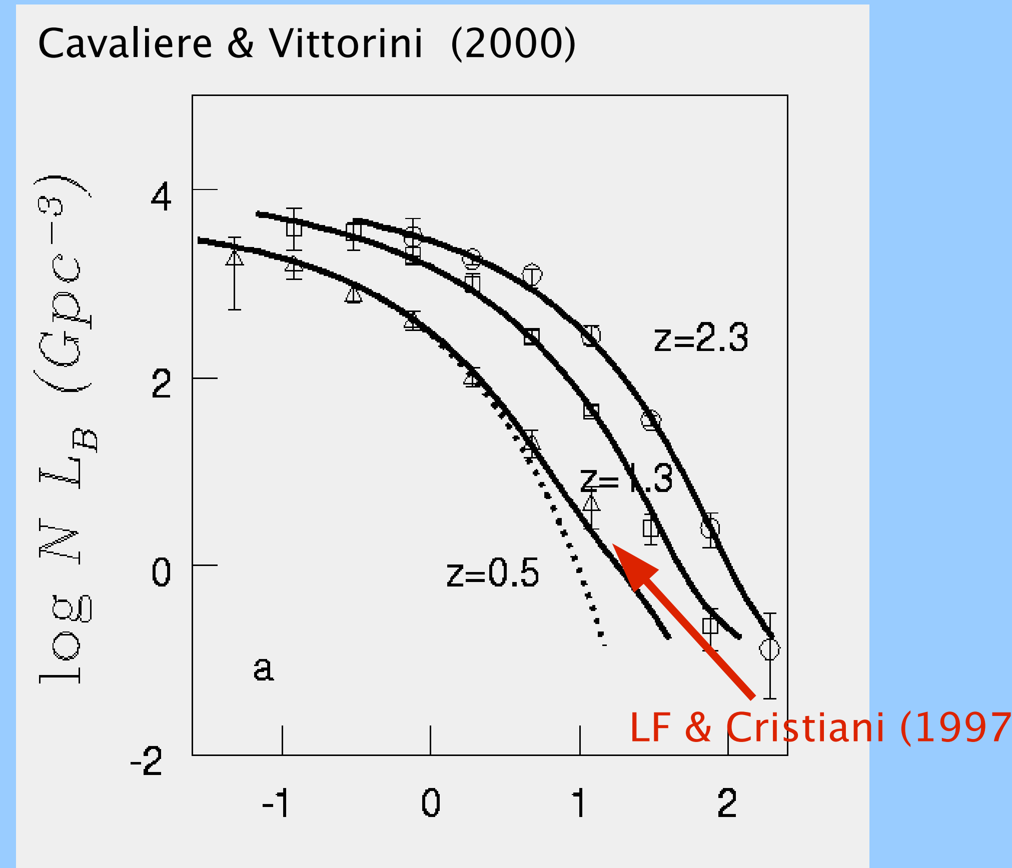

-Molti modelli semianalitici (e.g. Kauffmann & Haehnelt 00) hanno difficolta` a riprodurre il ripido declino della densita` di QSO a bassi z.

-Un appiattimento a bassi z della LF dei QSO e` previsto ad esempio dai modelli di Cavaliere e Vittorini (2000), nei quali il declino della LF a z<3 e` causato dagli effetti della crescita gerarchica delle strutture attorno ai BH in accrescimento, amplificata dall'esaurimento del gas disponibile per l'accrescimento. L'evoluzione si svolge in due regimi: all'inizio, al formarsi degli sferoidi avvengono dei violenti eventi di merging, mentre piu` tardi domina una fase di incontri con le altre galassie ad un tasso $\sim Gyr^{-1}$.

-The functional form of the AGN evolution was not entirely known: PLE, LDDE,... (downsizing?)

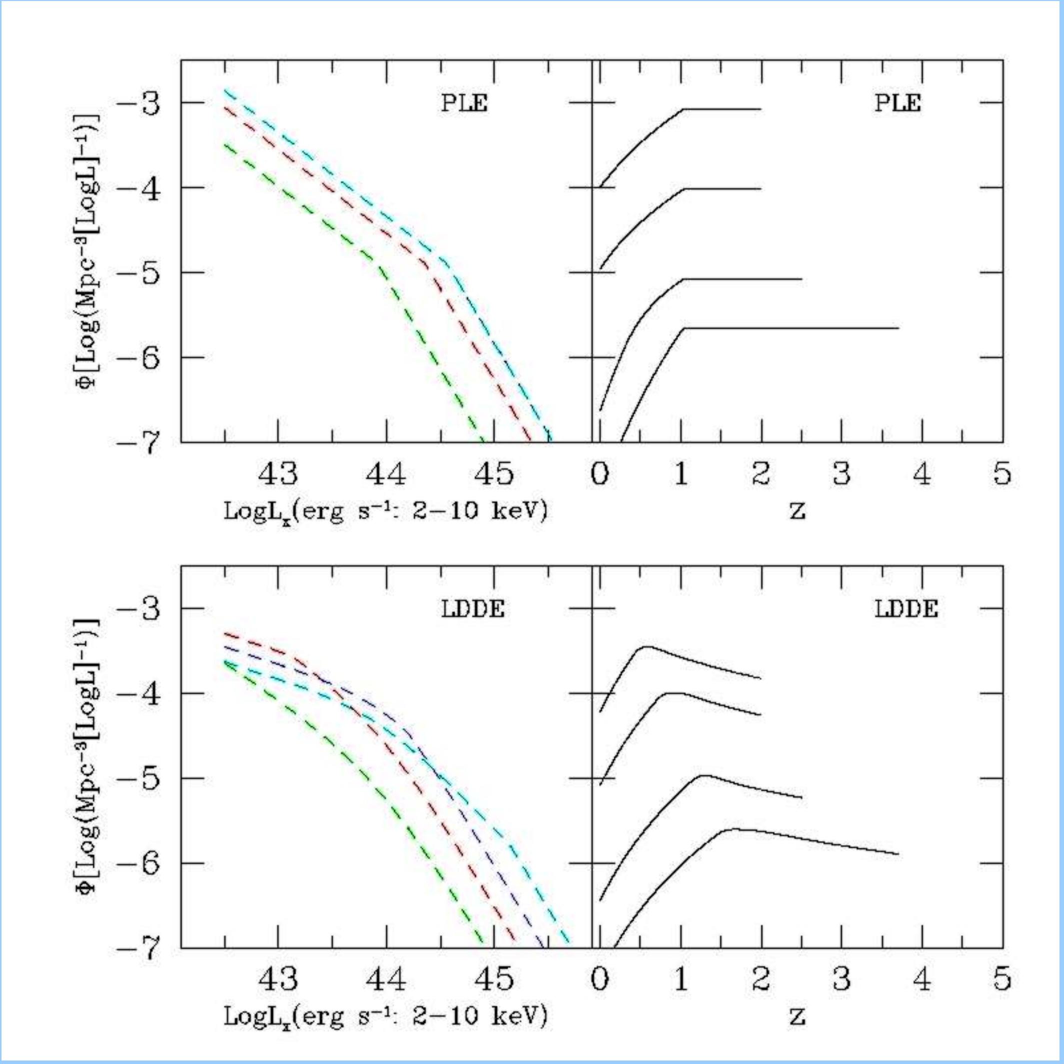

The density of AGN at high redshift (z>4) is still uncertain

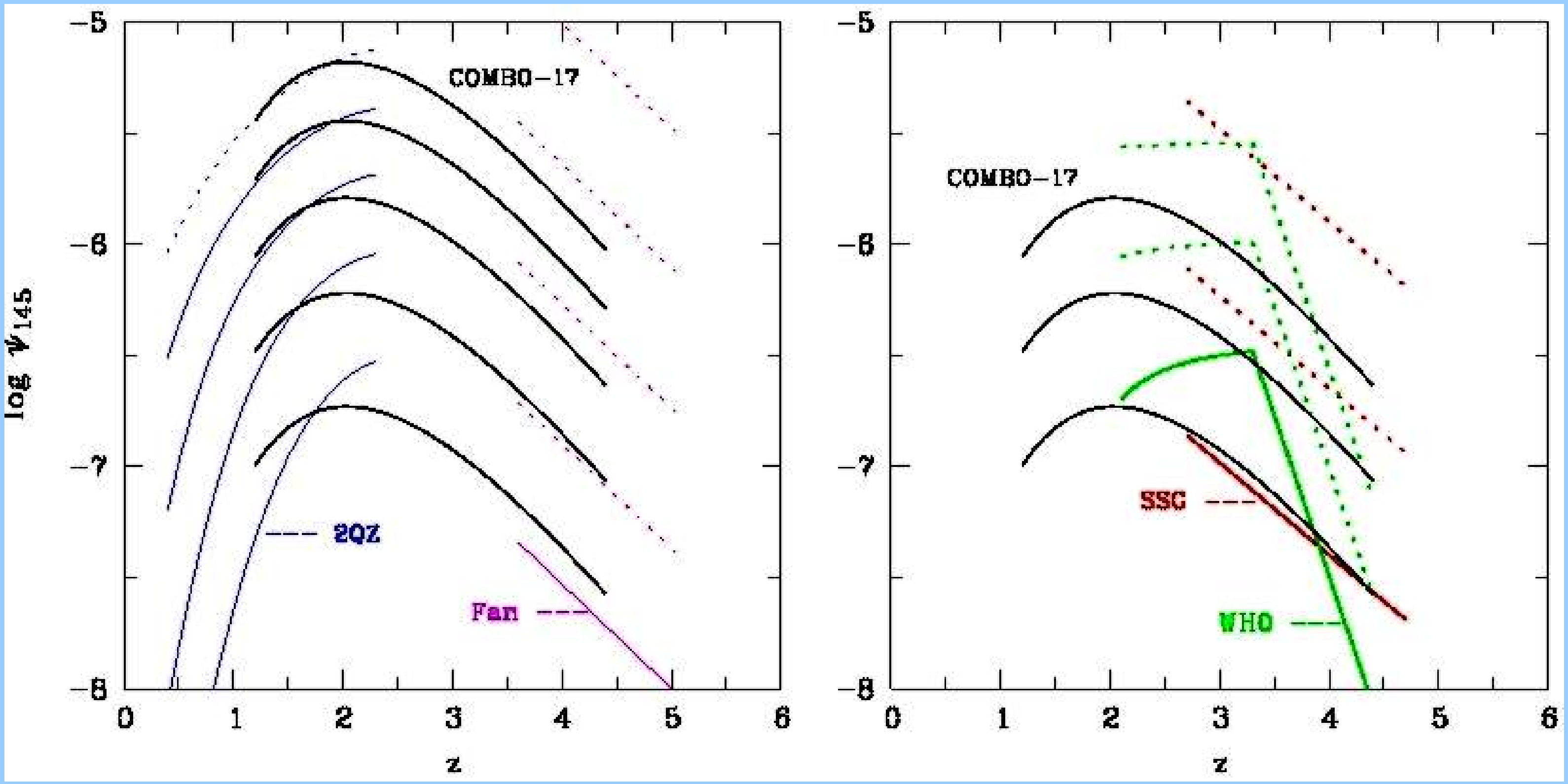

Wolf et al. (2003)

Chandra and XMM/Newton deep surveys
called for a revision of the standard evolutionary models: a faster evolution of absorbed AGN
linked to the starbust history of galaxies (Gilli et al. 2001; Franceschini et al. 2002; Gandhi & Fabian 2002)

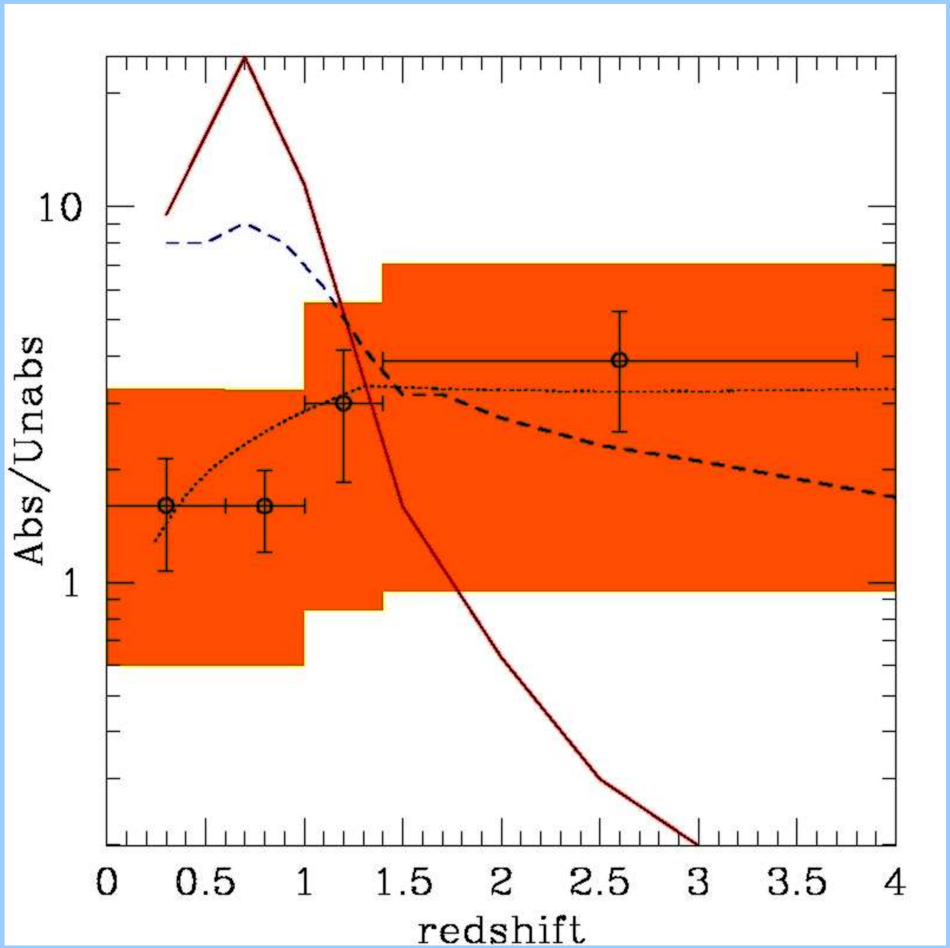

Gilli (2003)

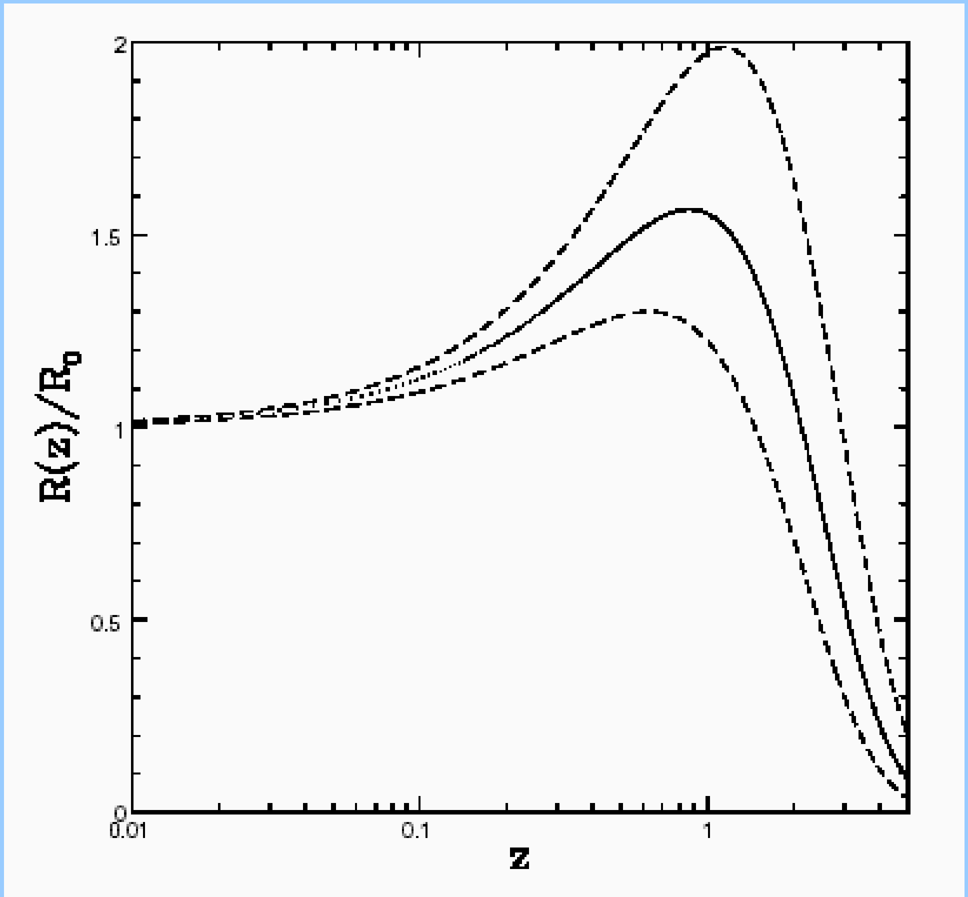

Pompilio, LF, Matt (2000)

Each evolutionary model fits the shape of the cosmic X-ray background (there is degeneracy in the solutions), whose normalization and shape at high energies is still uncertain

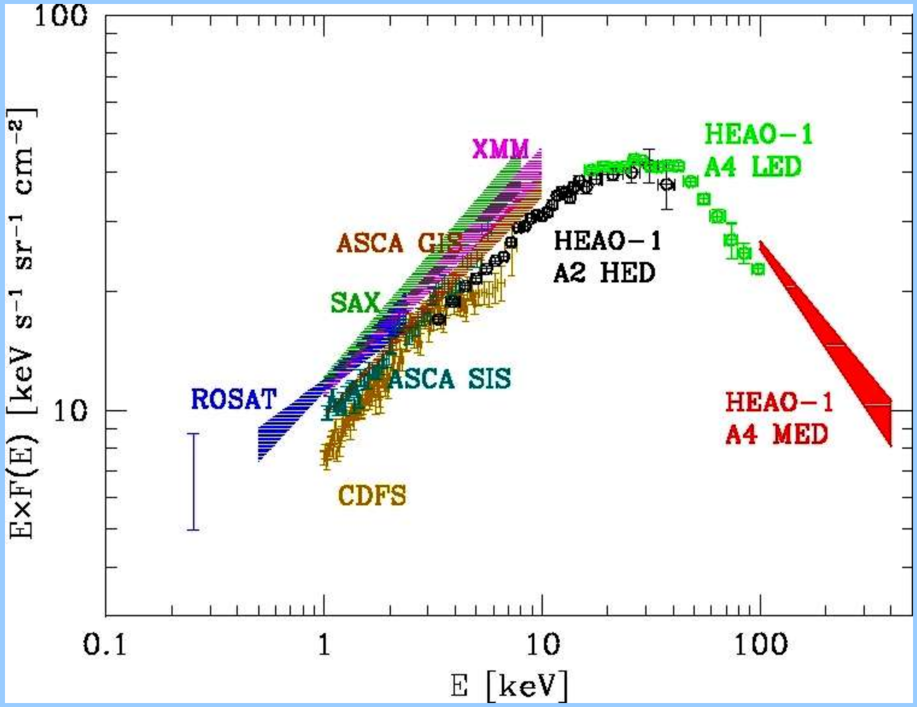

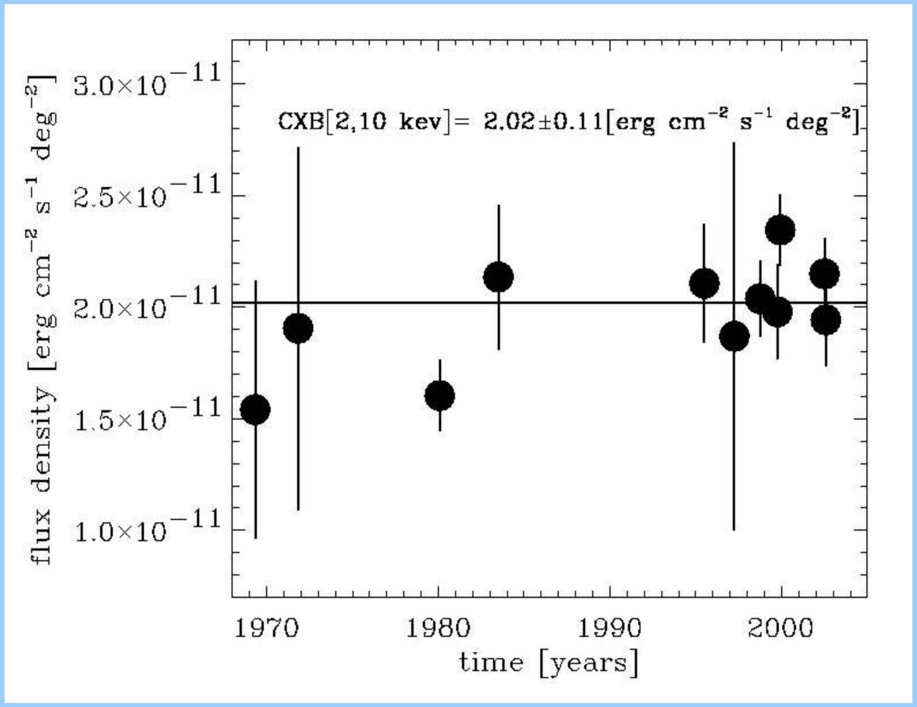

Moretti et al. (2003)

The models failed to reproduce the observed increase of the fraction of absorbed AGN with the flux.

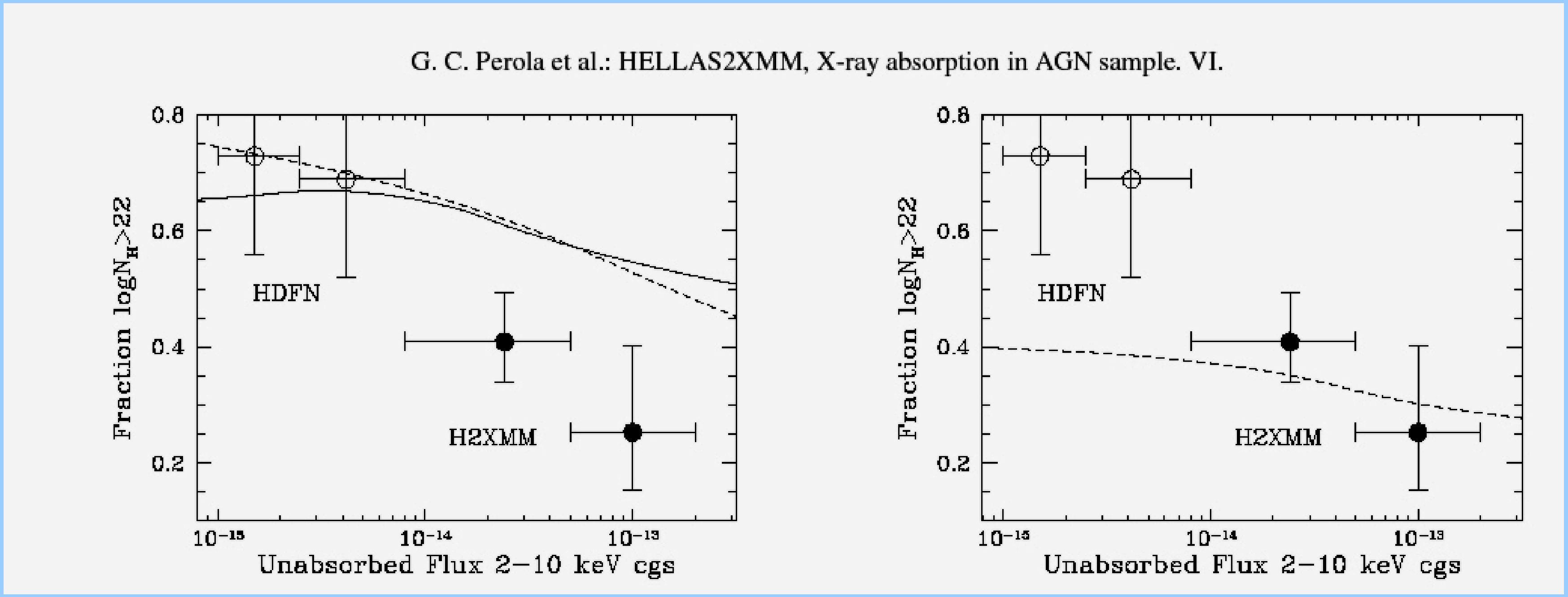

The deep samples reaches only 60% spectroscopic completeness and have to use phot-z for the remaining sources.

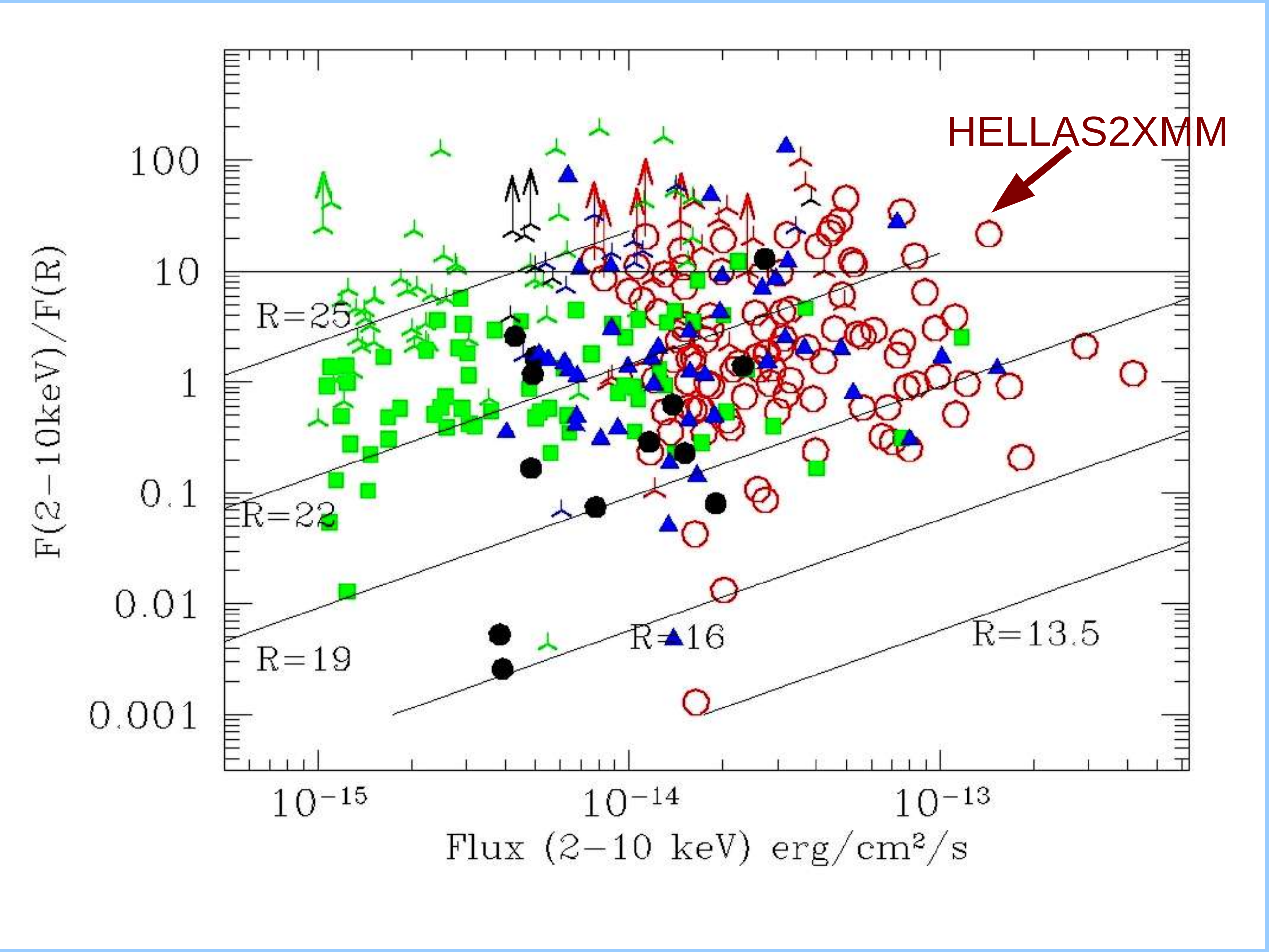

We have thus decided to measure the history of density of the AGN as function of luminosity and N_H absorbing columns, taking into account all the selection effects and incompleteness factors.

The samples used

690 AGNs

HELLAS2XMM
1.5 sq. deg.
137 sources with z
$F_X > 8 \times 10^{-15}$

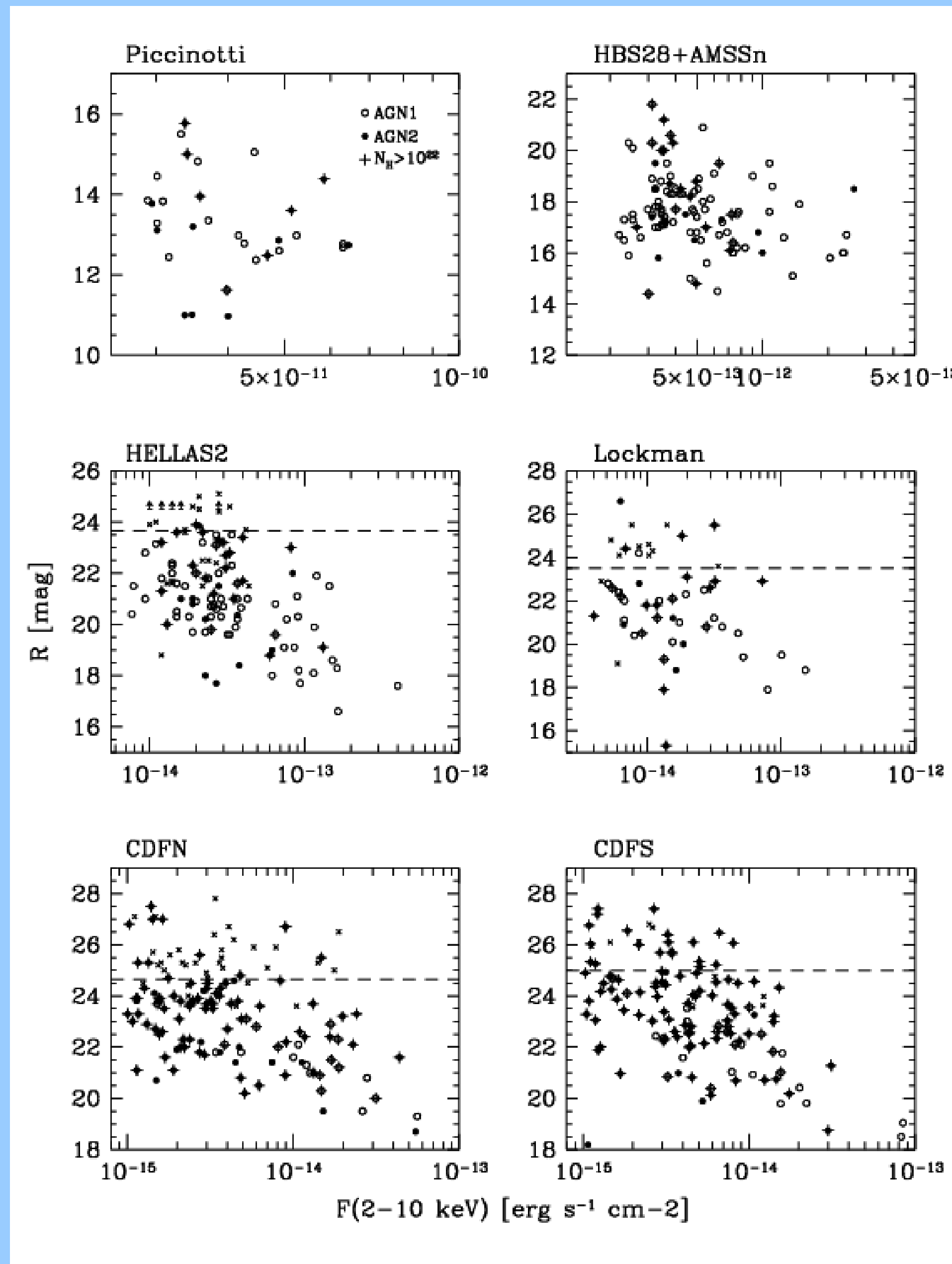

508 AGNs
in the
spectroscopic
complete
sample

The counts

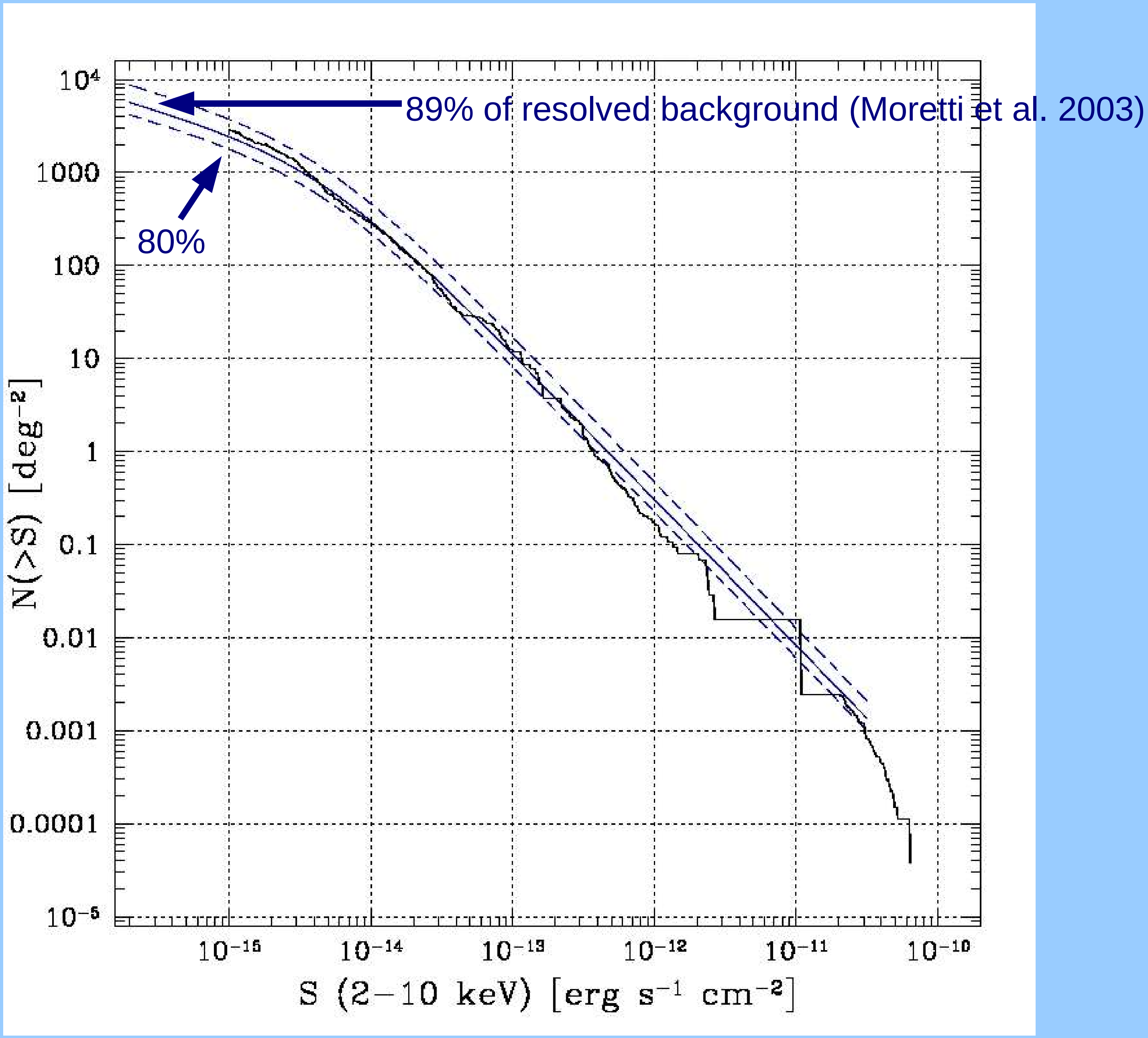
89% of resolved background (Moretti et al. 2003)
80%
10^4
1000
100
10
1
0.1
0.01
0.001
0.0001
10^{-5}
$N(>S)$ [deg^{-2}]
10^{-15}
10^{-14}
10^{-13}
10^{-12}
10^{-11}
10^{-10}
S (2–10 keV) [erg s^{-1} cm^{-2}]

The counts

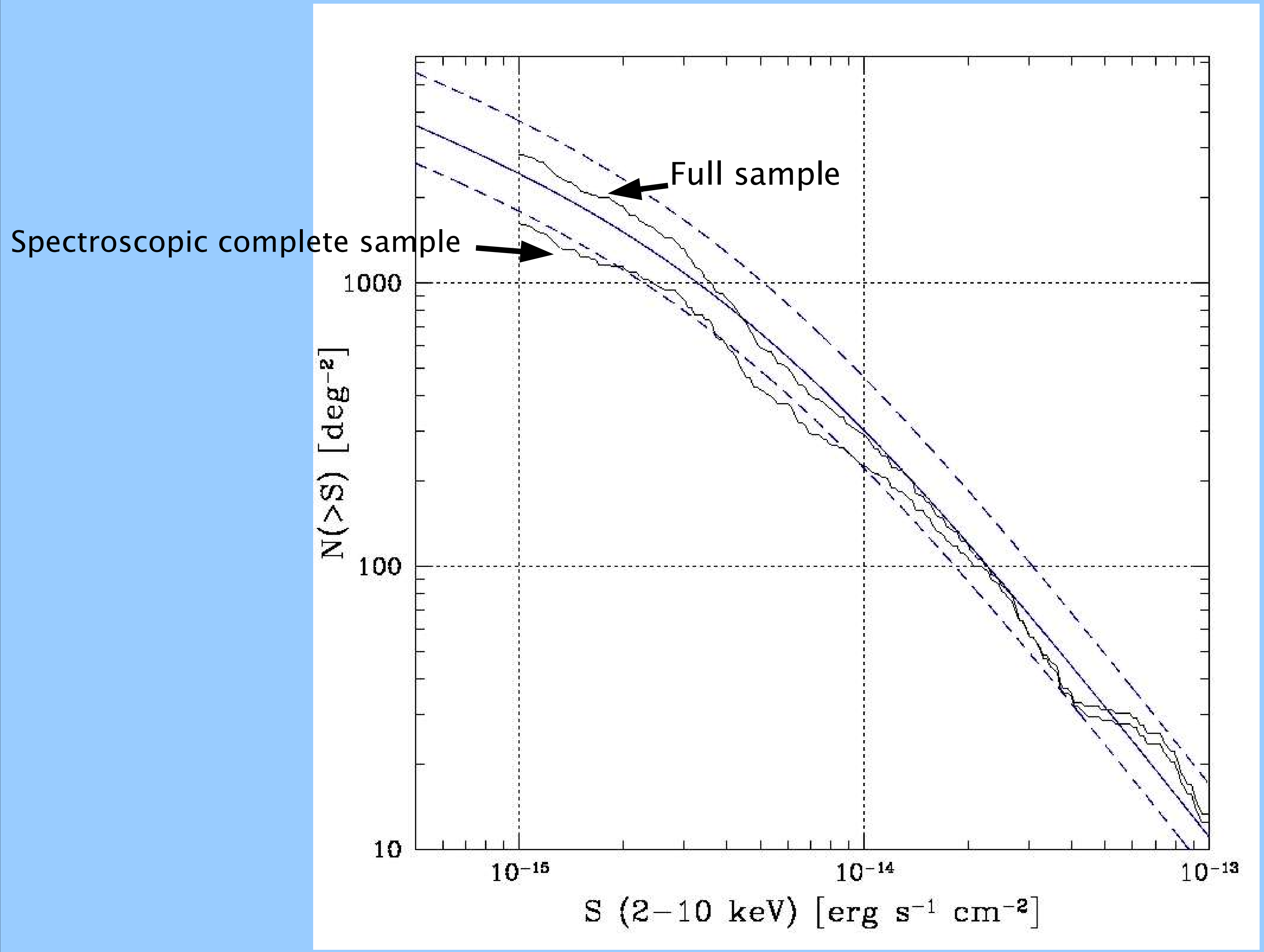

Full sample
Spectroscopic complete sample
1000
100
10
N(>S) [deg^{-2}]
10^{-15}
10^{-14}
10^{-13}
S (2–10 keV) [erg s^{-1} cm^{-2}]

The Lx-z plane

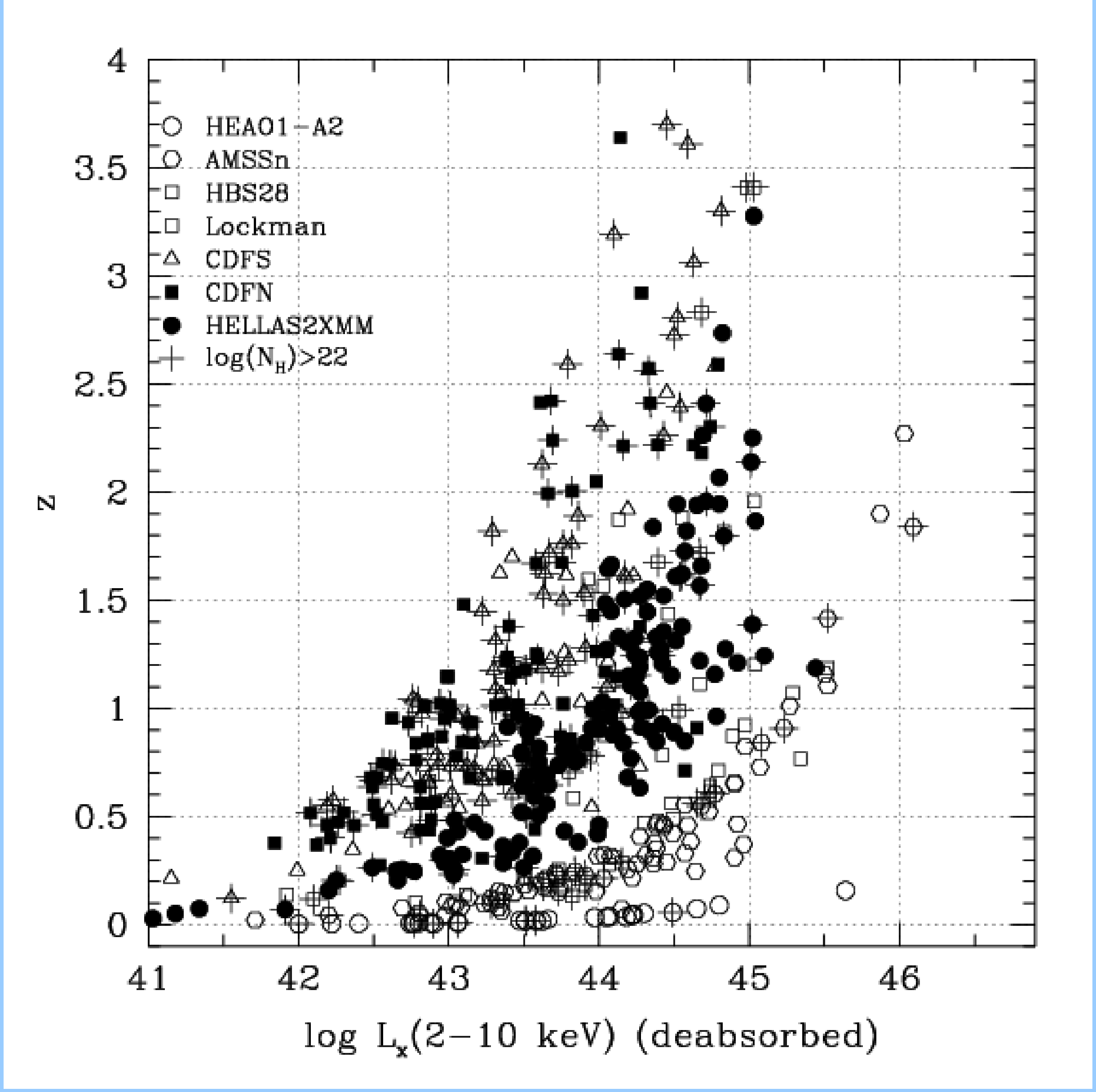

The samples used

690 AGNs

HELLAS2XMM
1.5 sq. deg.
137 sources with z
$F_X > 8x10^{-15}$

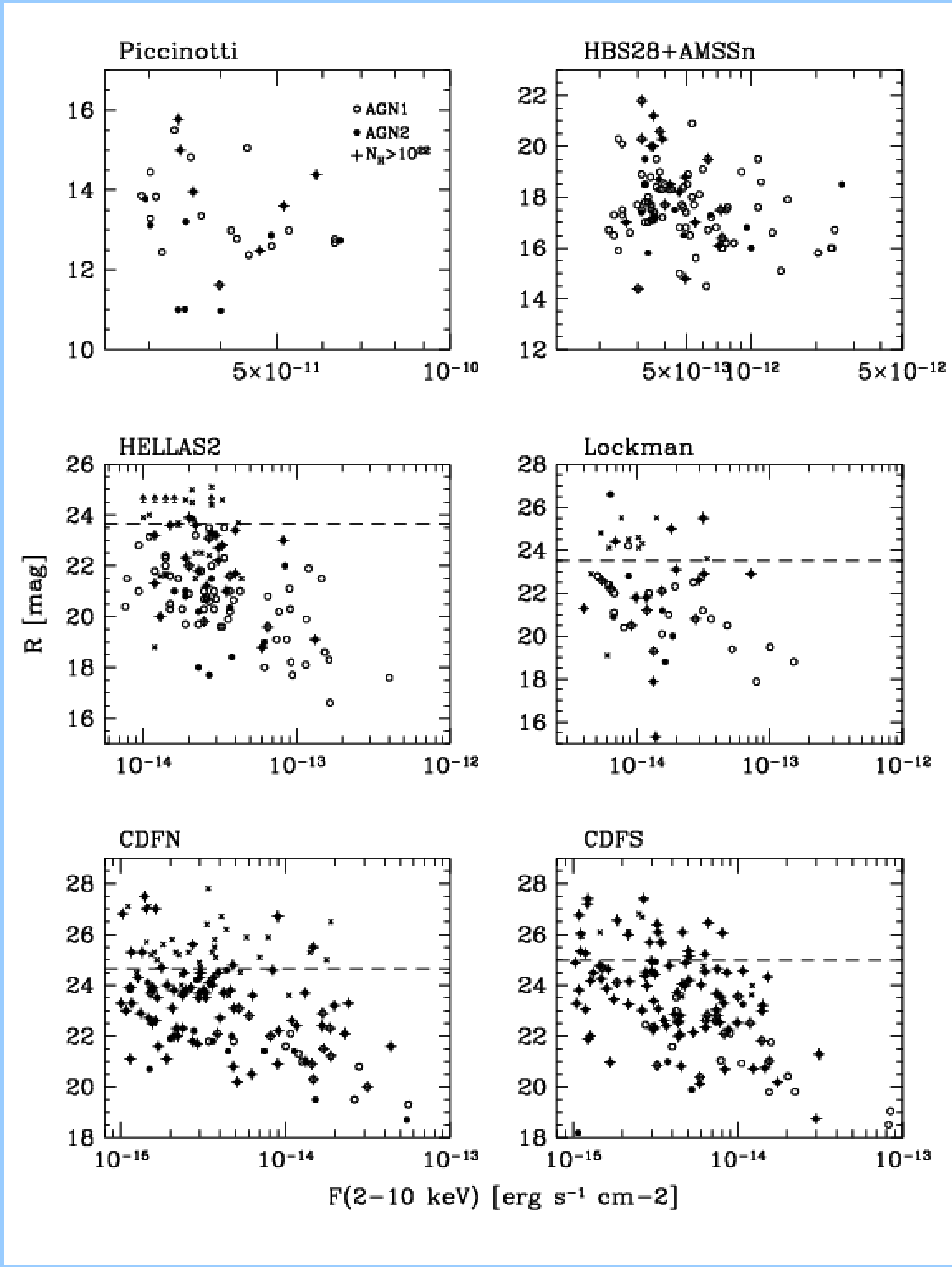

508 AGNs
in the
spectroscopic
complete
sample

The L_X–L_O relationship

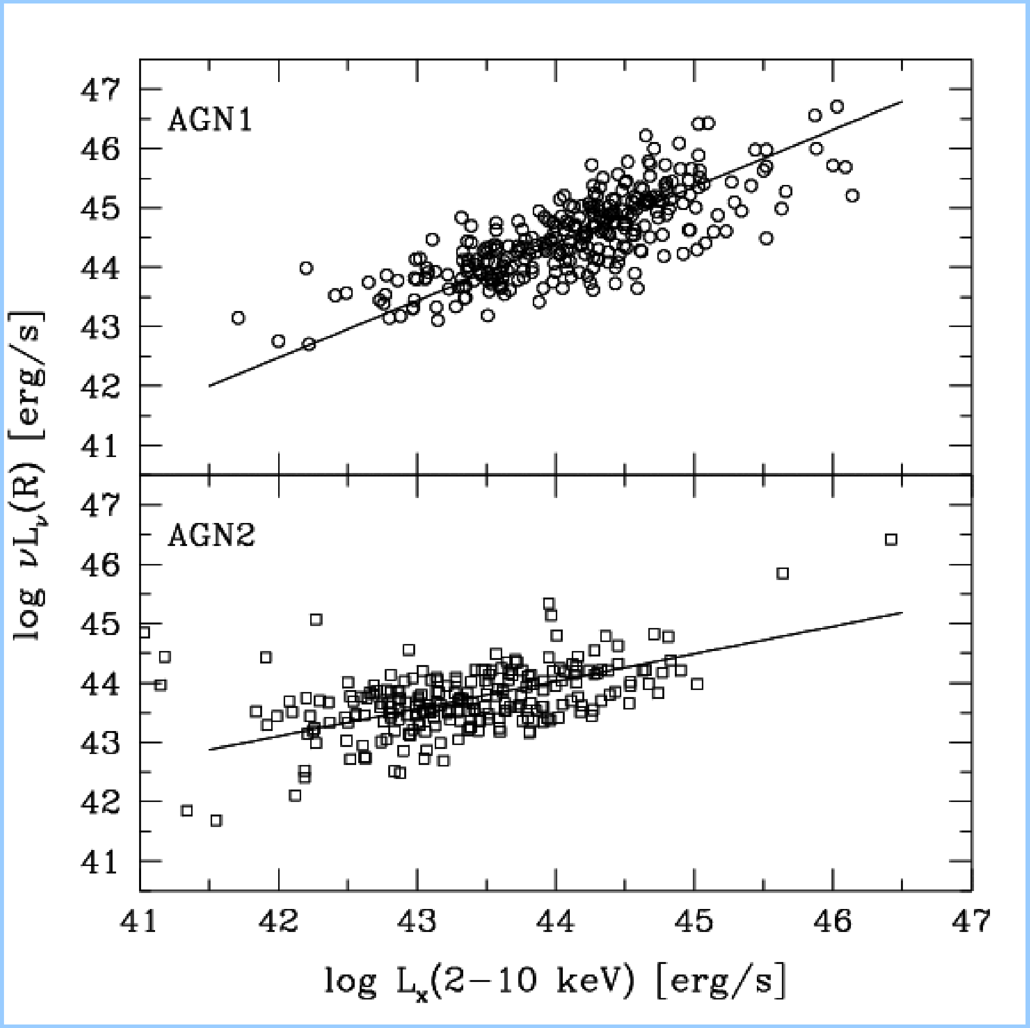

In order to correct for spectroscopic incompleteness we need to predict the optical luminosity of AGNs

The fitting method

1) Assume a XLF: $N(L_X,N_H,z) = A(L_X,z)Prob(N_H)$;
where $Prob(N_H)=f(L_X,z)$

2) For each L_X,N_H compute the probability to appear as optical AGN1 or AGN2: f1+f2=1

3a) From the $Lo=f(L_X)$ for AGN1 compute the probability of having an AGN1 with apparent magnitude R brighter than the optical spectroscopic limit: $Prob_1(R<R_{LIM})$

3b) From the $Lo=f(L_X)$ for AGN2 compute the probability of having an AGN2 with apparent magnitude R brighter than the optical spectroscopic limit: $Prob_2(R<R_{LIM})$

$$Prob(R<R_{LIM}) = Prob_1(R<R_{LIM})+Prob_2(R<R_{LIM})$$

The Expected number of AGN in each bin is

$$E(L_X,N_H,z)= A(L_X,z) \times Prob(N_H) \times Prob(R<R_{LIM}) \times Volume$$

Change the parameters in order to minimize $(E-O)^2/E$

The fraction of AGN1 as a function of L_X and N_H

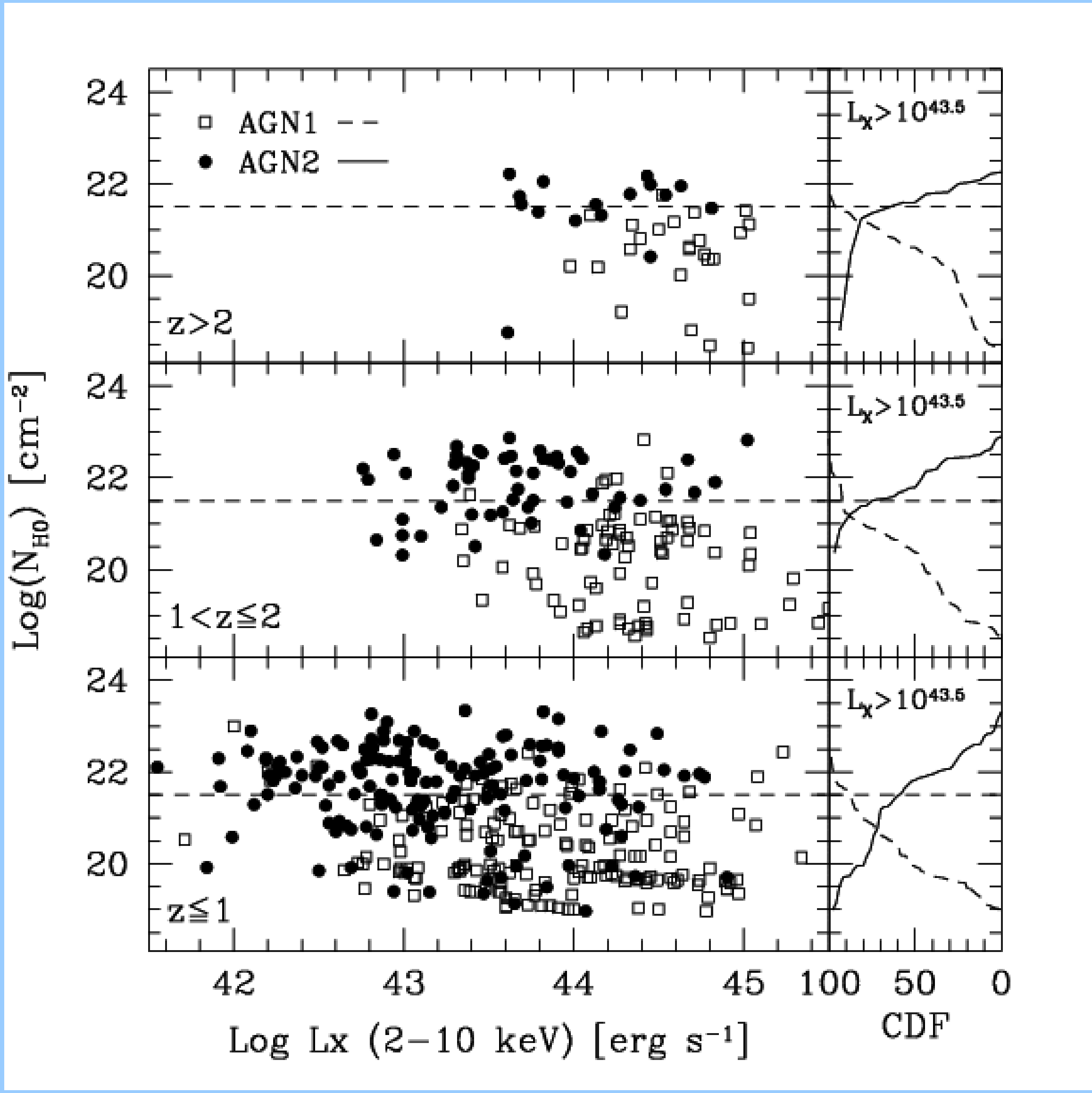

The fraction of AGN1 as a function of L_X and N_H

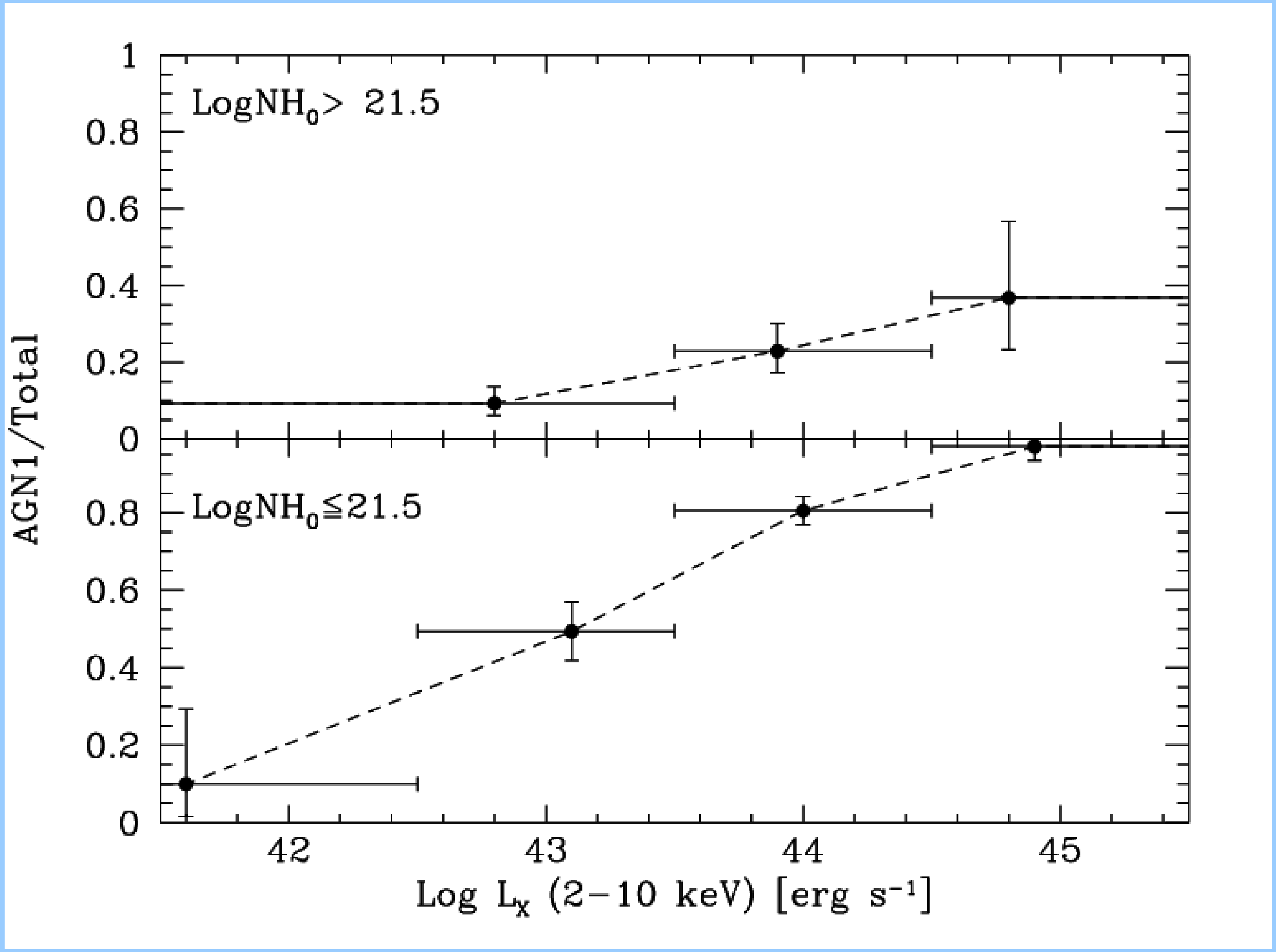

The fitting method

The number of observed AGN in the L_X–z space is compared with the number of expected AGN taking into account: 1) a spectroscopic completeness correction, and 2) and an N_H distribution.

X-ray spectroscopic completeness correction

$$E = \sum_{i=1}^{N_{\rm samp}} \int\int\int \frac{{\rm d}\Phi(L_{\rm X}, z)}{{\rm dLog}L_{\rm X}} f(L_{\rm X}, z; N_{\rm H}) g_i(L_{\rm X}, z, N_H) \times$$

$$\Omega_i(L, N_H, z) \frac{dV}{dz} {\rm dLog}L_{\rm X} {\rm d}z {\rm d}N_H .$$

$$\int_{20}^{26} f(L_{\rm X}, z; N_{\rm H}) {\rm dLog}N_{\rm H} = 1.$$

N_H column density distribution

Pure Luminosity Evolution (PLE) or Luminosity Dependent Density Evolution (LDDE) ?

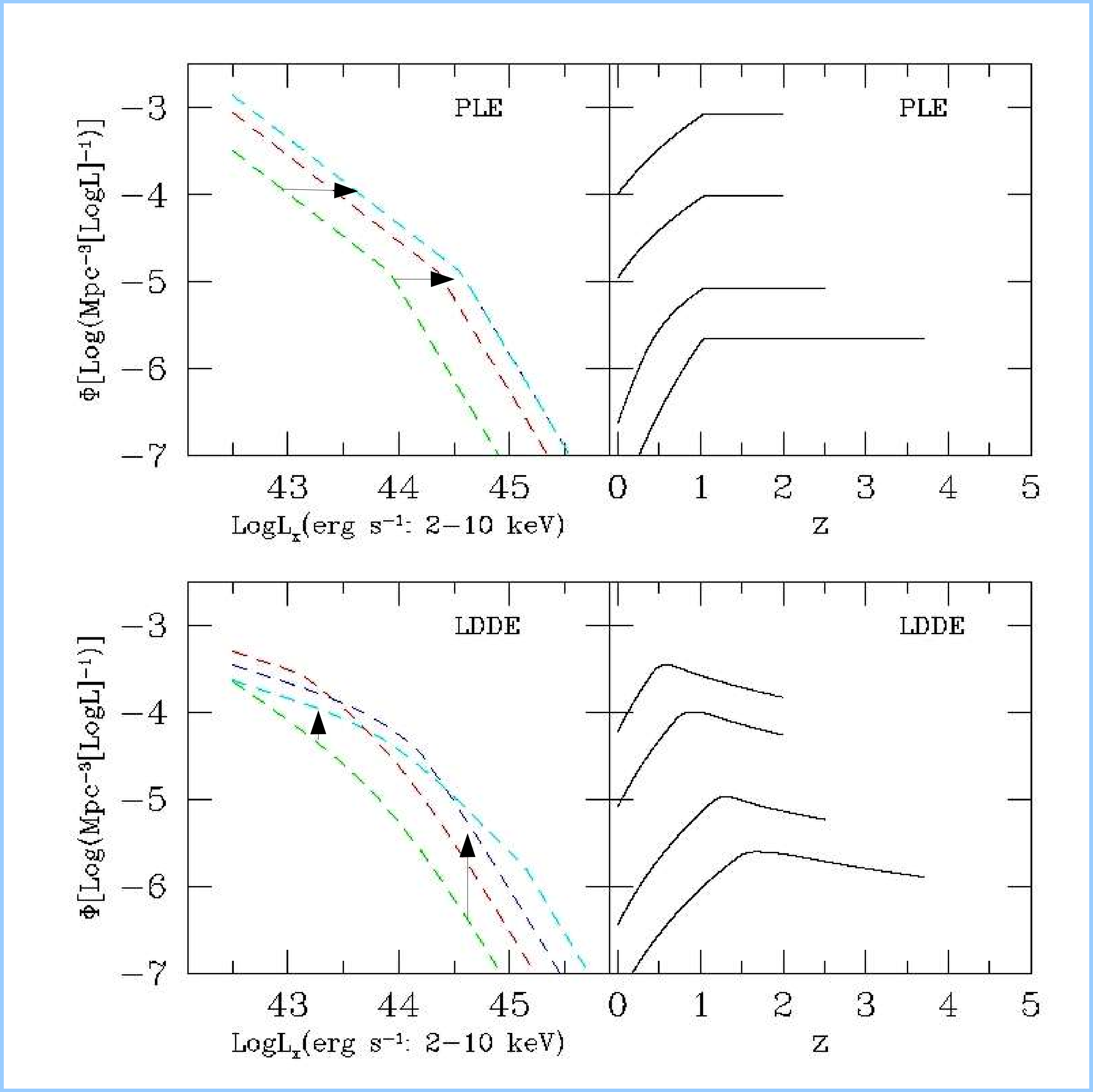

The observed density of AGN

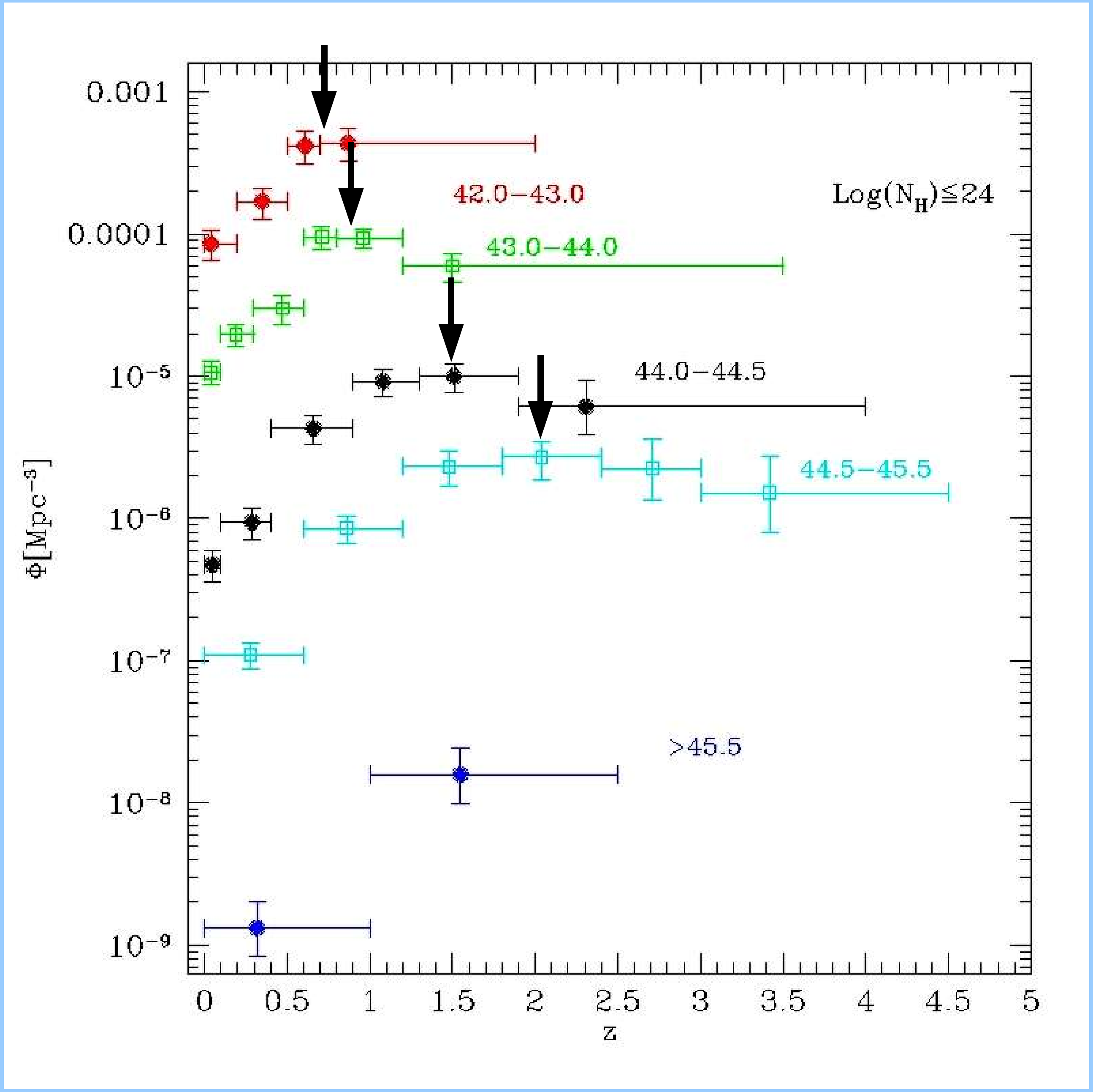

The data and the models

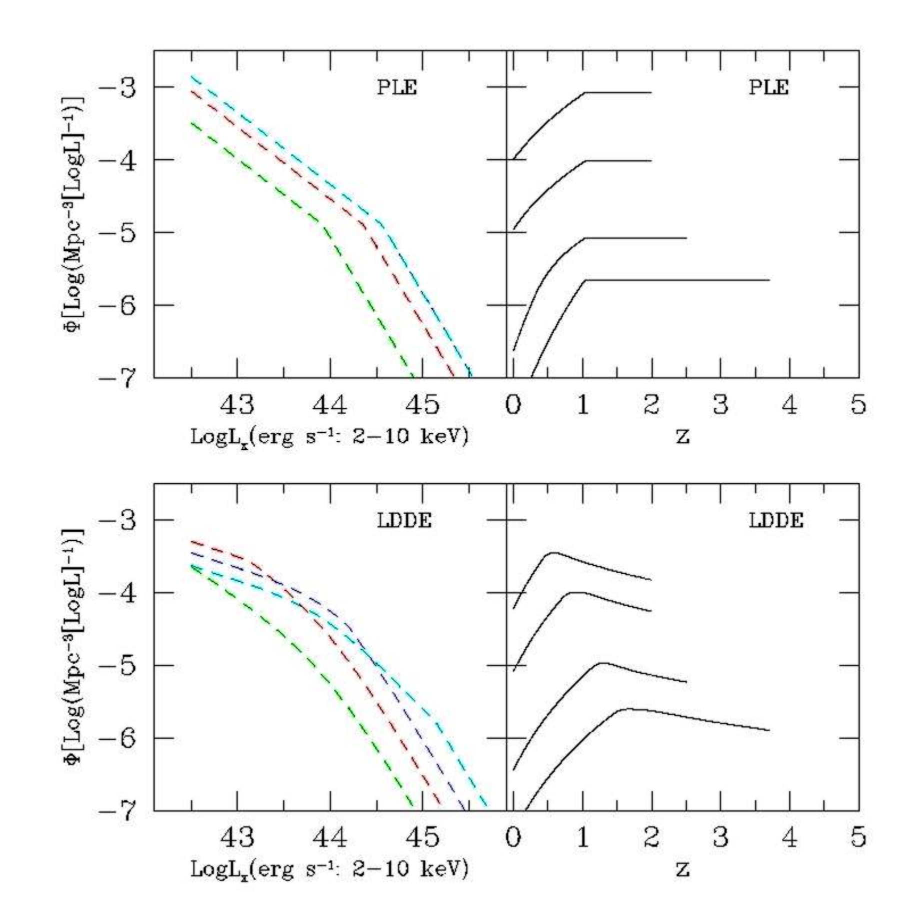

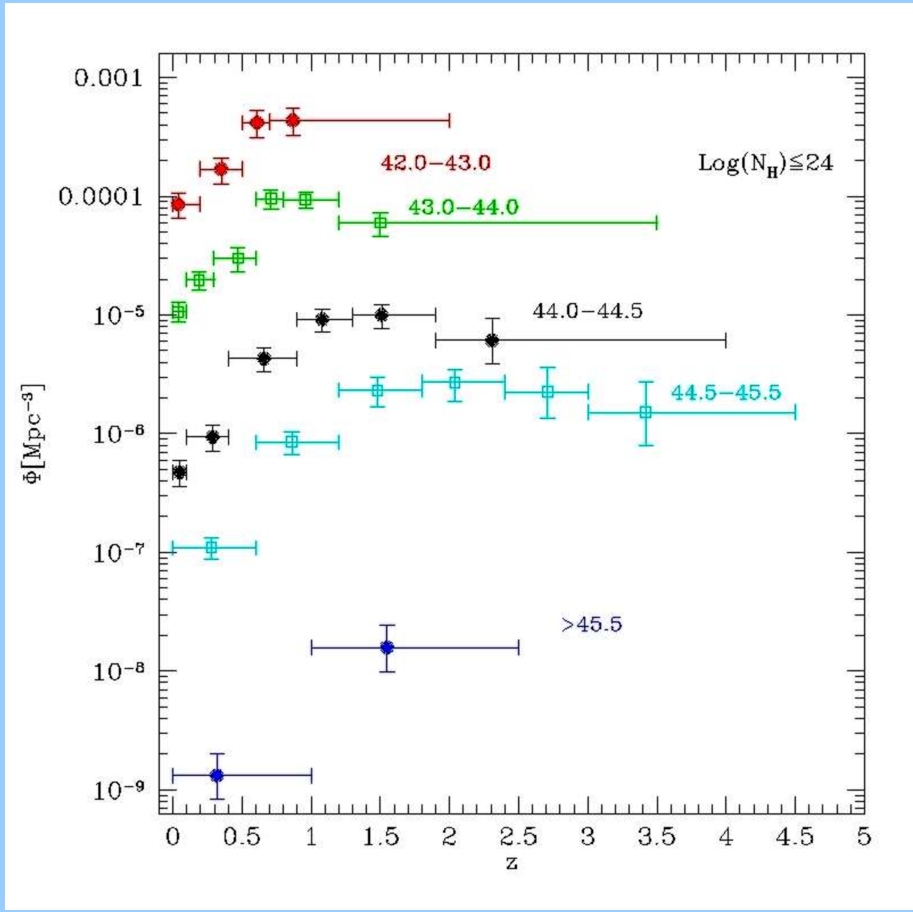

PLE or LDDE?

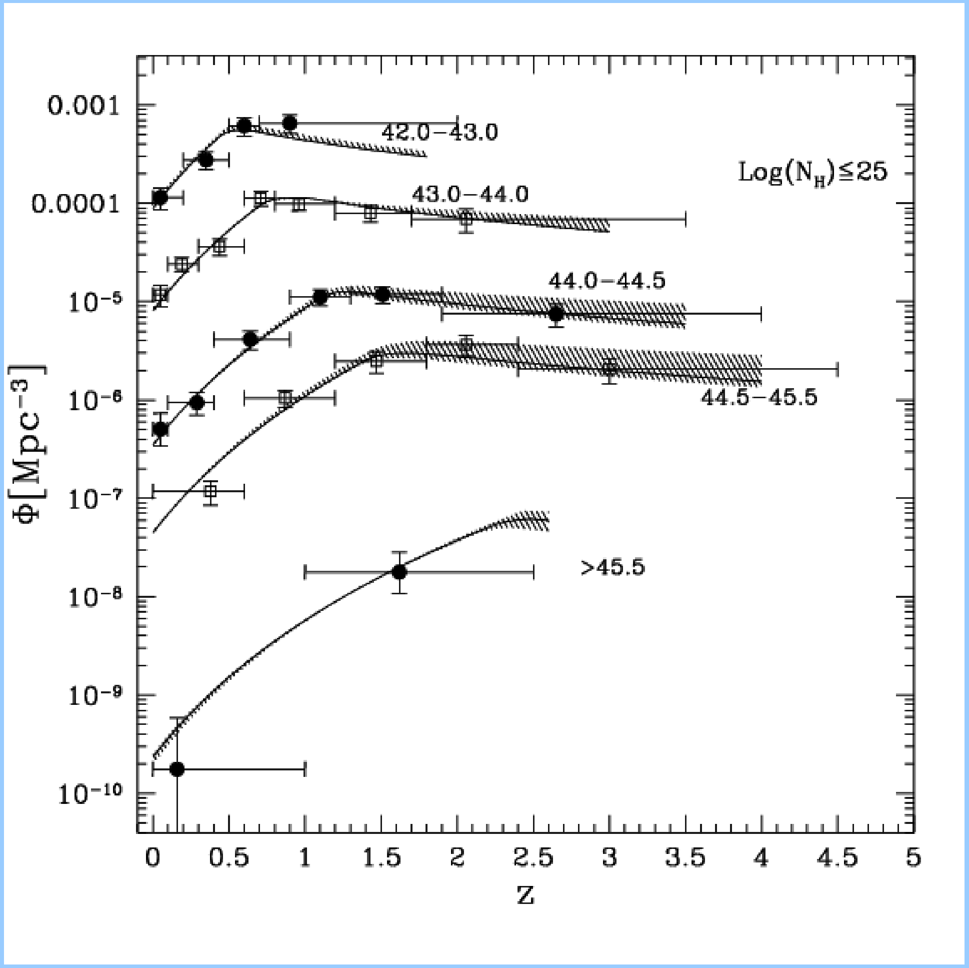

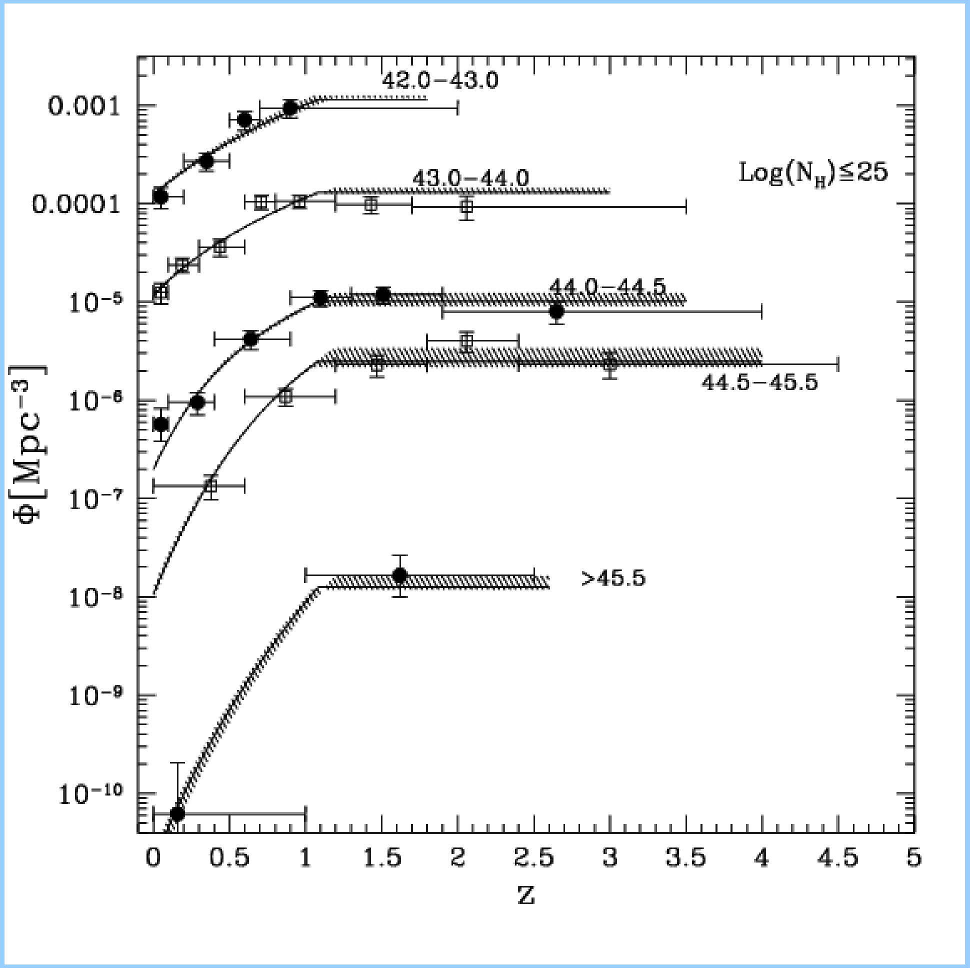

$P(\chi^2)$=20%

$P(\chi^2)$=9% (with z_{cut}=1.1 !!!)
$P(\chi^2)$=0.0001% (with z_{cut}=2.0)

The observed and predicted counts

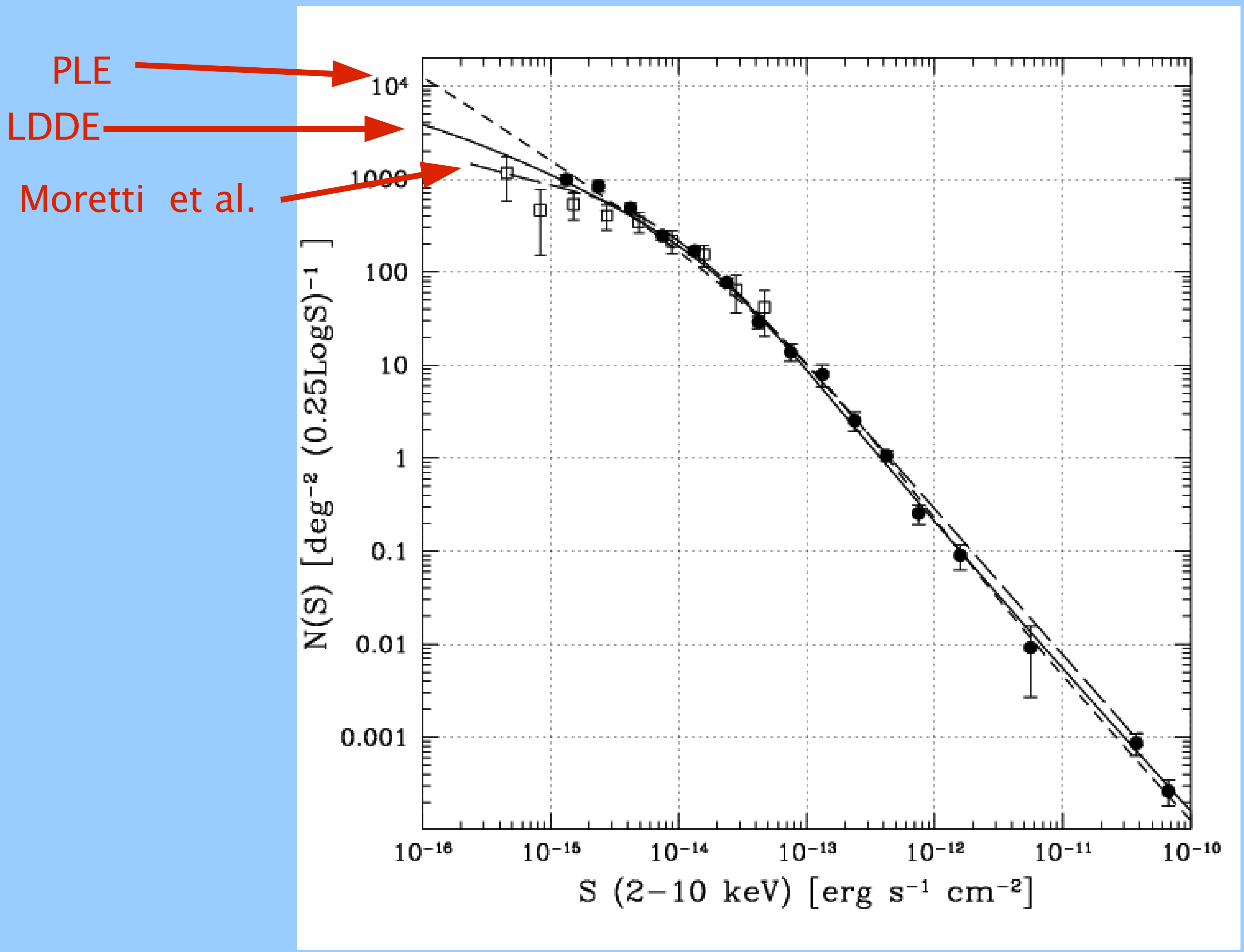

The N_H column density distributions

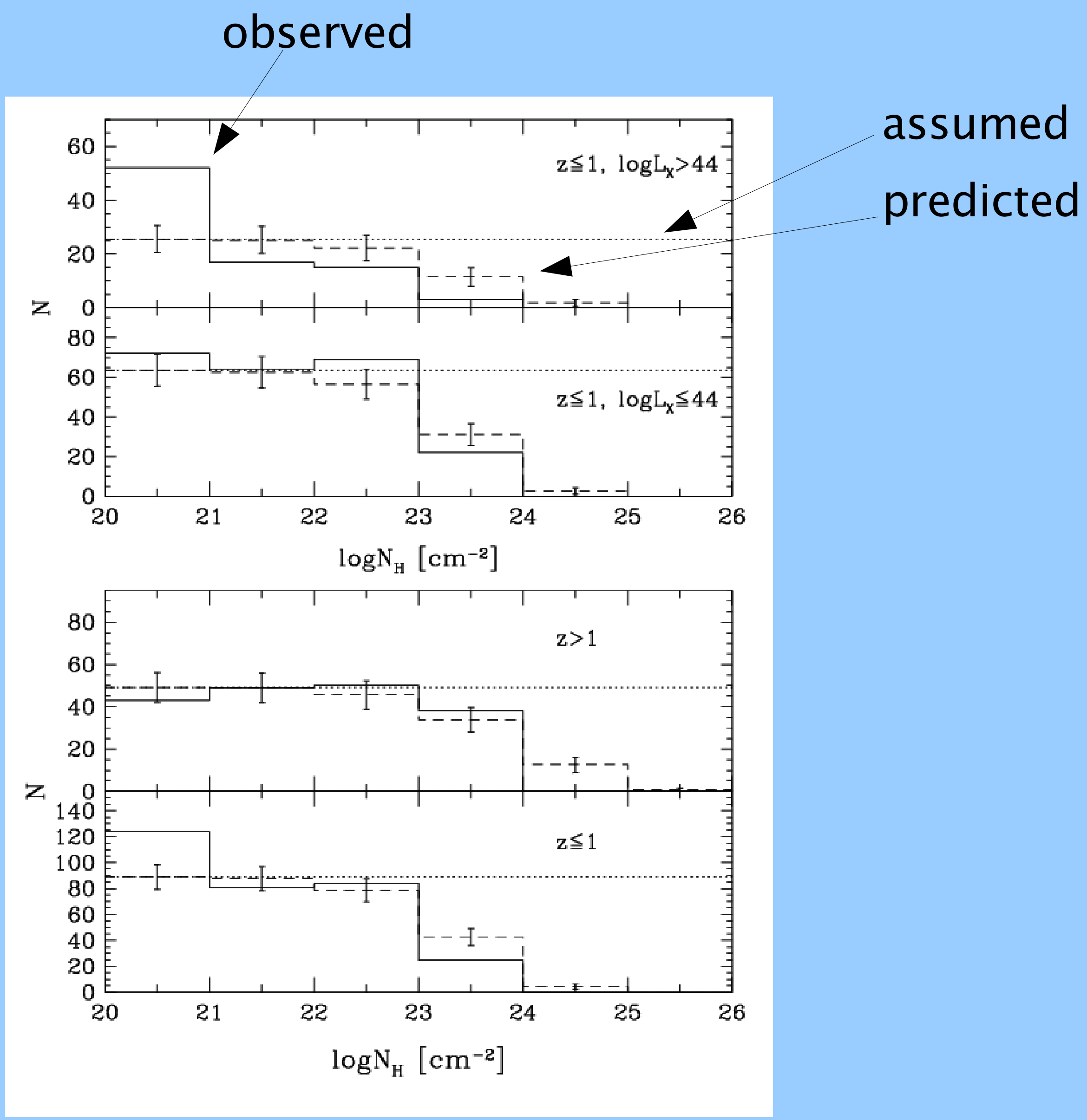

The N_H column density distributions

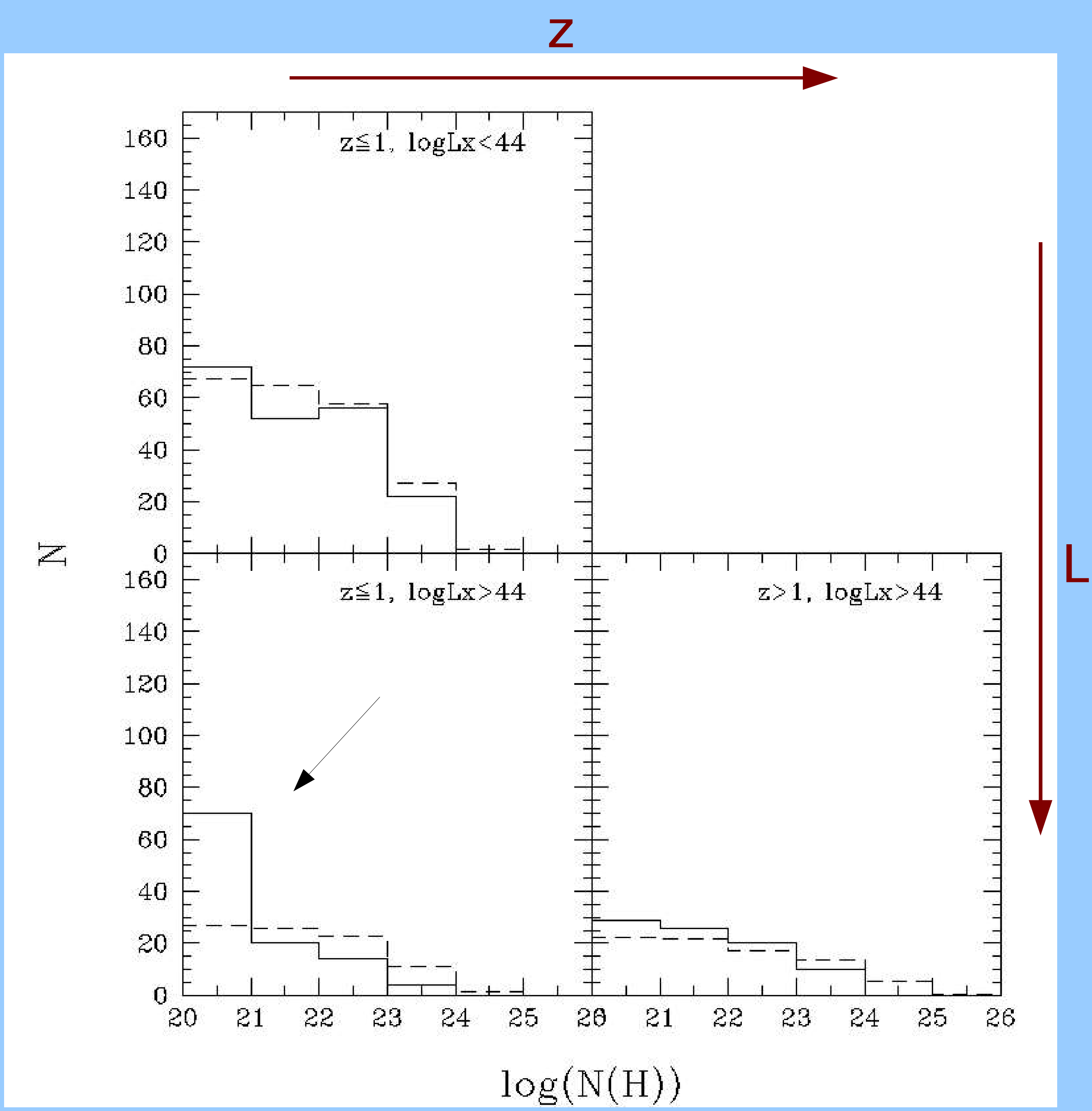

The fraction of absorbed AGN as function of L_X and z

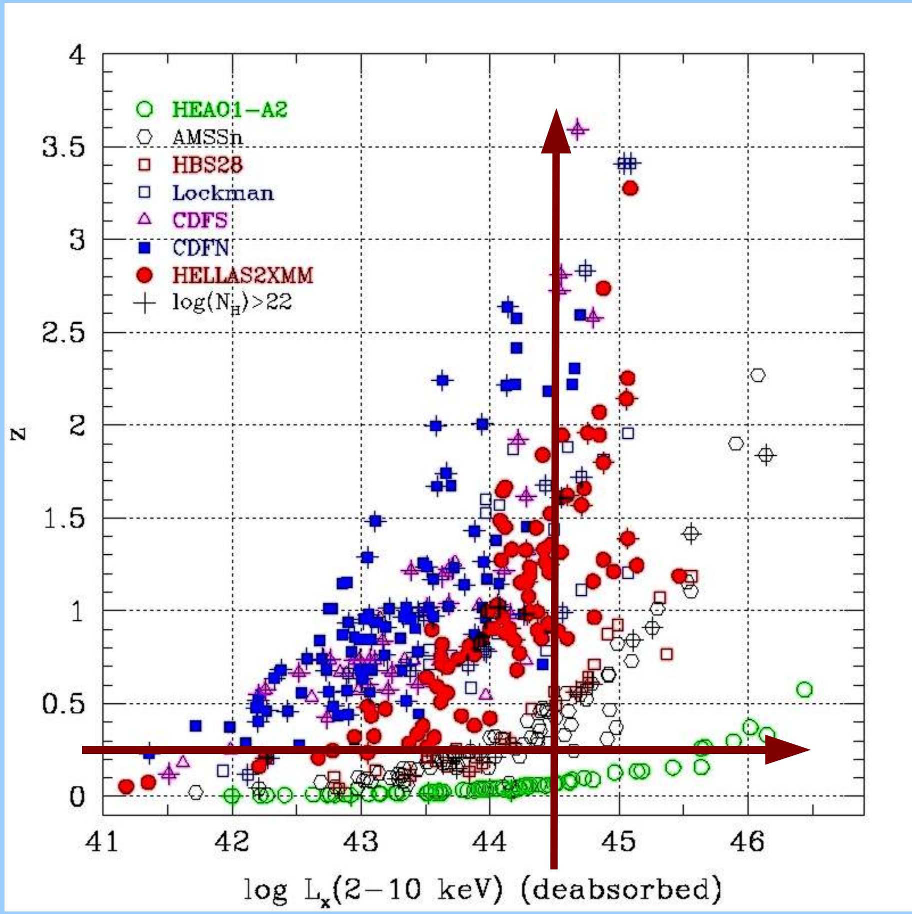

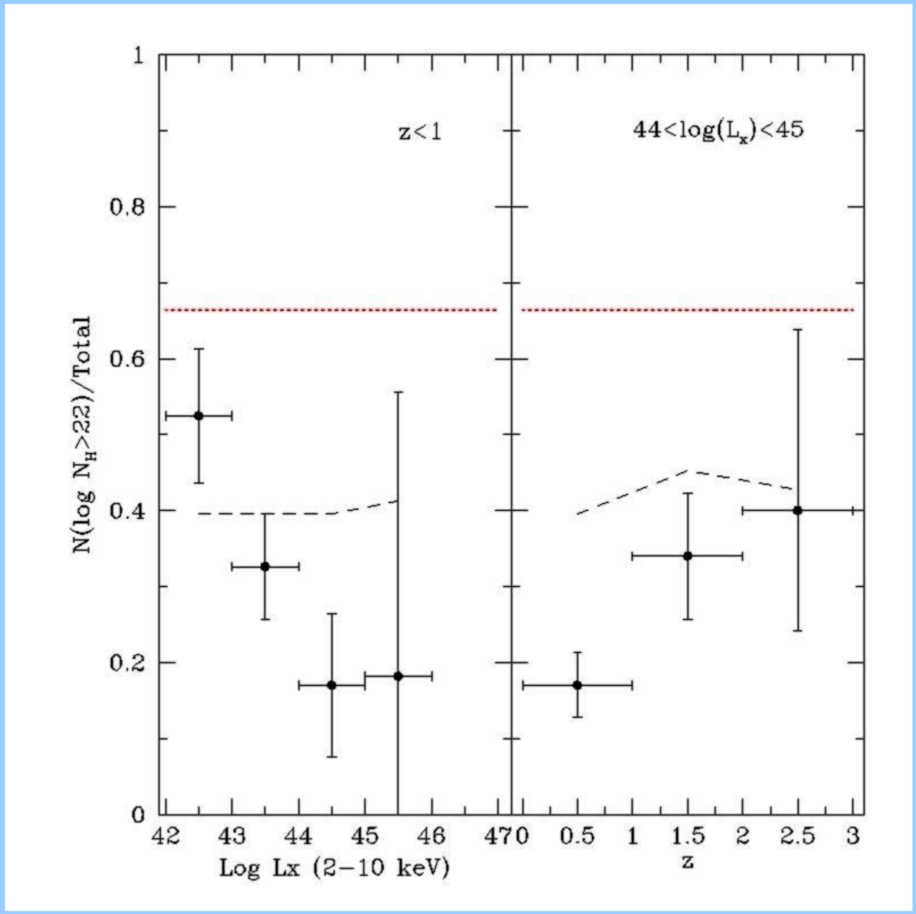

Without luminosity and redshift dependences

The fraction of absorbed AGN as function of L_X and z

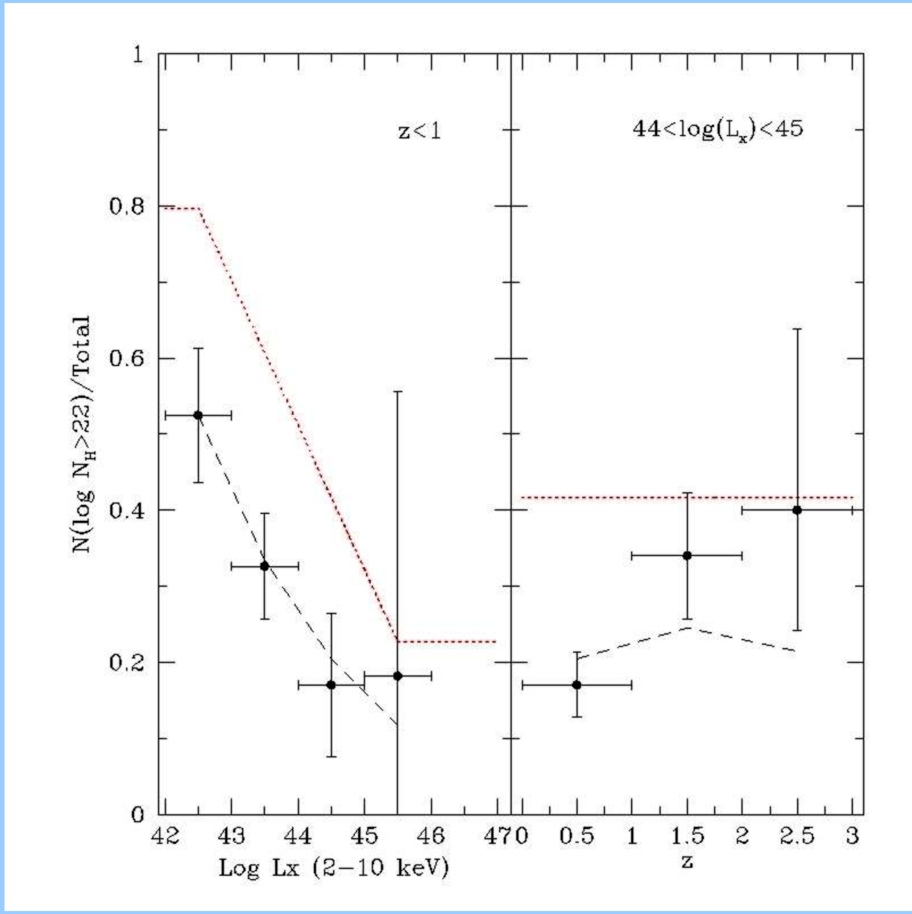

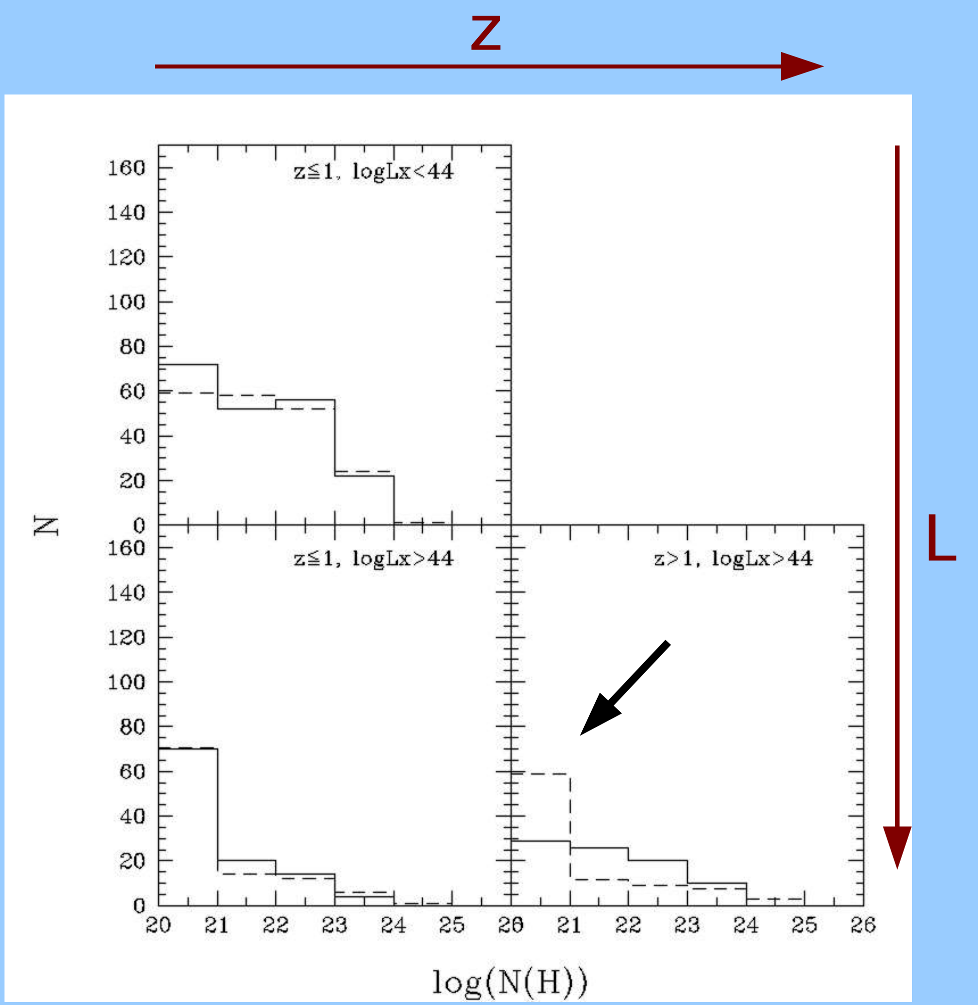

Without z dependence

The fraction of absorbed AGN as function of L_X and z

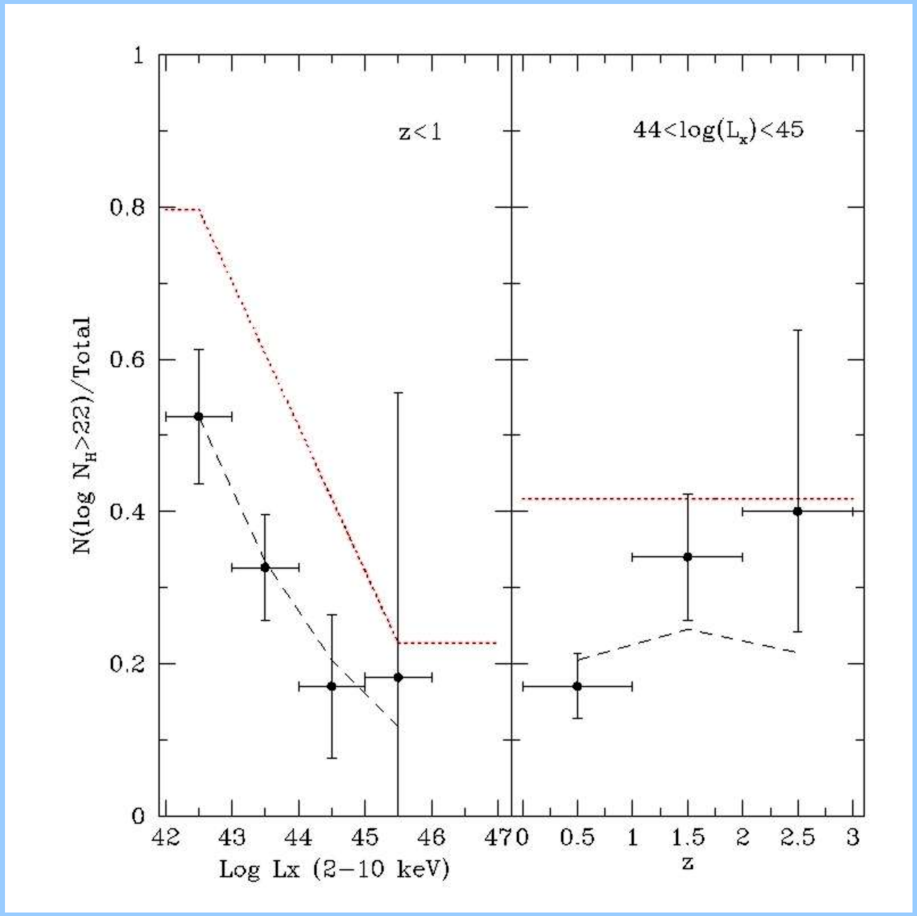

Without z dependence

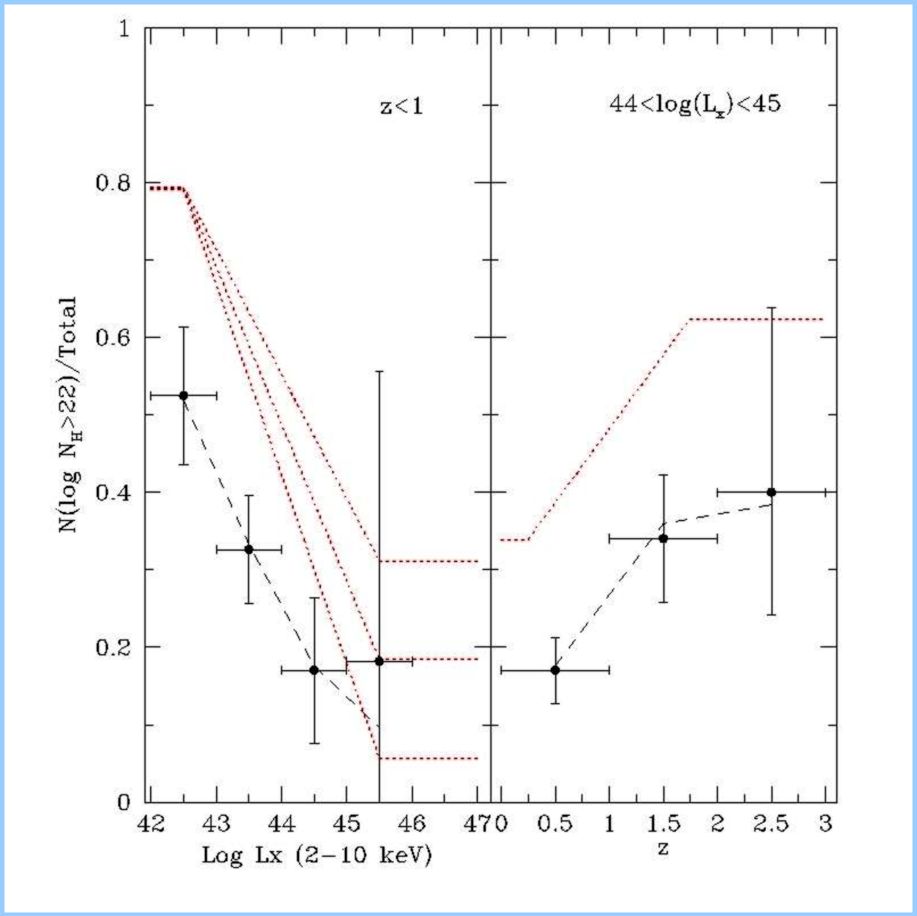

With z dependence

The fraction of absorbed AGN as function of L_X and z

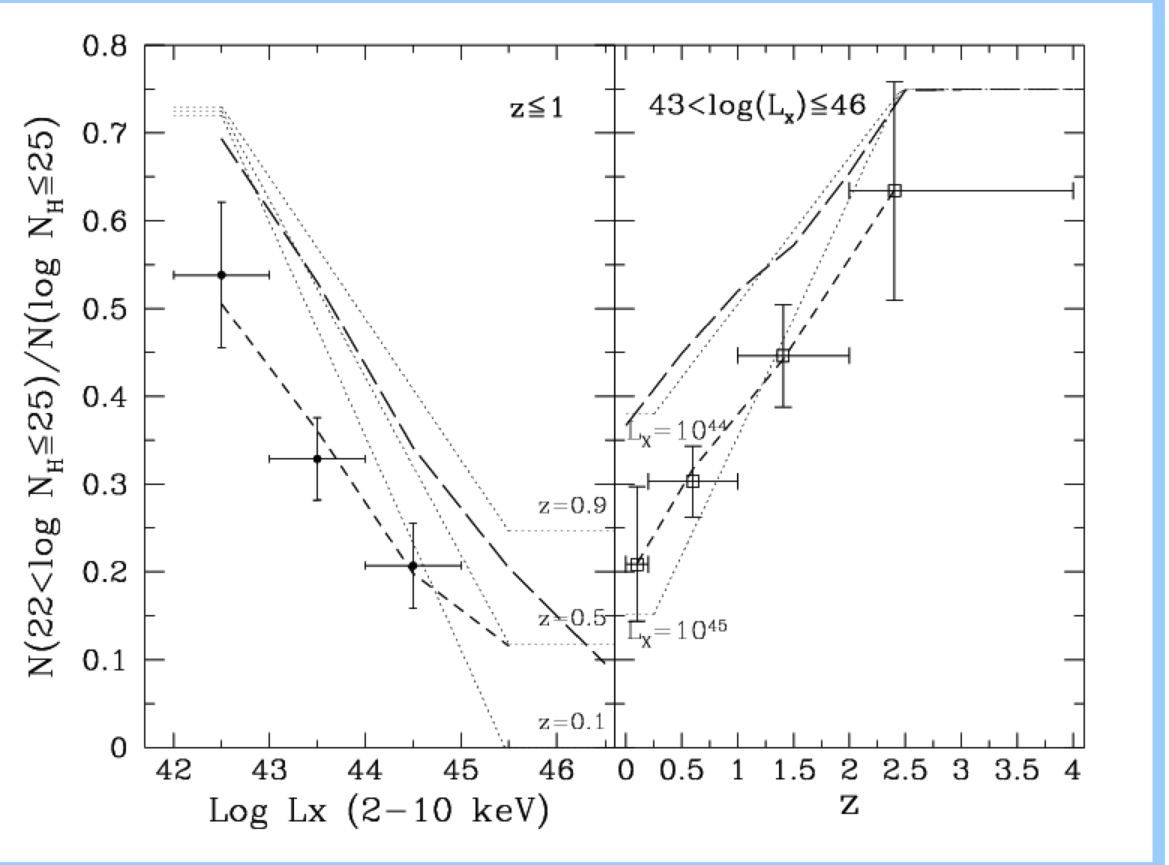

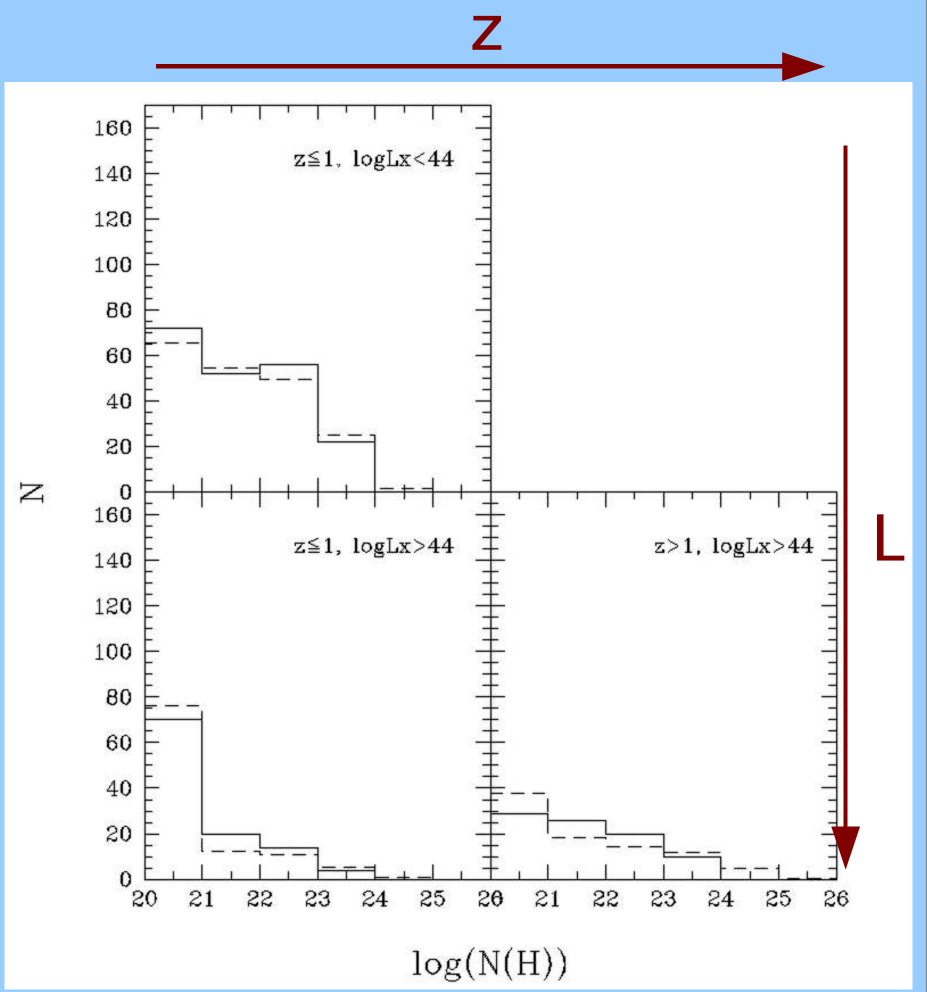

With L and z dependence

Fraction of absorbed AGN as function of z

Using X-ray spectral fits only, from CDFS-H2XMM-HBS28-Lockmann-Piccinotti

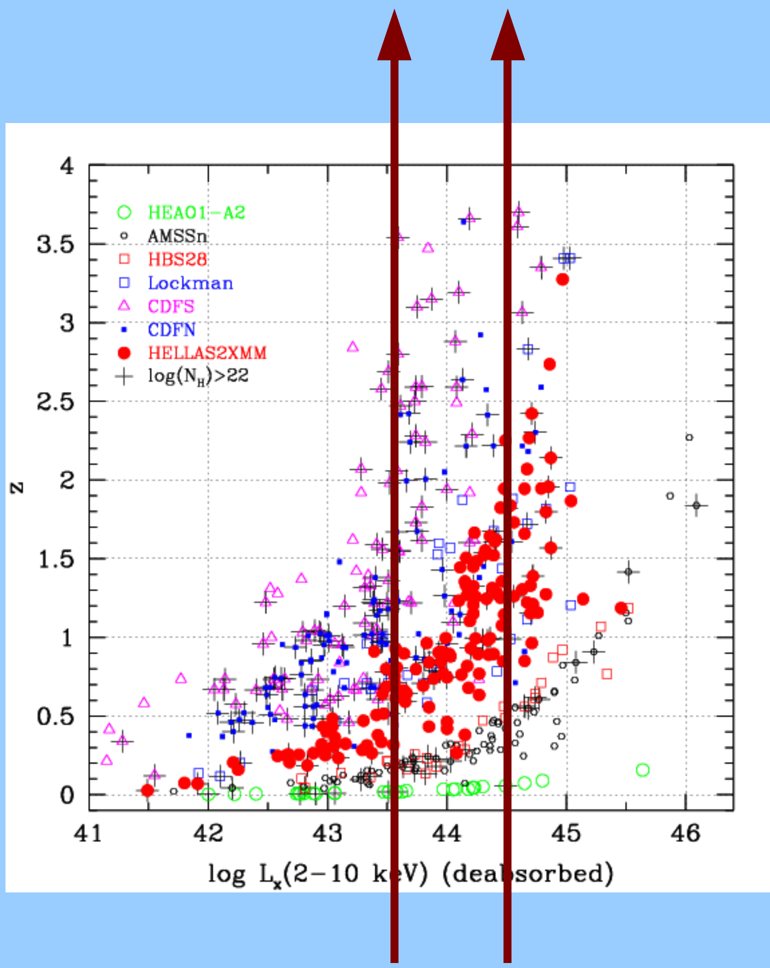

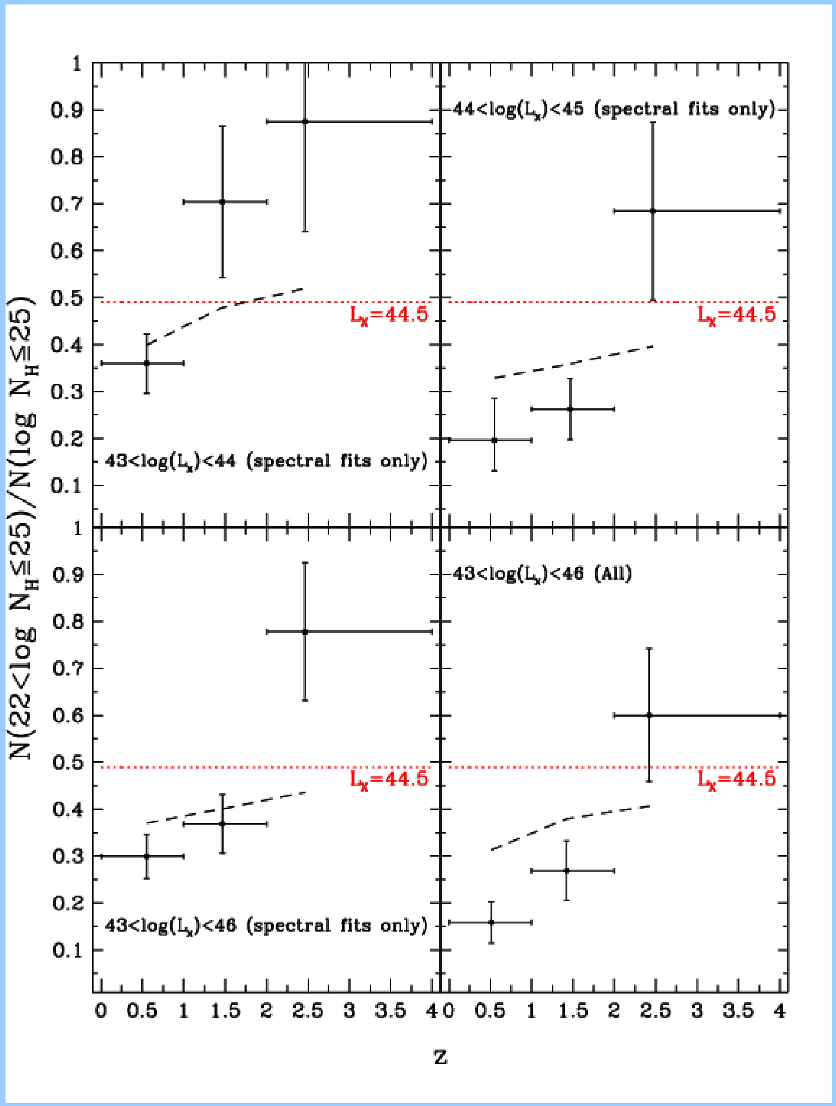

The decrease of absorbed AGN with increasing luminosity

Model 1

The Receding Torus Model: the opening angle of the torus increases with ionising luminosity (Simpson 1998; Lawrence 1991; Grimes et al. 2003)

Model 2

The gravitational effects of the BH on the molecular gas disk of galaxies

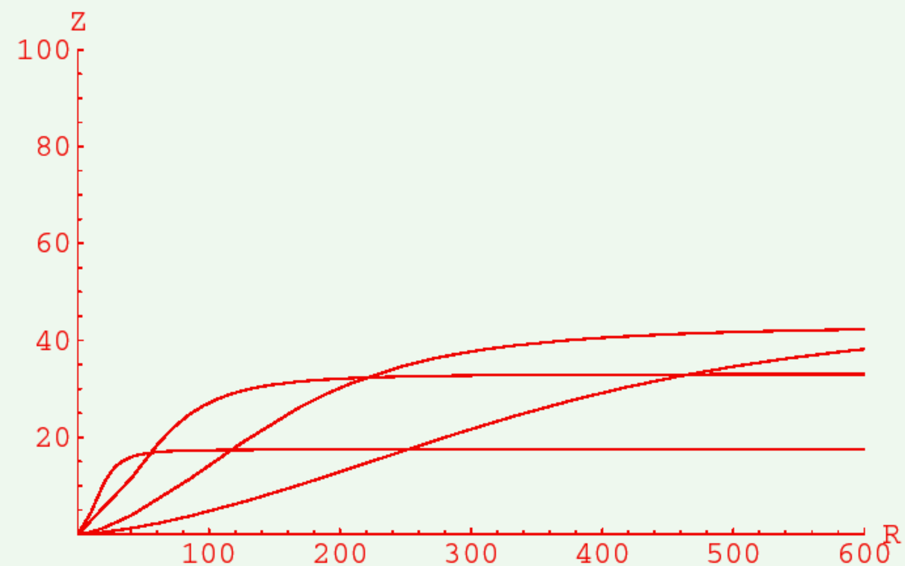

Fig. 2. Scale height of the clouds as a function of R when M_{BH} = $10^6\ M_\odot$, $10^7\ M_\odot$, $10^8\ M_\odot$ and $10^9\ M_\odot$.

Lamastra, Perola & Matt (2006)

The fraction of absorbed AGN as a function of flux

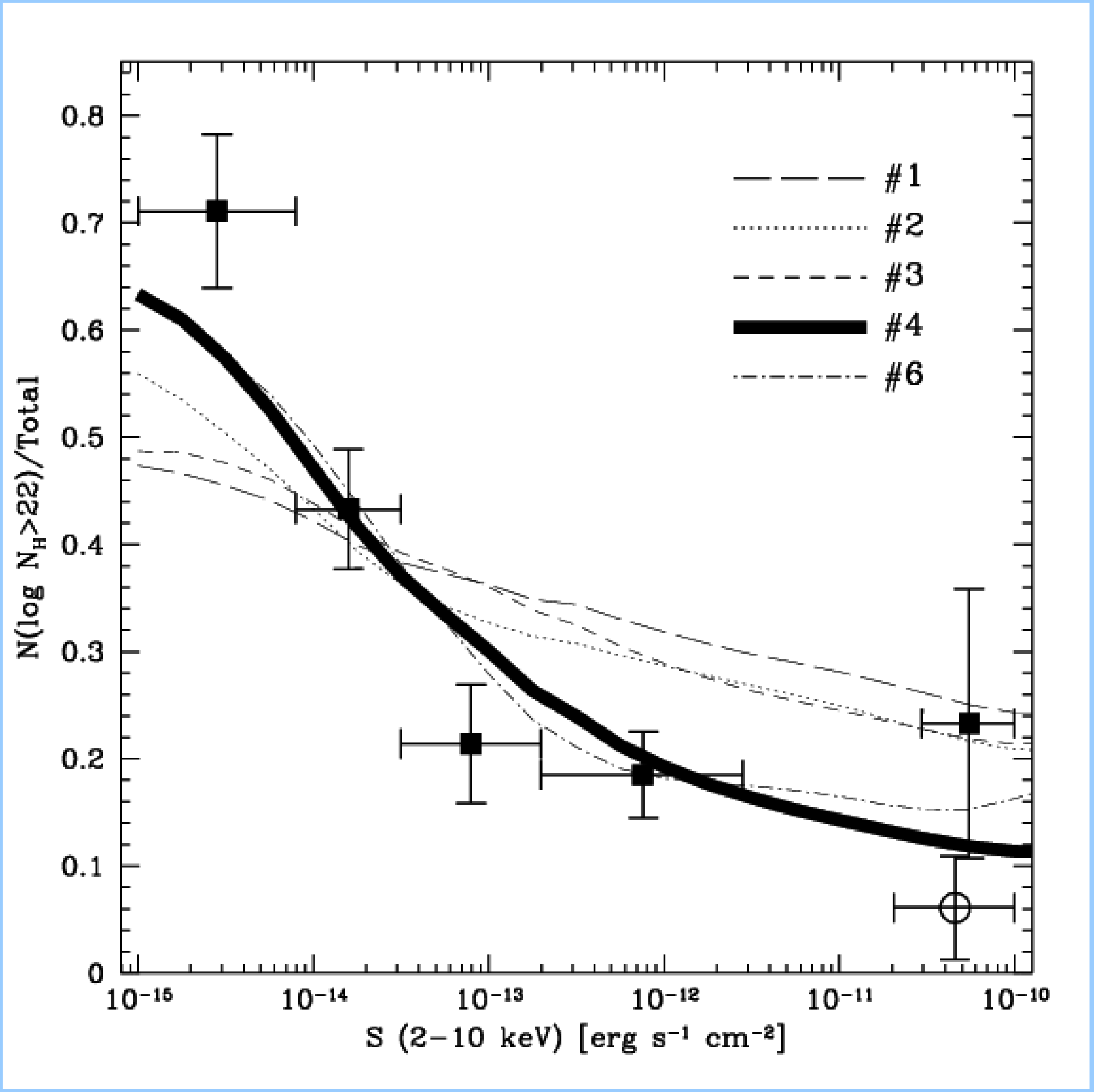

The observed and predicted counts

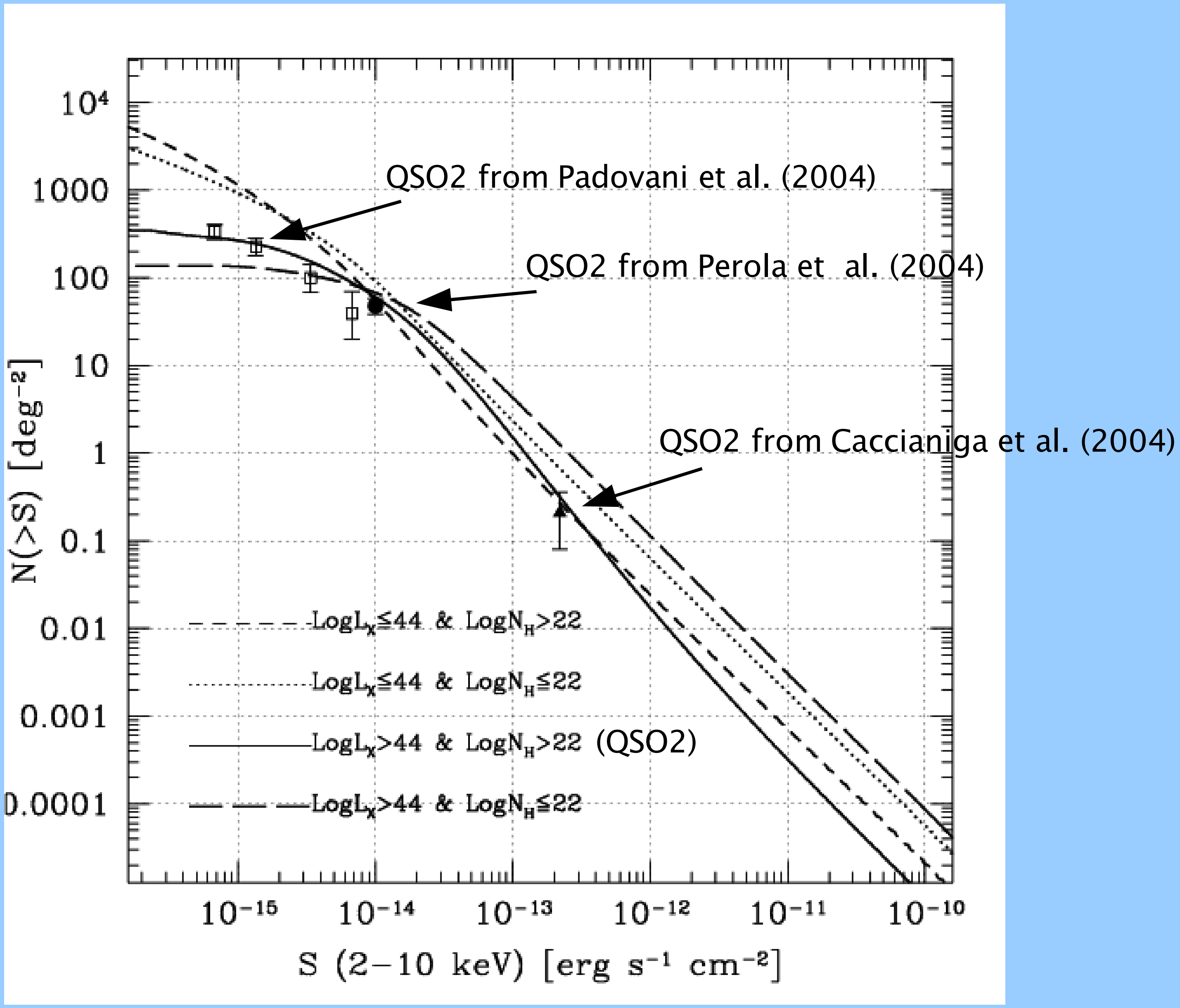

The synthesis of the X-ray background

We reproduce 92% of the 2-10 keV XRB as estimated by Revnivtsev et al. (2005) and 108% of the original HEAO1 A2 measure.

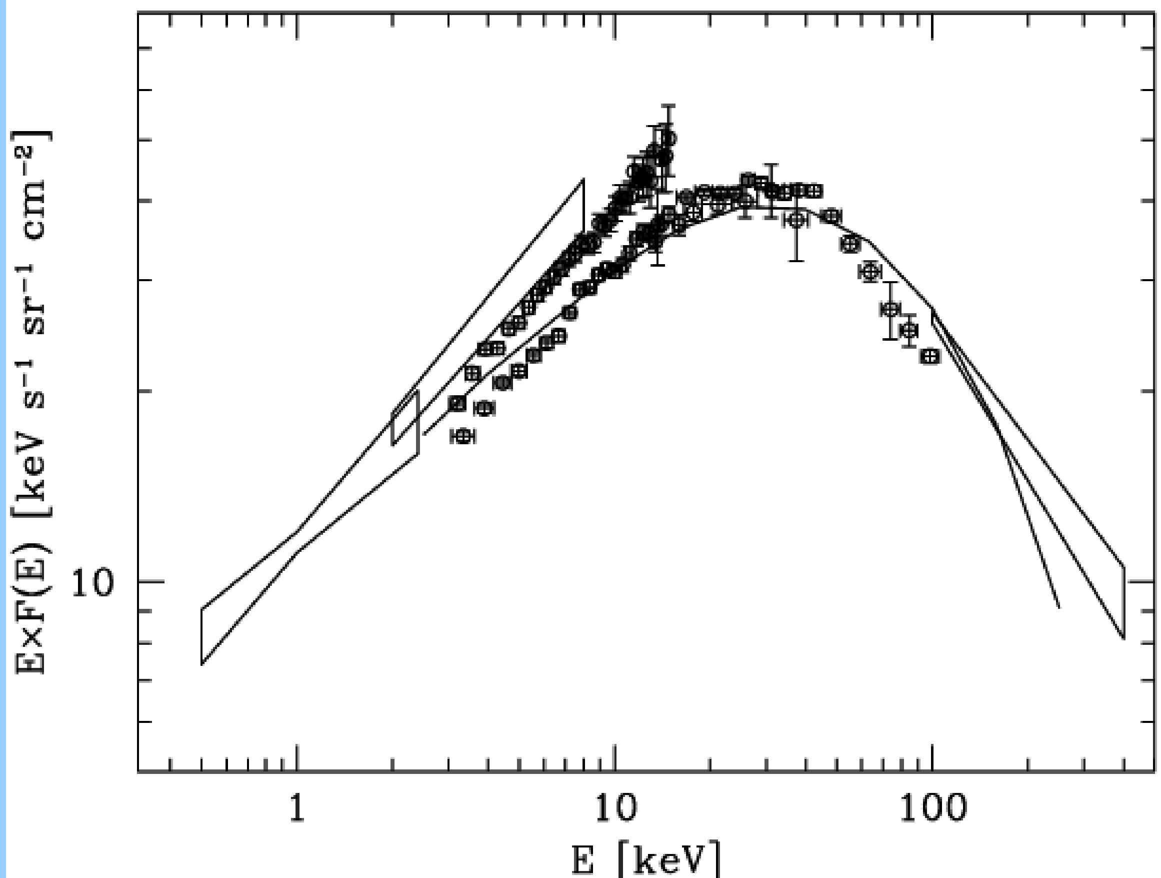

The evolution of absorbed and un-absorbed AGN

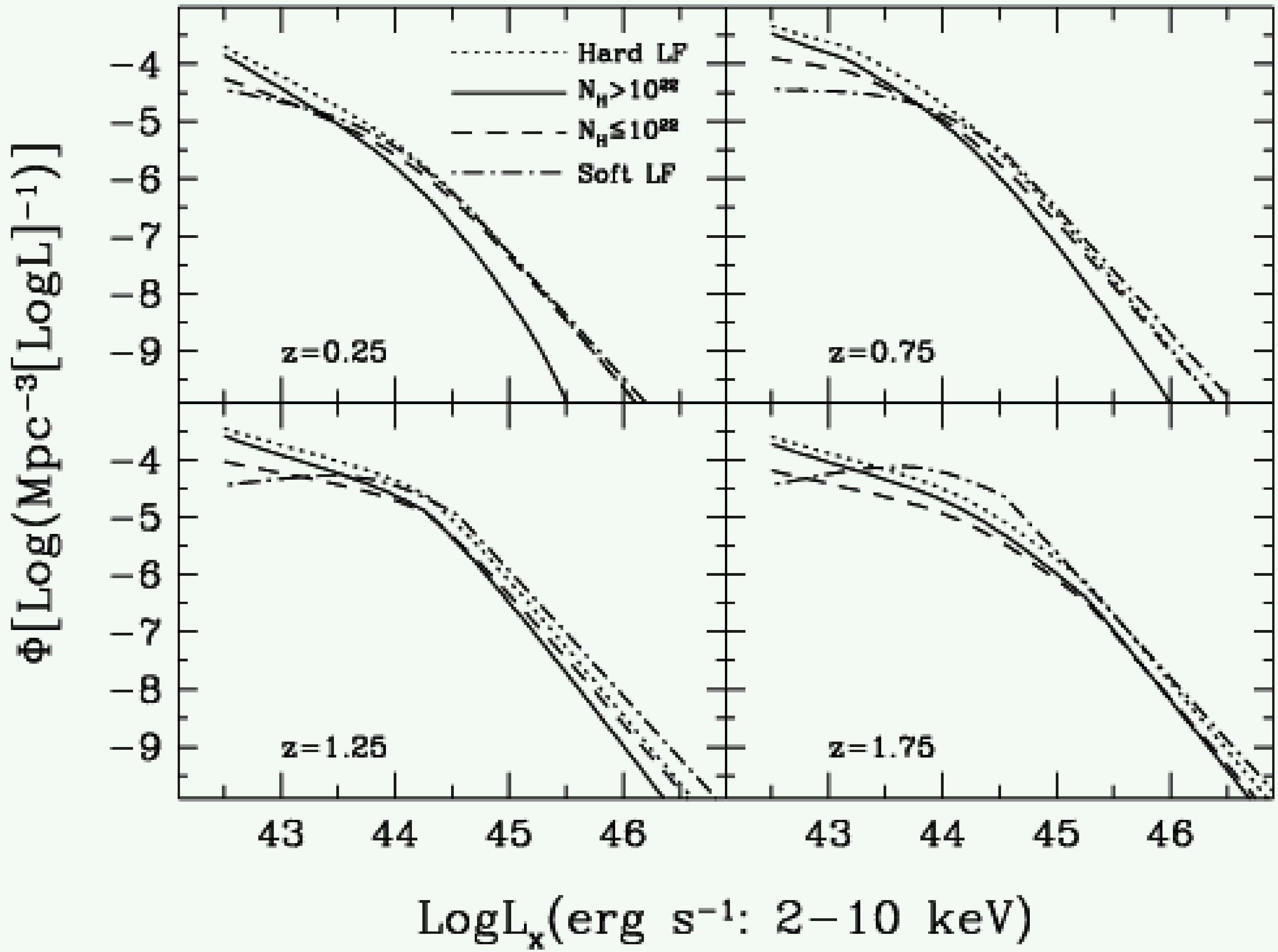

AGN1

righe : larghe+strette

non assorbito in X

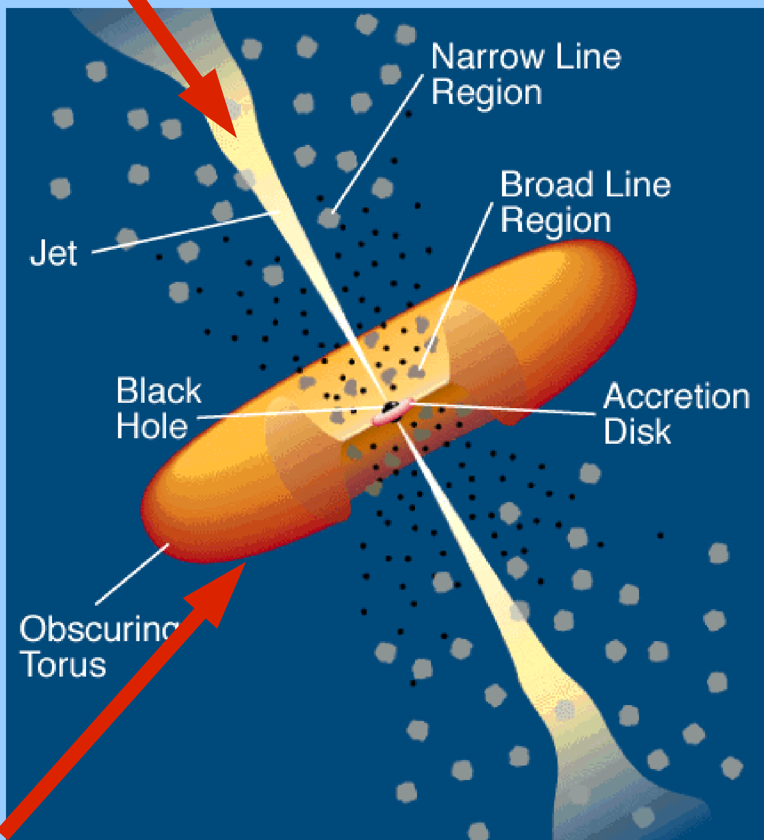

AGN2

righe : strette

assorbito in X

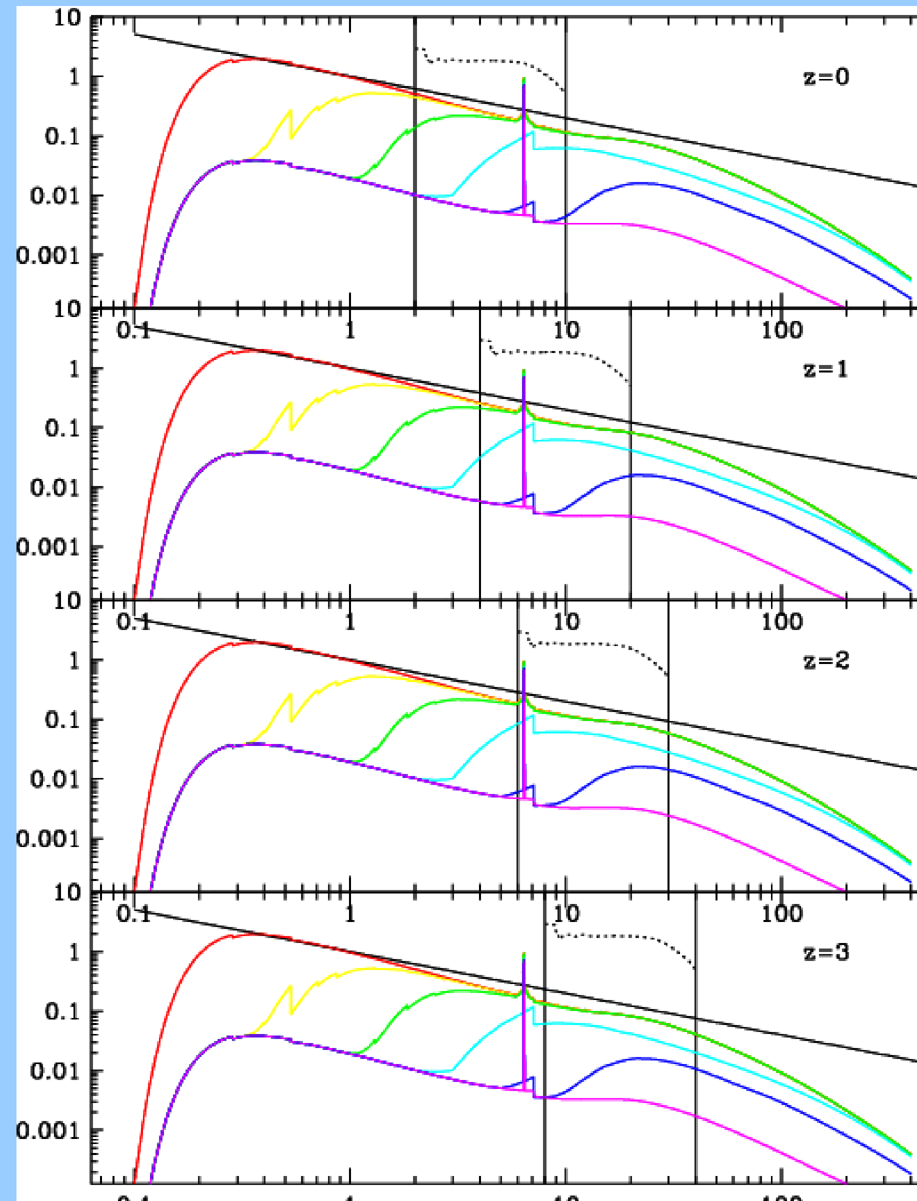

keV

The separate evolution of AGN1 and AGN2

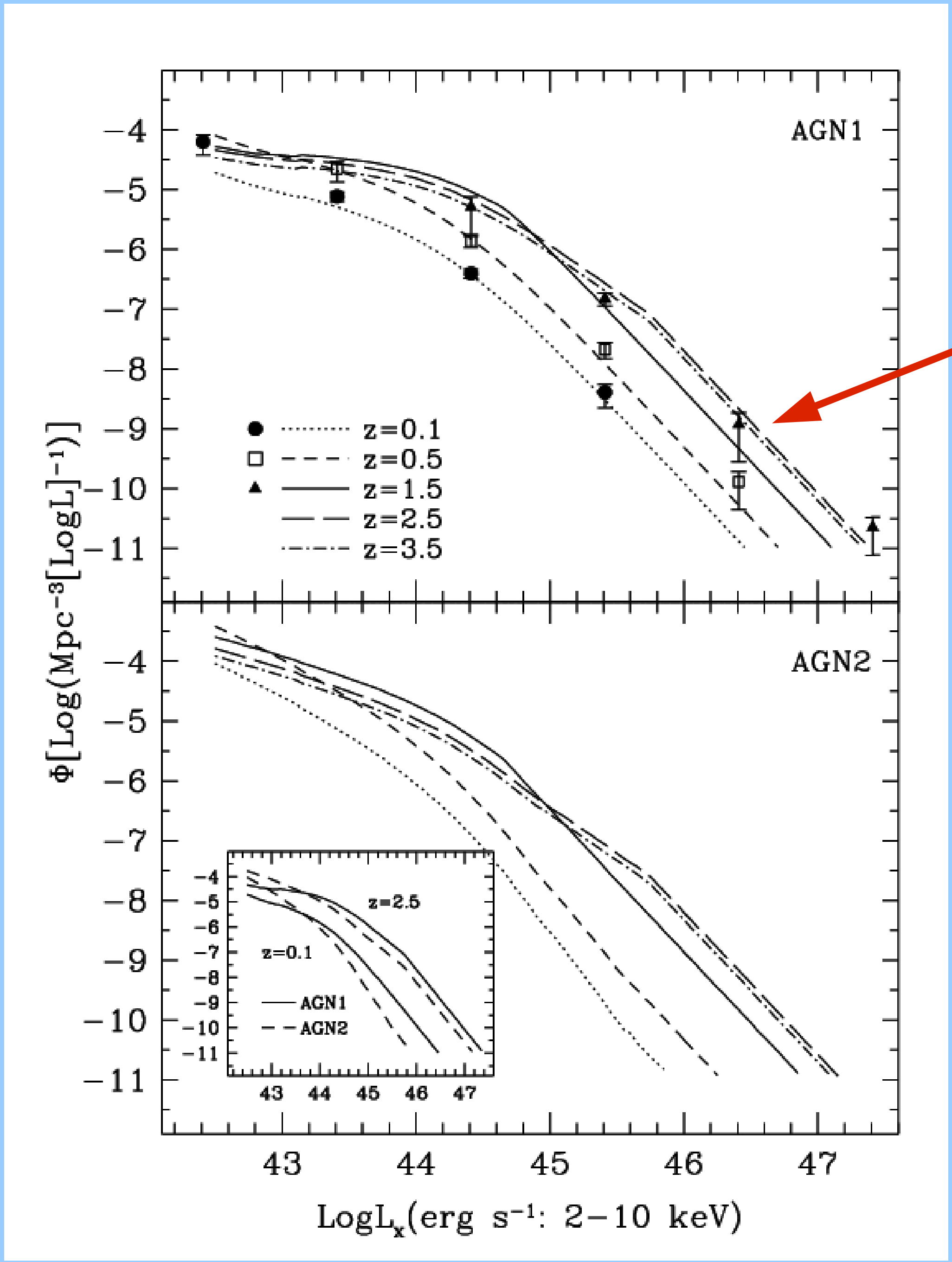

LF, Fiore, Vignali et al. 02
(BeppoSAX + other data)

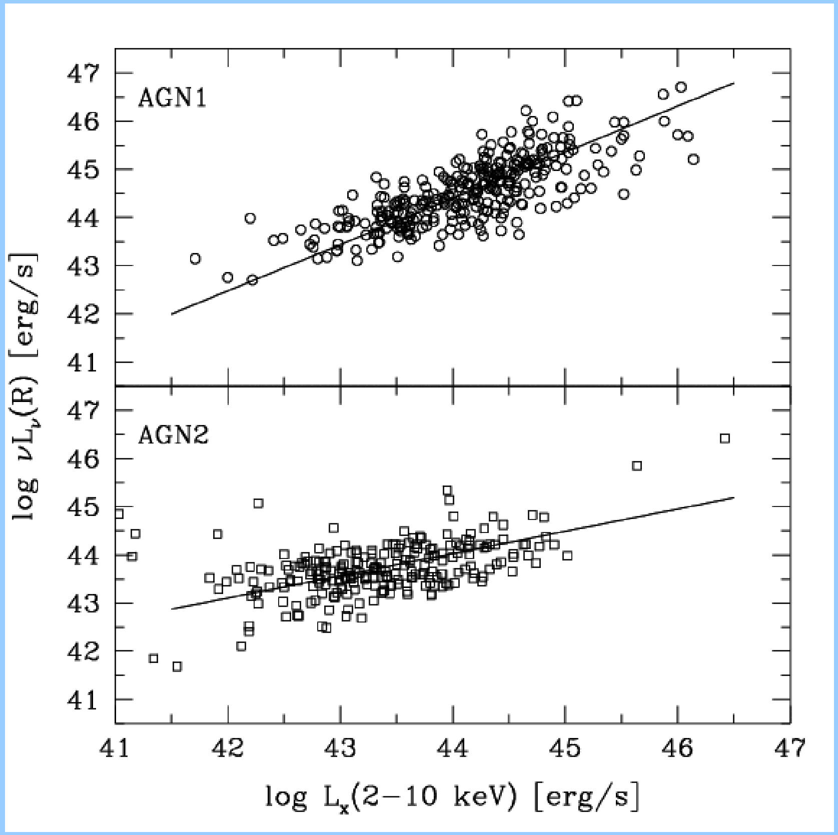

Accretion history of the Universe

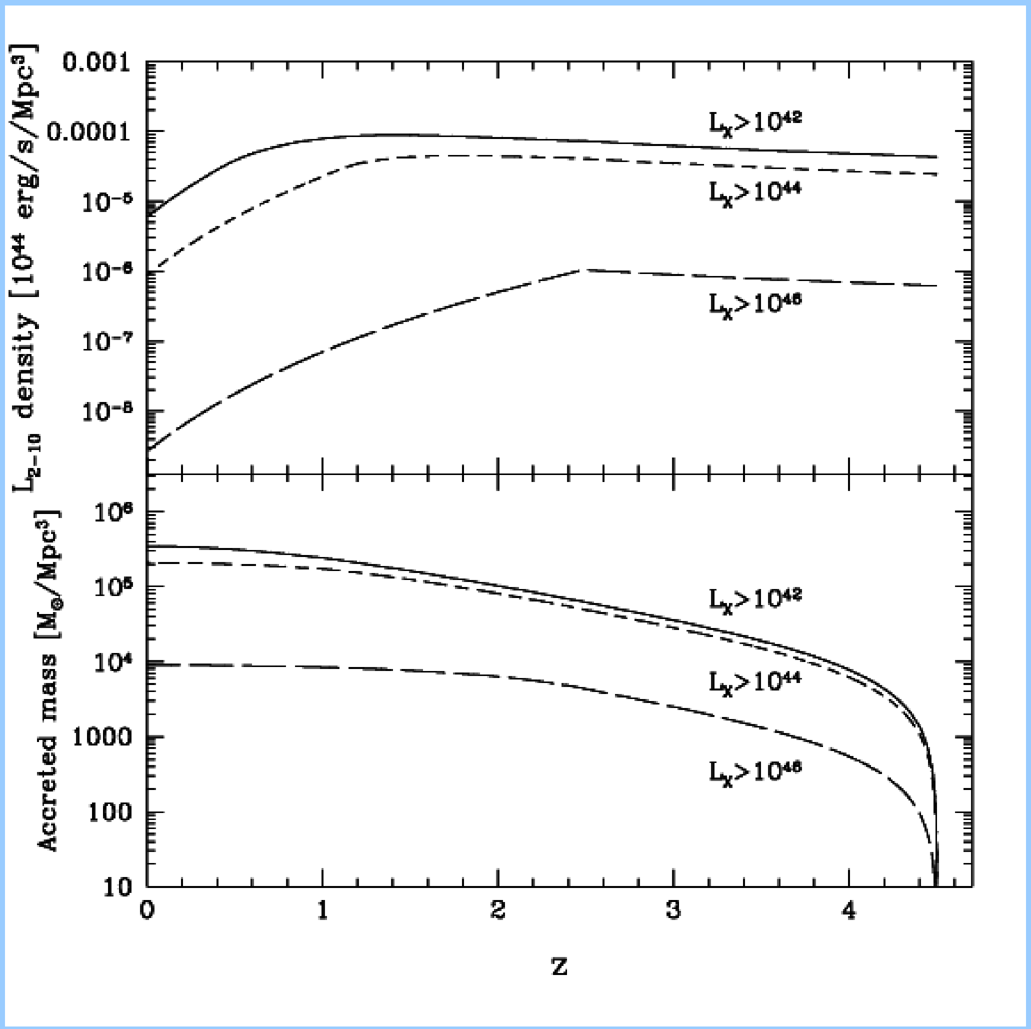

Luminosity density

$$\int L_X \Phi(L_X, z)\, d\log L_X.$$

Accretion rate density

$$\dot{\rho}_{BH}(z) = \frac{1-\epsilon}{\epsilon c^2} \int K\, L_X \Phi(L_X, z)\, d\log L_X,$$

Mass density in BH

$$\rho_{BH}(z) = \int_z^{z_s} \dot{\rho}_{BH}(z)\, \frac{dt}{dz}\, dz.$$

$$\rho_{BH} = 3.2\, h_{70}^2 \times 10^5\, M_\odot\, \mathrm{Mpc}^{-3}$$

Marconi et al. (2004): 4.6 (+1.9;-1.4) $M_\odot$ Mpc^{-3}

McLure & Dunlop (2004): 2.8 (+/- 0.4) $M_\odot$ Mpc^{-3}

·Seguendo il modello di Cavaliere e Vittorini (00), Menci et al. (04) hanno sviluppato un modello gerarchico semianalitico di formazione delle galassie connesso con l'accrescimento sui BH. L'accrescimento e` innescato dagli incontri (non necessariamente mergers) fra le galassie.

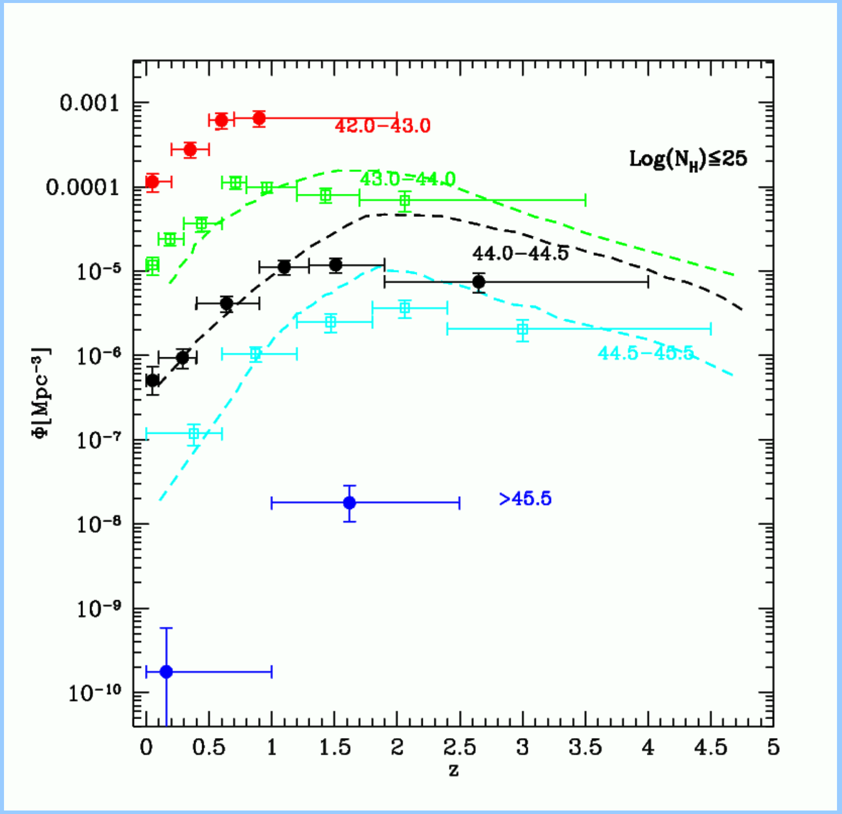

Confronto fra la HXLF di La Franca et al. (05) e le predizioni di Menci et al. (04)

Conclusions I

- LDDE model better reproduces the data

-The LDDE is more probable and better reproduces the high z decline of the density of AGNs and the faint counts

-It is observed an increase of the fraction of absorbed AGN at lower luminosities and higher redshifts

-The fitting model fully reproduces the counts, the XRB and the observed fraction of absorbed AGN as a function of flux.

The ELAIS-S MIR (15 μm) survey

The Mid-Infrared View on the Evolution of AGN ***and Starburst Galaxies***

Fabio La Franca
Dipartimento di Fisica
Universita' degli Studi Roma Tre

ELAIS-S people

- Matute, Israel (MPE Garching)
- Gruppioni, Carlotta (INAF- OA Bologna)
- Lari, Carlo (CNR Bologna)
- Pozzi, Francesca (INAF-OA Bologna)
-
- Alexander, D.M. (IoA Cambridge)
- Ciliegi, P. (INAF-OA Bologna)
- Danese, L. (SISSA Trieste)
- Franceschini, A. (Univ. Padova)
- Mignoli, M. (INAF-OA Bologna)
- Oliver, S. (Univ. Sussex)
- Rowan-Robinson, M. (IC London)
- Serjeant, S. (Univ. Kent)
- Vaccari, M. (Univ. Padova)
- Zamorani, G. (INAF-OA Bologna)
-
- plus the ELAIS consortium

The ELAIS Survey

- ELAIS was the largest Open Time Project conducted by ISO
- The ELAIS* survey covered ~12 deg^2 *(Oliver et al. 2000; Rowan-Robinson et al. 2003)*
- The entire area has been surveyed at 15 µm (CAM) and 90 µm (PHOT). 7 deg^2 also at 6.7 and 175 µm.
- Four main areas: three in the north (N1,N2,N3) and one in the south (*S1*) + some smaller areas (e.g. S2...)

Here we present the results from the southern fields: S1 and S2

*) ELAIS: http://astro.imperial.ac.uk/elais/

IR Integrated Counts at 15 μm

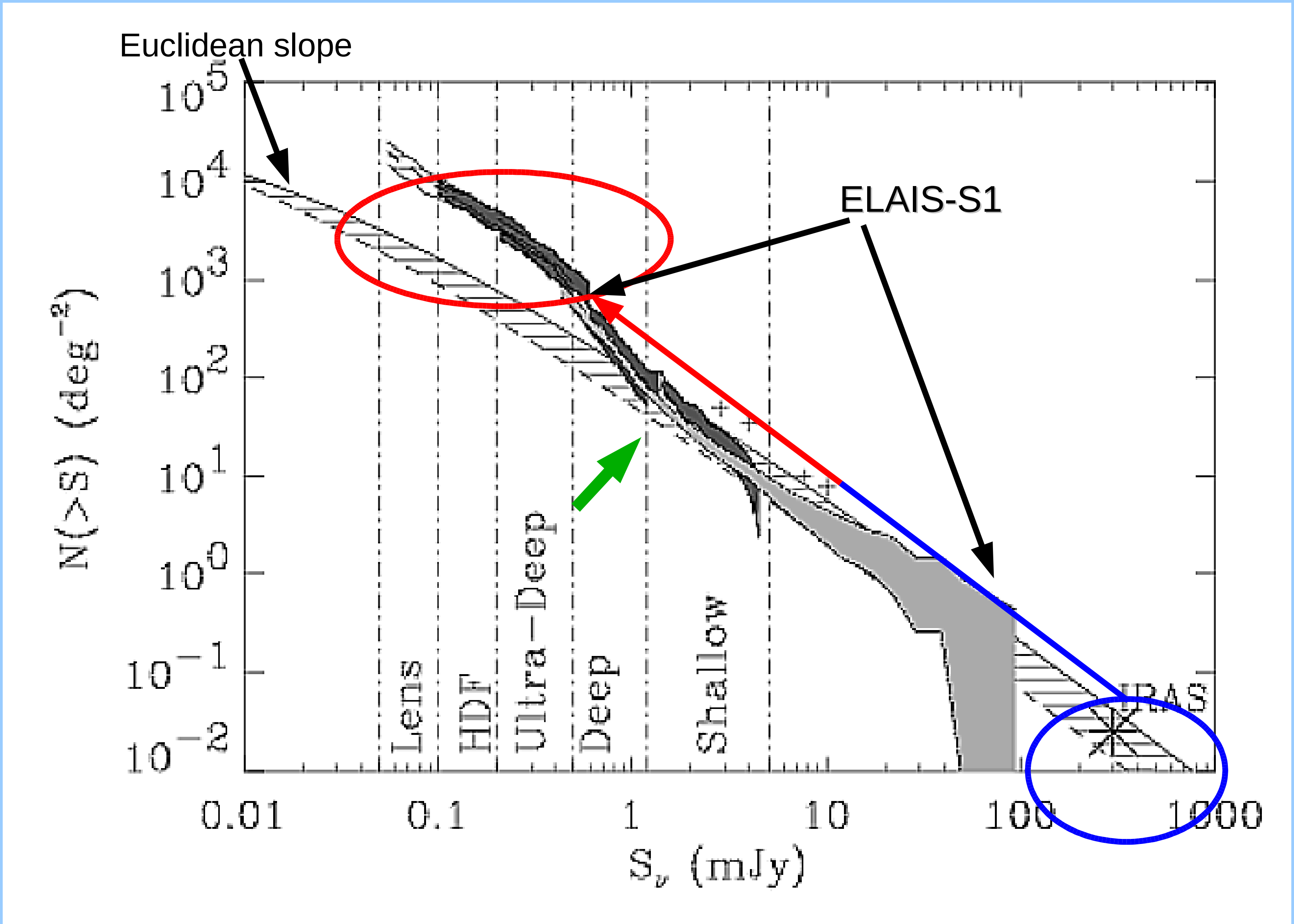

Gruppioni et al. 2002, MNRAS, 335, 831

Mid-IR SURVEYS (ISOCAM 15 μm)

Field	Type	Area (arcmin^2)	Flux (mJy)	# Obj
A2390	UD	5.3	$0.05<f<0.20$	31
HDF-S	UD	28	$0.1<f<0.3$	63
HDF-N	UD	27	$0.1<f<0.3$	44
MFB-UD	UD	90	$0.2<f<1.0$	100
MF	UD	70	$0.2<f<1.0$	82
MFB-D	D	710	$0.4<f<1.5$	144
LHD	D	510	$0.6<f<1.5$	70
LHS	S	1944	$1.0<f<5.0$	80
ELAIS-S1	S	14400	$0.5<f<150$	406

ELAIS-S1: the Final IR Catalog

- $\alpha(2000) = 00^h\, 34^m\, 44^s$
  $\delta(2000) = -43^o\, 28'\, 12''$
- 9 rasters for a total of 4 deg²
- 406 sources at 15 µm extracted with the 'Lari technique' :
  - 0.45 < flux < 100 mJy
  - S/N >5

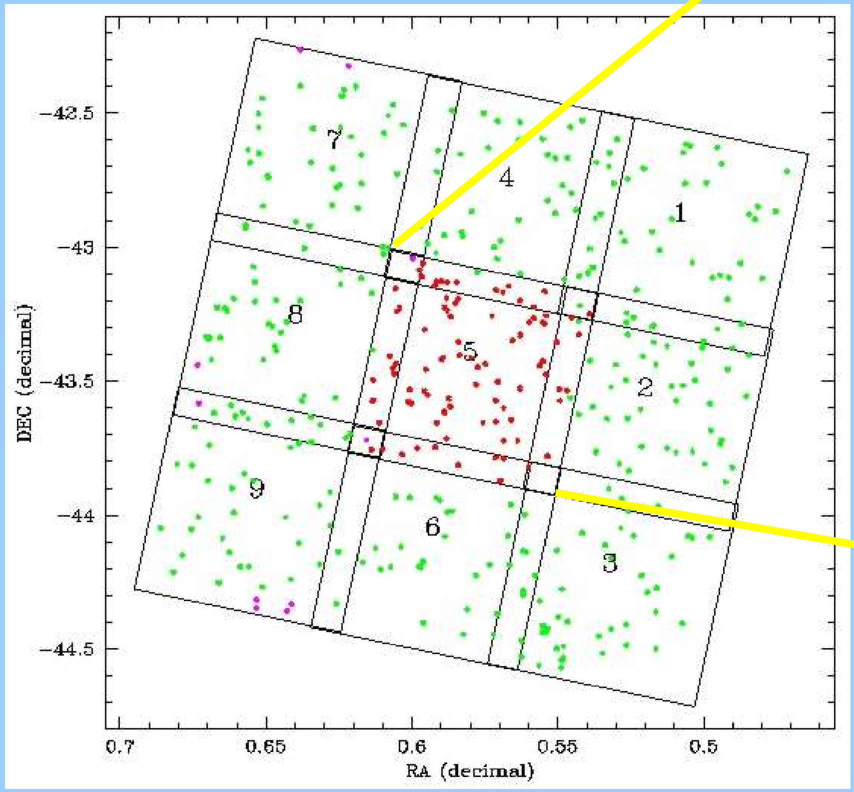

Fainter sources detected in S1_5 (~0.5 deg²) which was observed 3 times

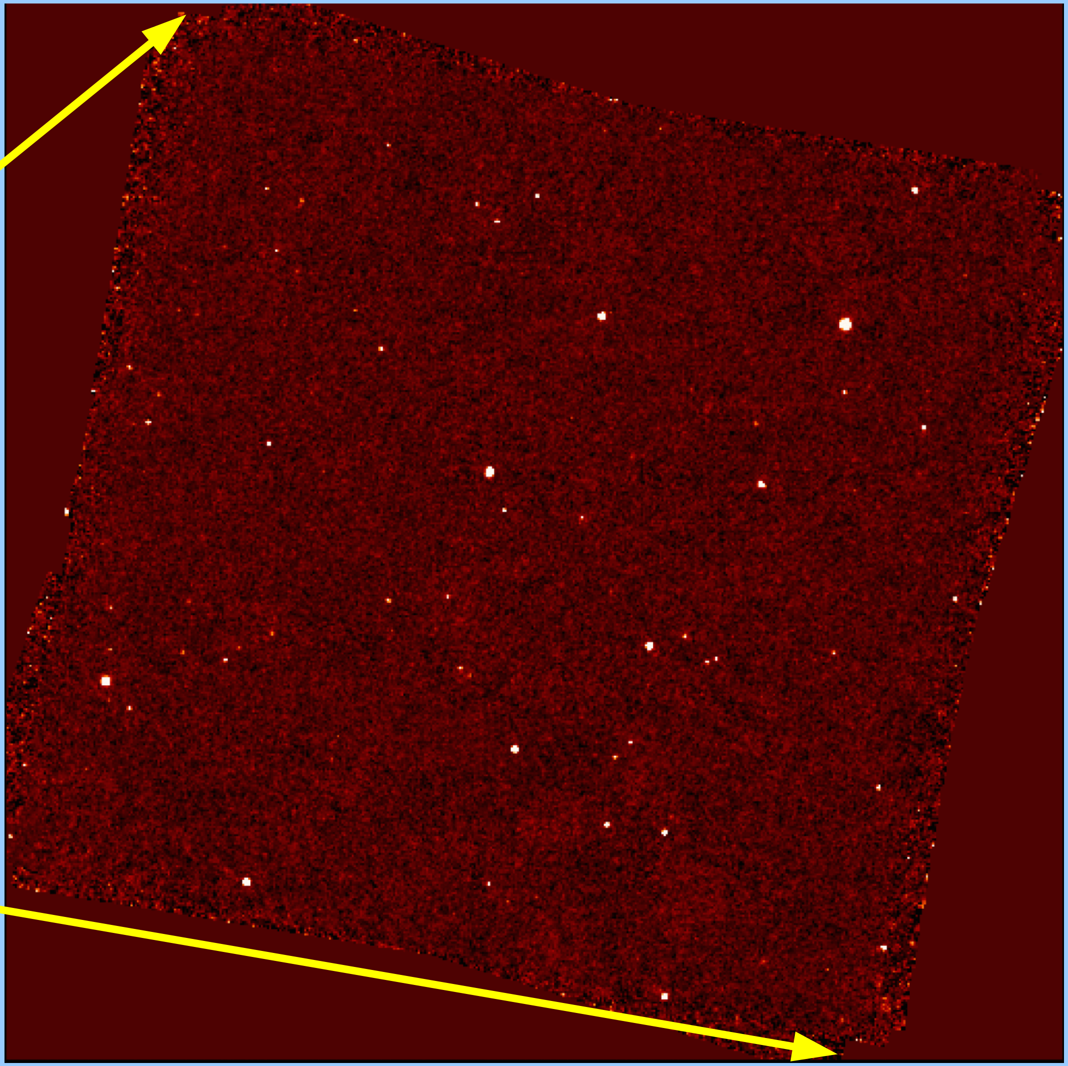

Lari, C. et al, 2001, MNRAS, 325, 1173

Multiwavelength data in ELAIS-S1

- Completely covered in the radio at 1.4 GHz down to 0.3 mJy. (Gruppioni et al. 1999, MNRAS, 305, 297)
- 50% observed in the X-rays with BeppoSAX (Alexander, LF, Fiore et al. 2001, ApJ, 554, 18)
- Observed in the central ELAIS-S1_5 raster (~0.6 sq.deg.) by 4x100 Ks XMM pointings (PI F. Fiore, see Puccetti et al. 2006)
- Fully included in the SIRTF SWIRE survey

Multiwavelength data in ELAIS-S1

~20% of MIR sources detected in the 0.5-10 keV band
(preliminary result)

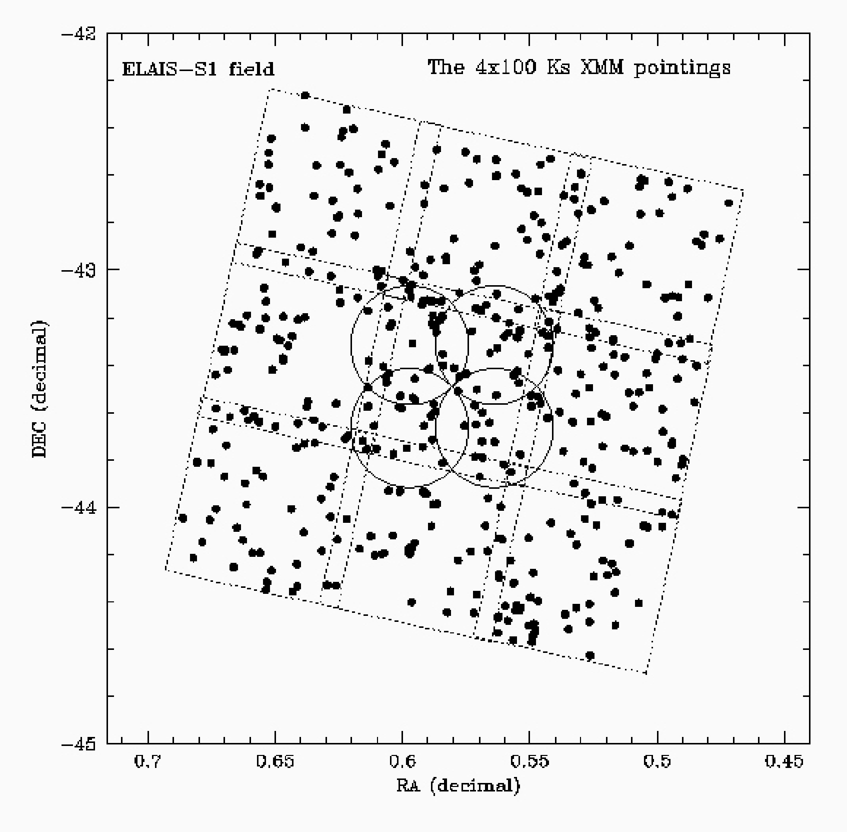

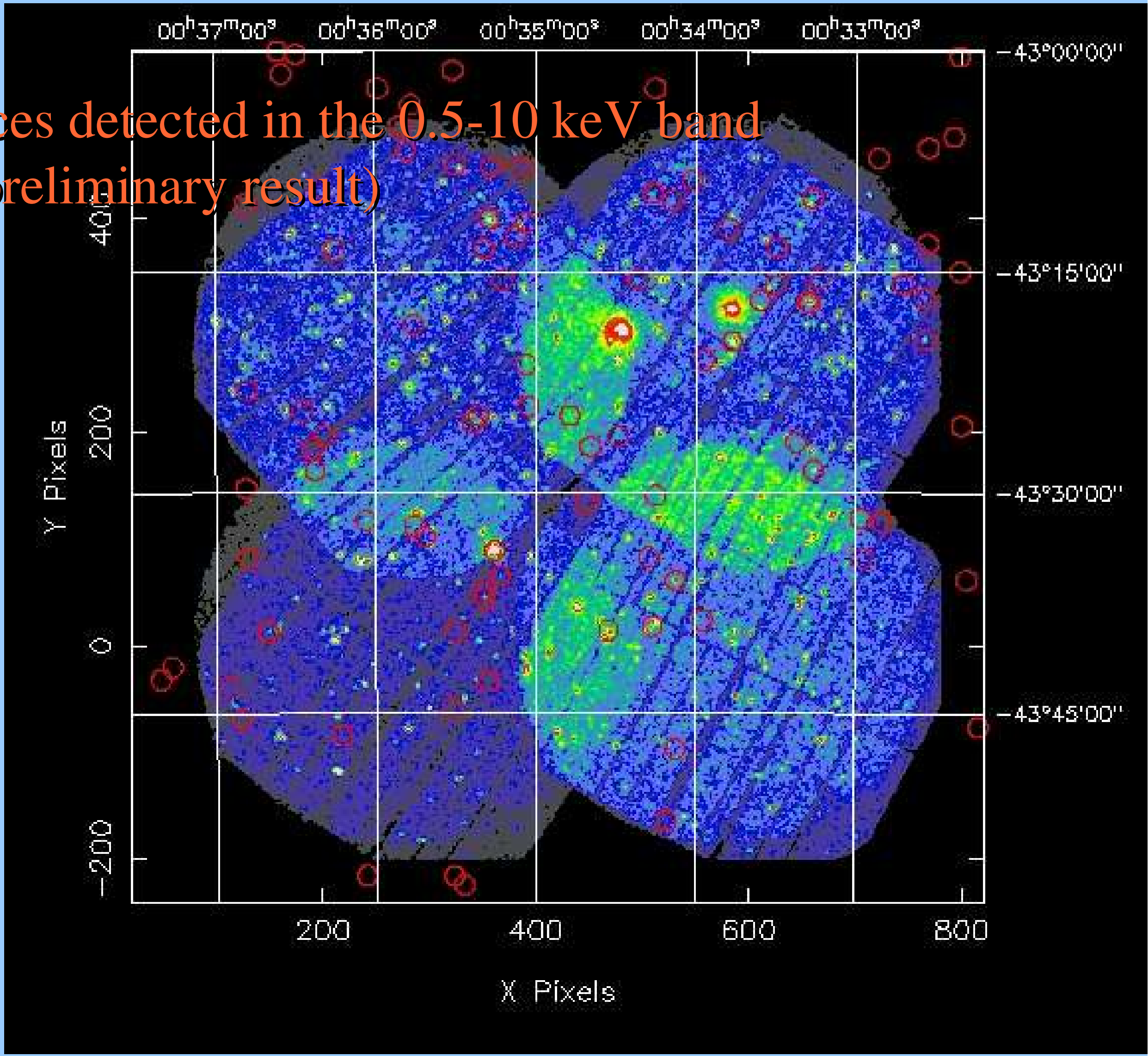

4x100 Ks XMM pointings

The Spectroscopic Catalog

- All S1 covered in R-band down to R=23 at ESO/La Silla.
- Spectroscopic follow-up carried out at 2dF/AAT and NTT,3.6 and 1.5 Danish telescopes at ESO/La Silla.
- 81% (330/406) of the 15 μm sources optically identified
- 71% (290/406) spectroscopically classified

LF, Gruppioni, Matute et al., (2004)

The spectroscopic classification

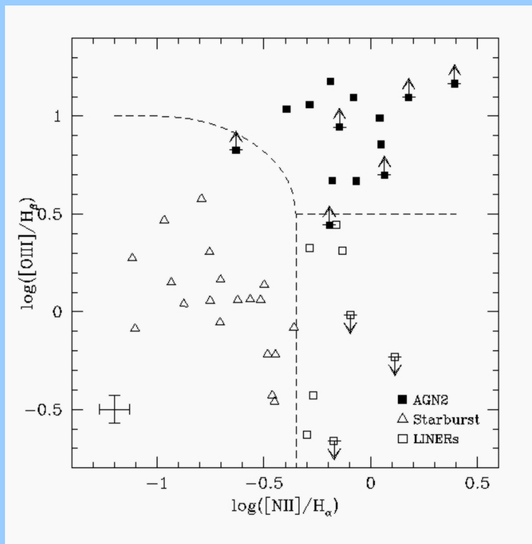

AGN2: standard line ratios

GLX: [OII] & Hδ lines (Poggianti et al. 1999)

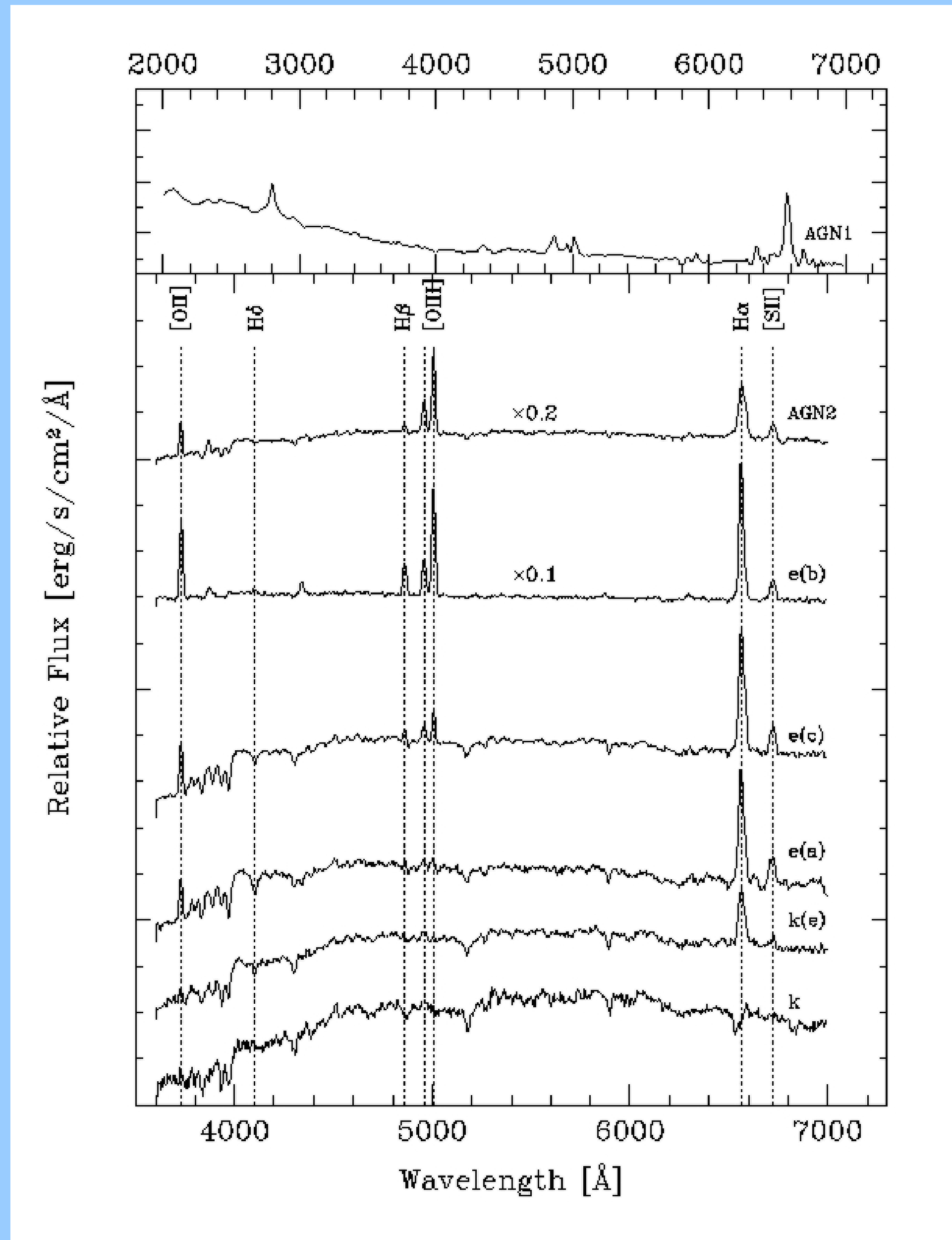

AGN1: 8%

AGN2: 7%

e(b) strong STB: >4%

e(c) normal STB: >22%

e(a) absorb. STB: >12%

k(e) only Hα: >10%

k passive ell.: >1%

LF, Gruppioni, Matute et al., AJ (2004)

The counts in ELAIS-S1

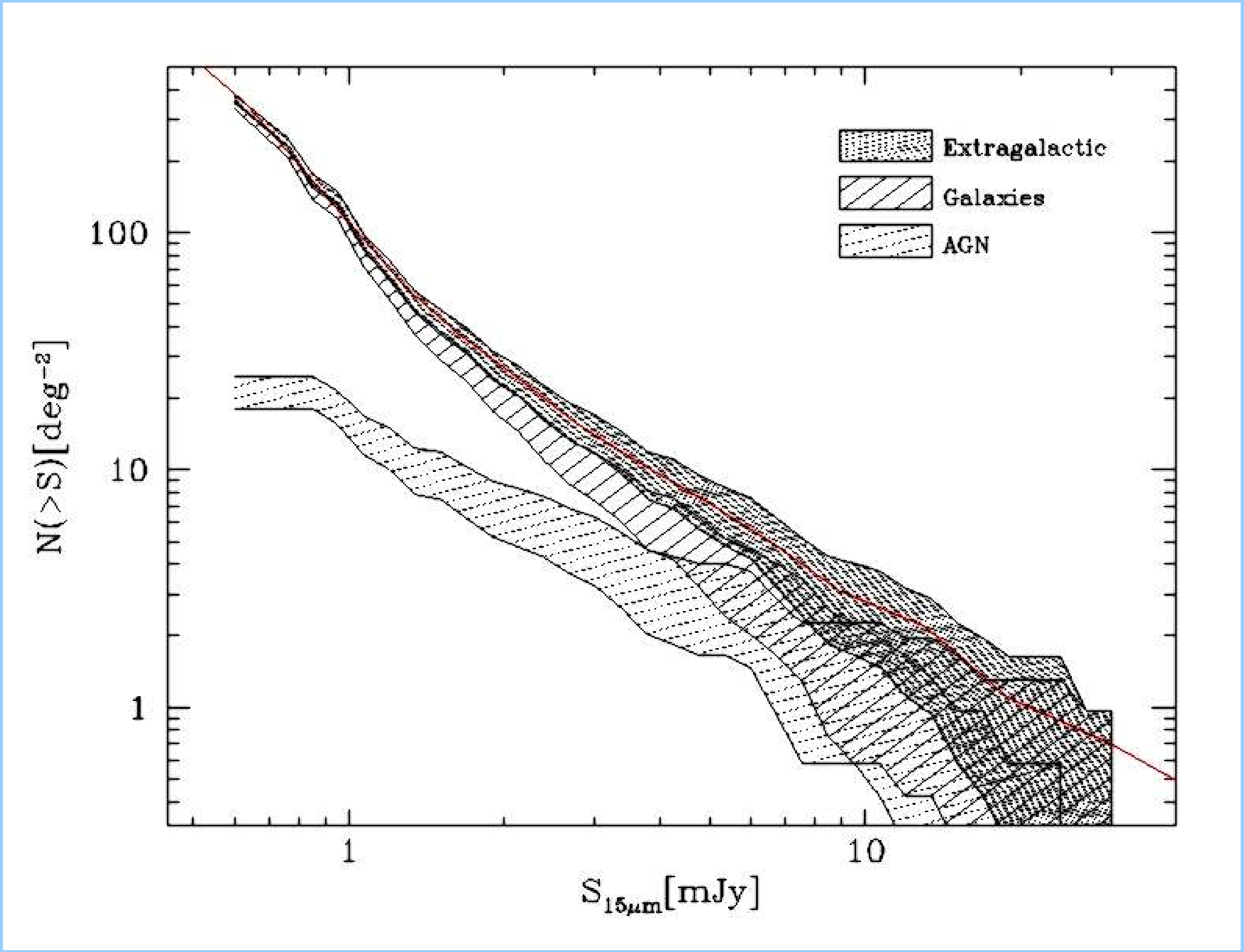

LF, Gruppioni, Matute et al., AJ (2004)

Nature of the ELAIS-S1 Sources

Total of 293 identifications distributed as follows:

- 48 -- AGNs (Type 1 + 2), 17% *
- 146 -- Emission Line Galaxies, 50% *
- 4 -- Early type Galaxies, 1% *
- 92 -- Stars, 32% *

(*)= percentages on the spectroscopically identified sample

ELAIS

vs

IRAS

		Type 1 AGN	Type 2 AGN	ELG
ELAIS-S1	%	~8	>7	48<...<85
	<z>	1.254	0.284	0.209
IRAS	%	6	16	77
	<z>	0.040	0.015	0.014

IRAS subsample from Alexander & Aussel 2000

The evolution of IR galaxies

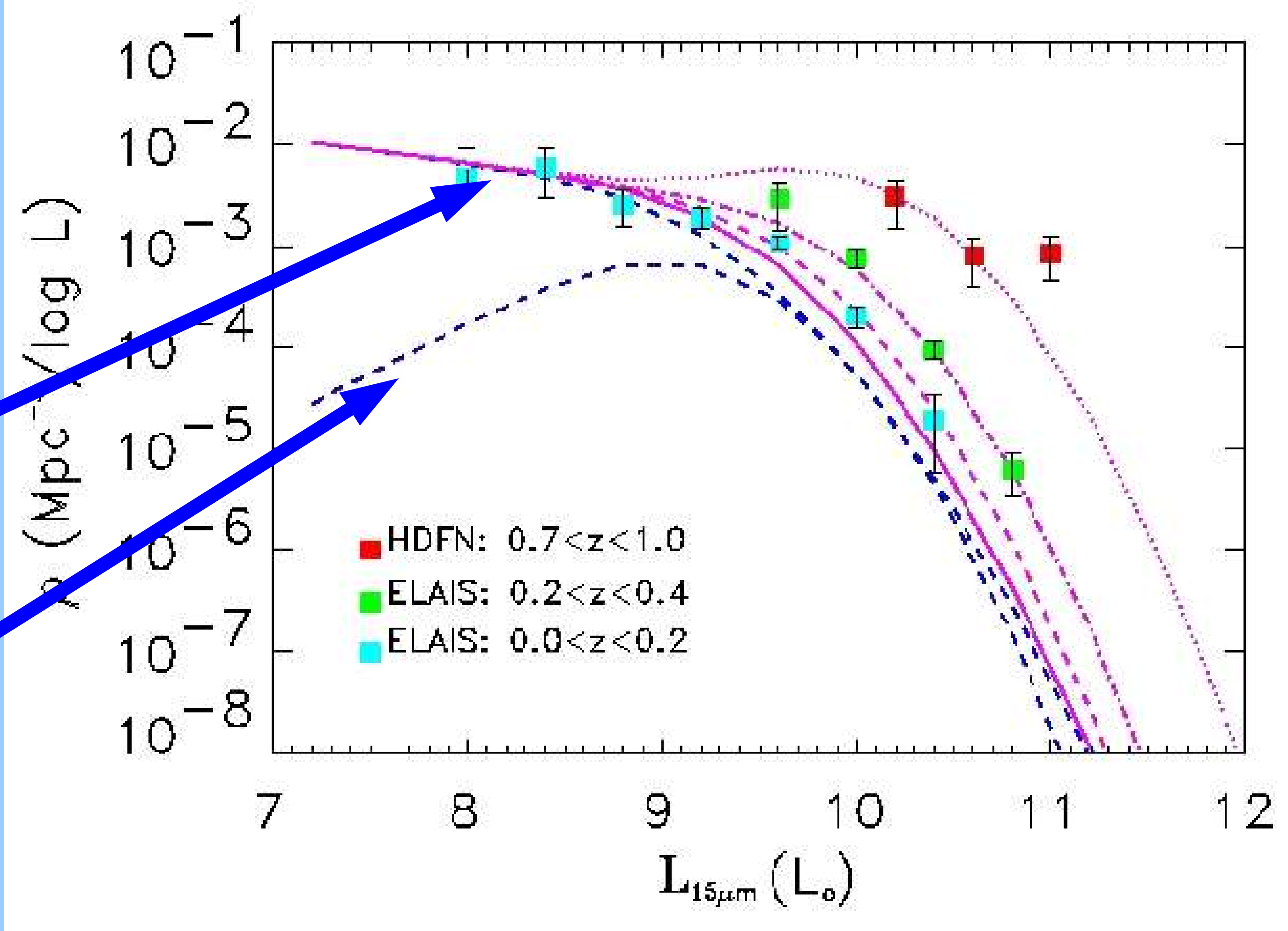

Not evolving spirals

Evolving Starburst

$$L(z)=L(0)(1+z)^{3.2}$$

$$n(z)=n(0)(1+z)^{3.5}$$

Pozzi et al., (2004)

The evolution of IR galaxies

Comparison with the local LF from Rush, Malkan and Spinoglio (93)

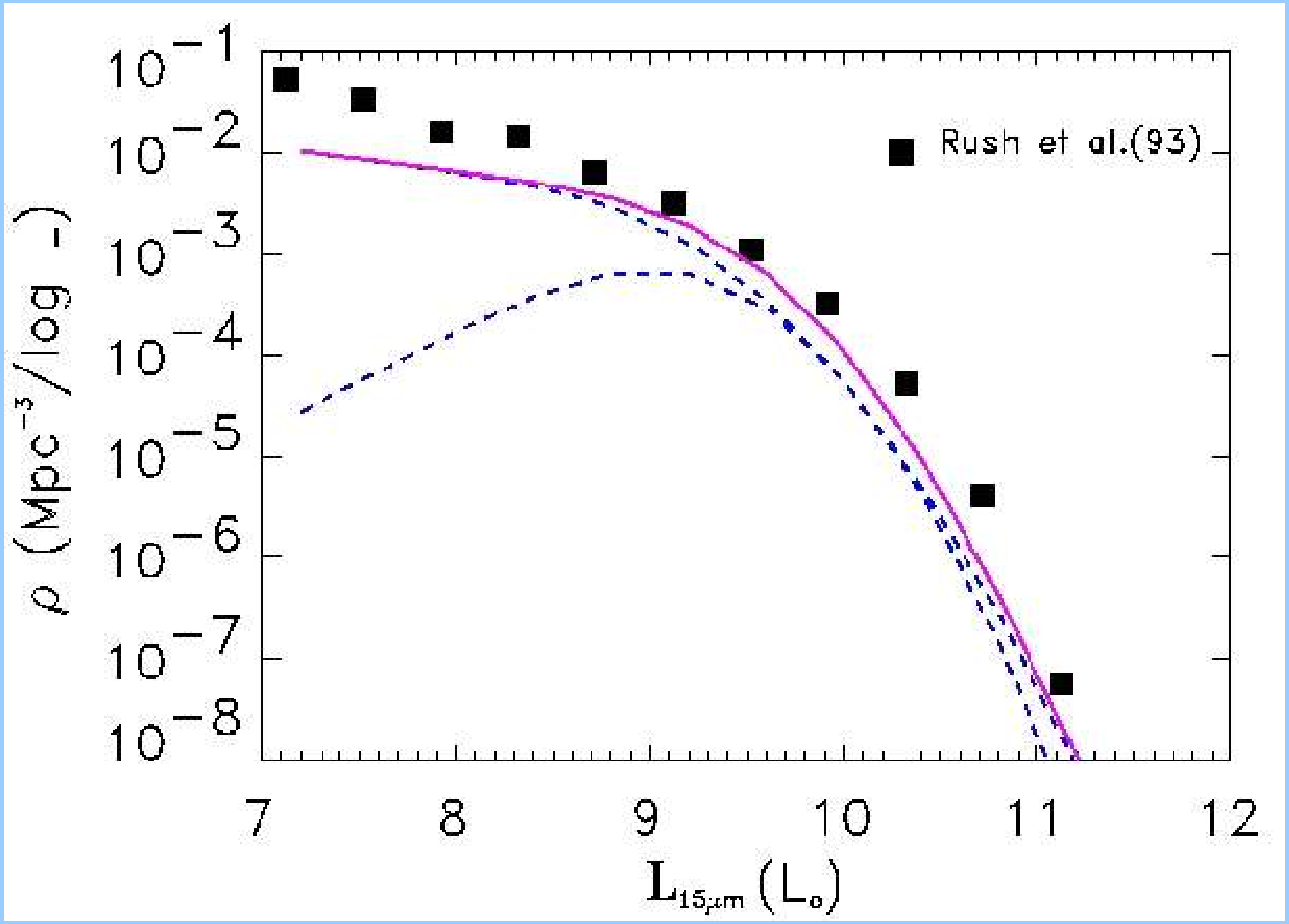

Pozzi et al. (2004)

The evolution of IR galaxies

Observed and expected extragalactic counts

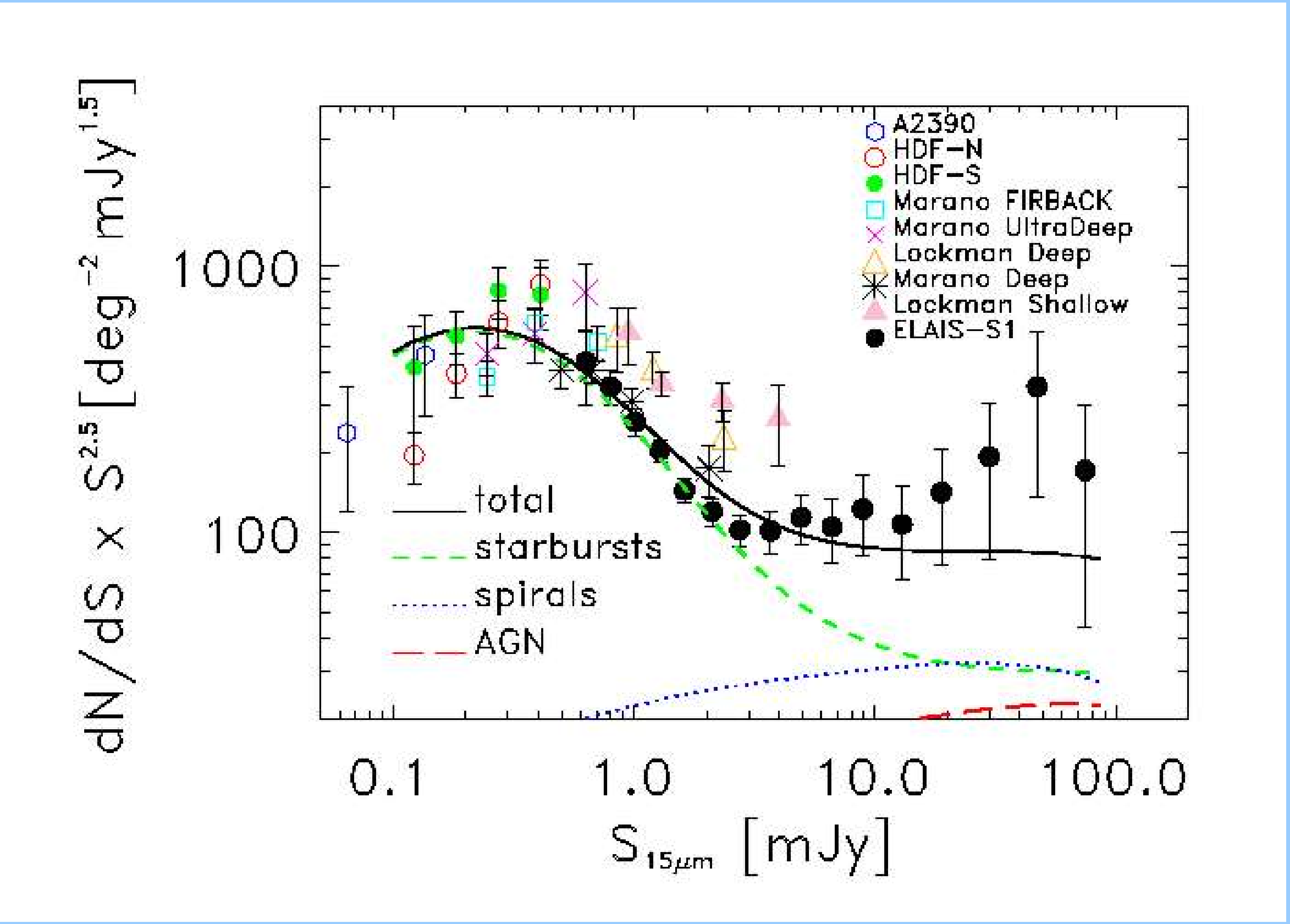

Pozzi et al., ApJ (2004)

AGN1 distribution in the L-z plane

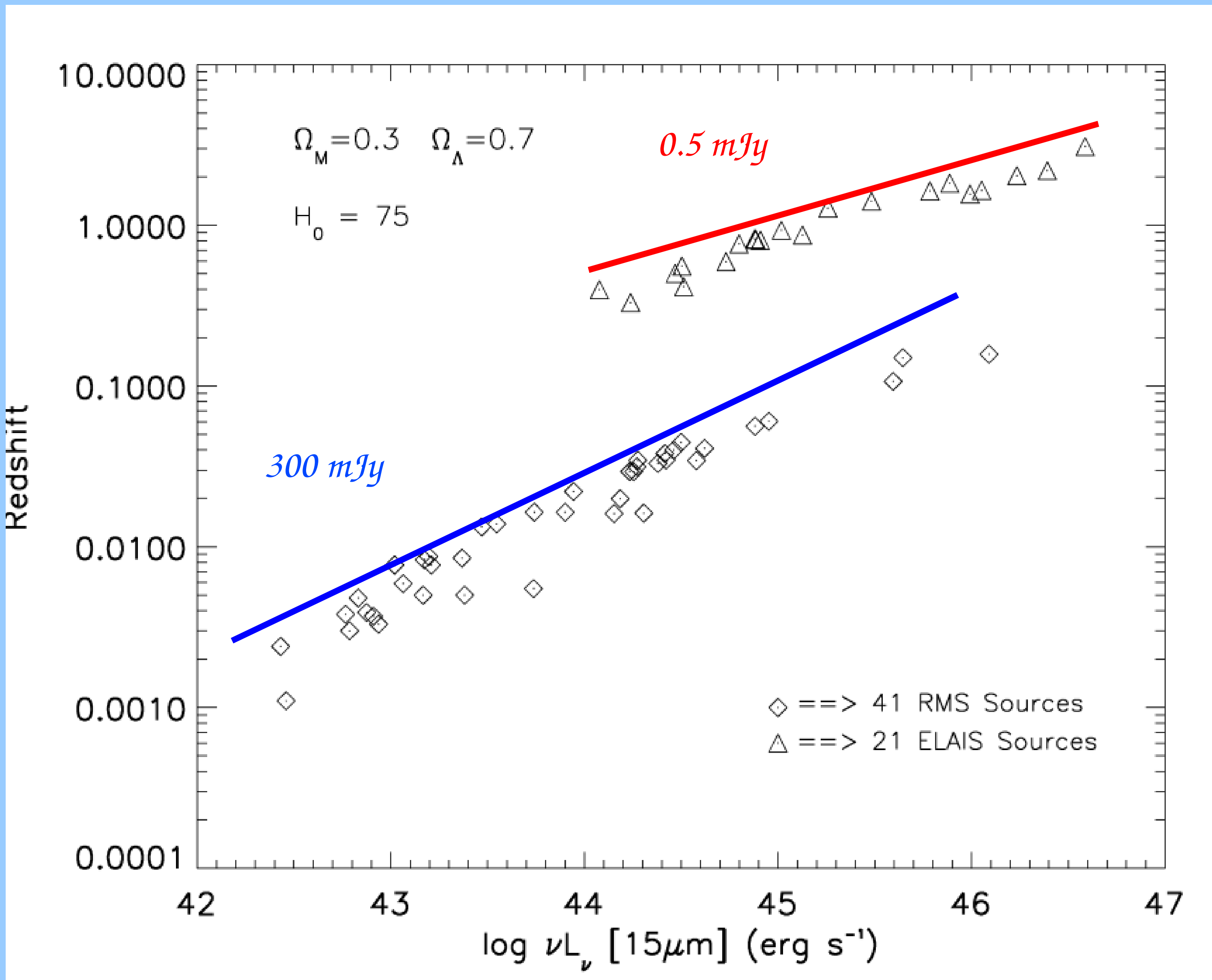

Matute, LF, et al. (2006)

The evolution of type 1 AGN

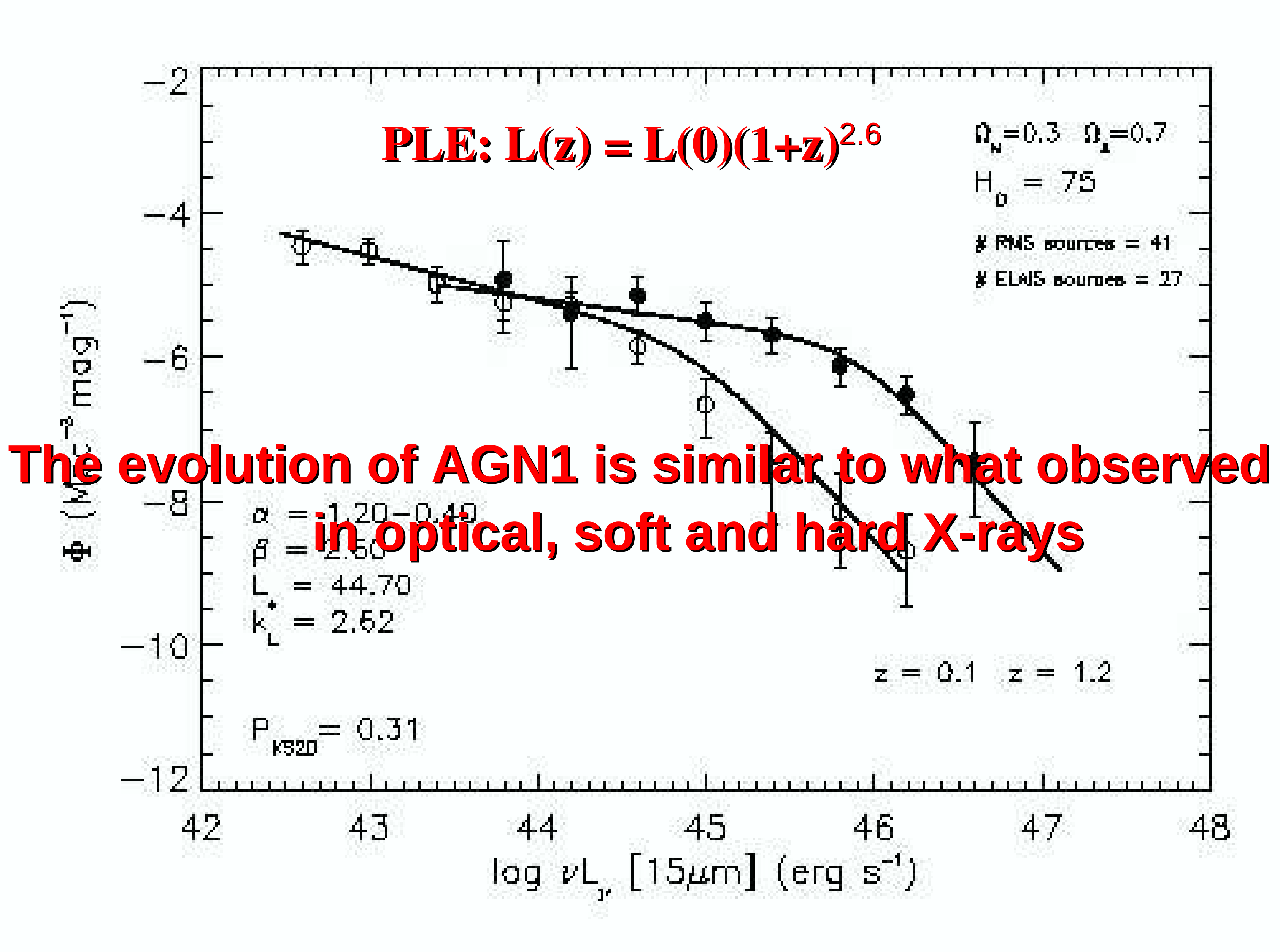

The evolution of AGN1 is similar to what observed in optical, soft and hard X-rays

Matute, LF, et al., 2002
Matute, LF, et al., 2006

Predictions: counts and z-distribution of AGN1

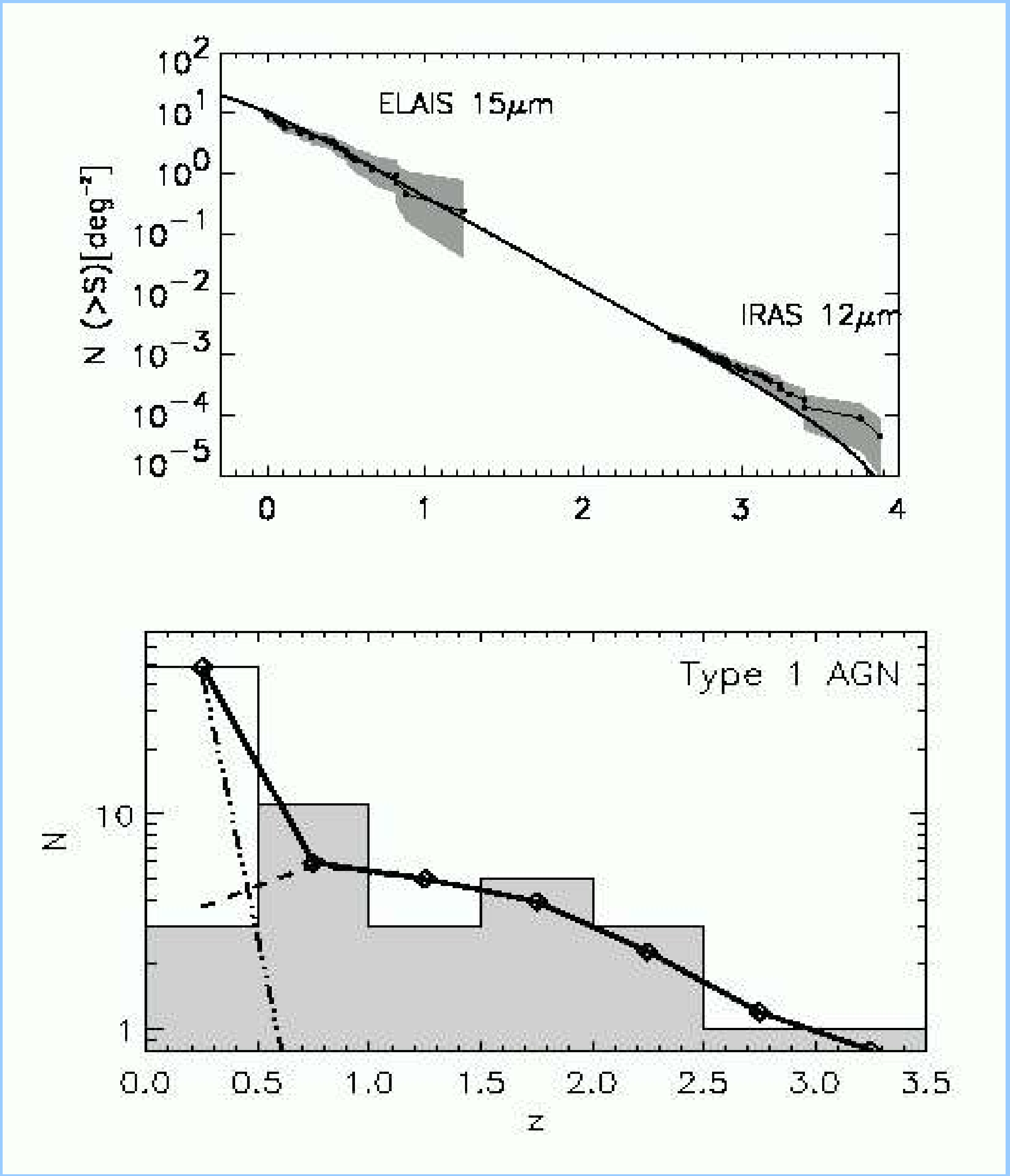

Matute, LF, et al., 2006

AGN2: L-z plane

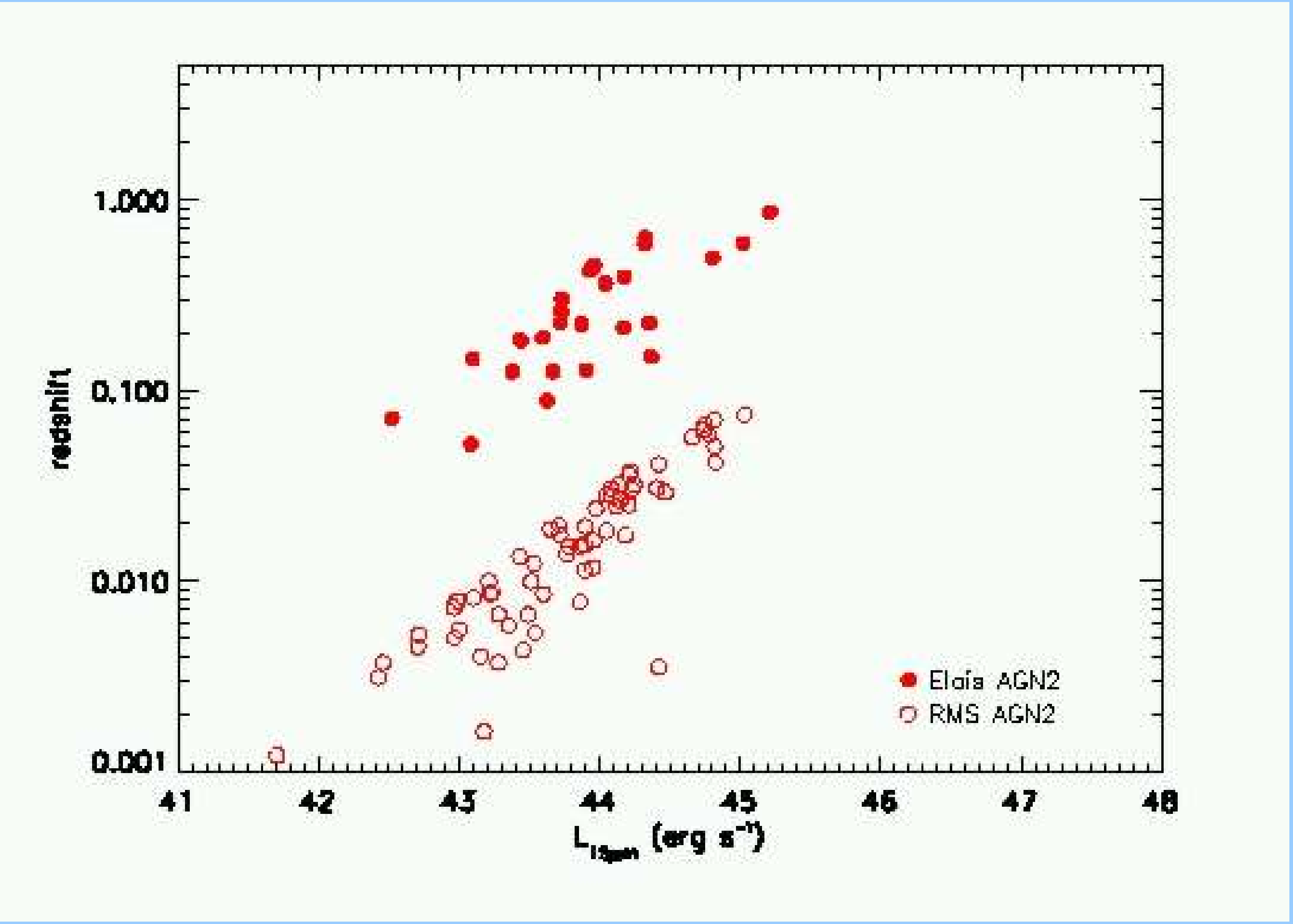

Matute, LF, et al., 2006

AGN2: evolution

Luminosity Function

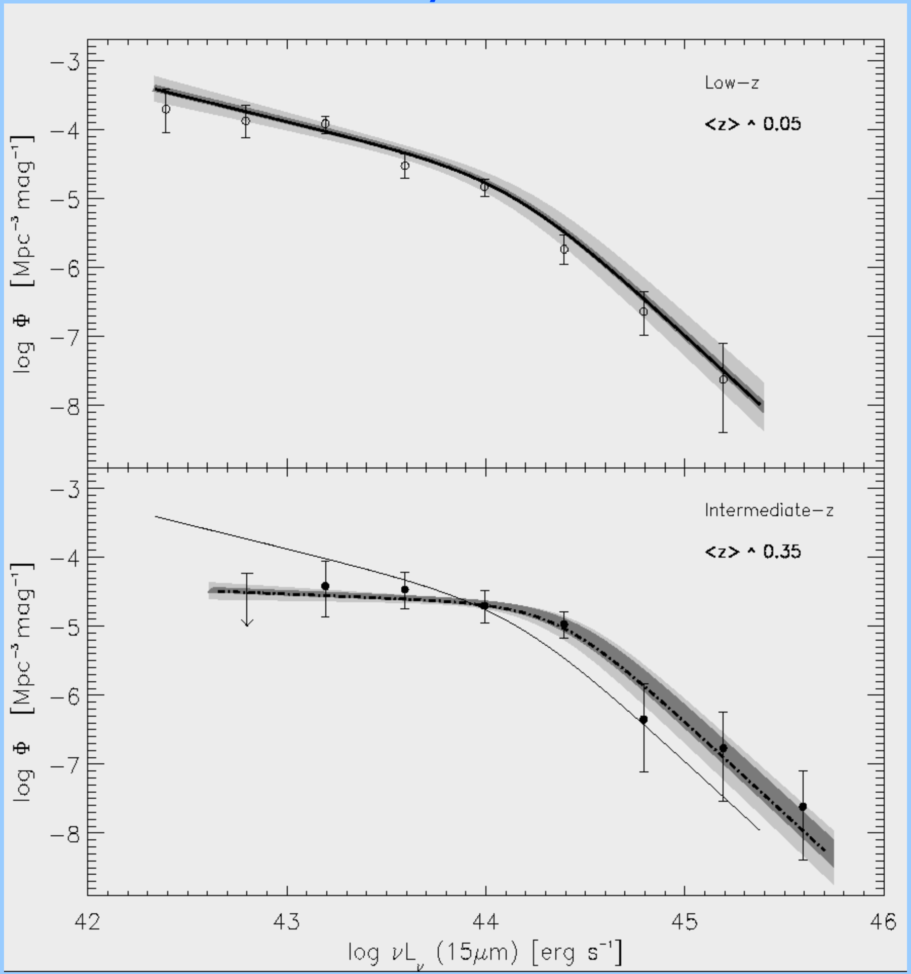

Completeness Function

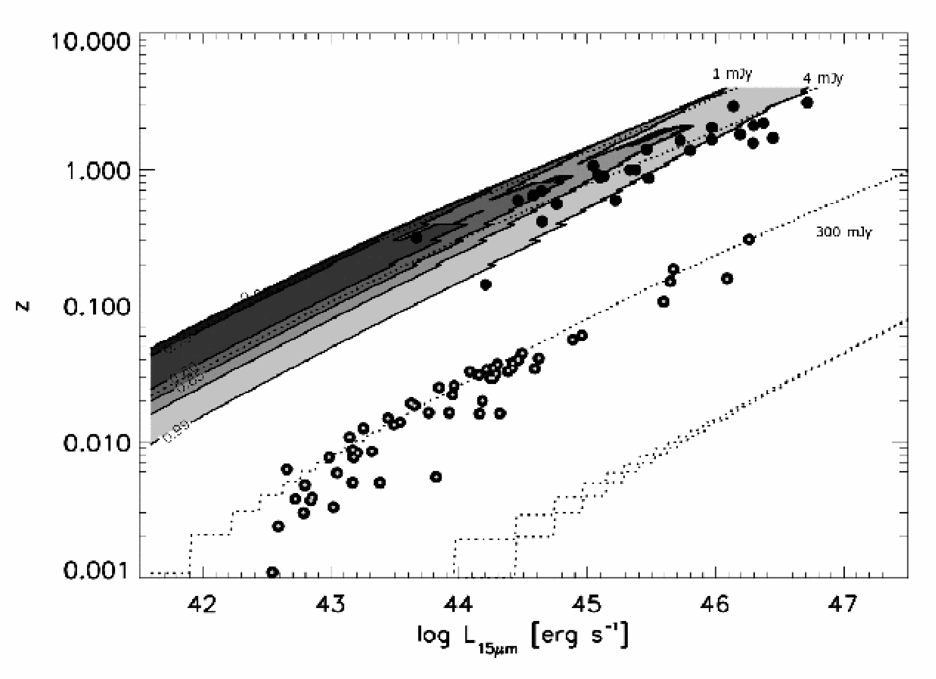

PLE: $L(z) = L(0)(1+z)^{1.8\text{-}2.6}$

Matute, LF, et al., 2006

Contribution of AGNs to the 15μm background (CIRB)

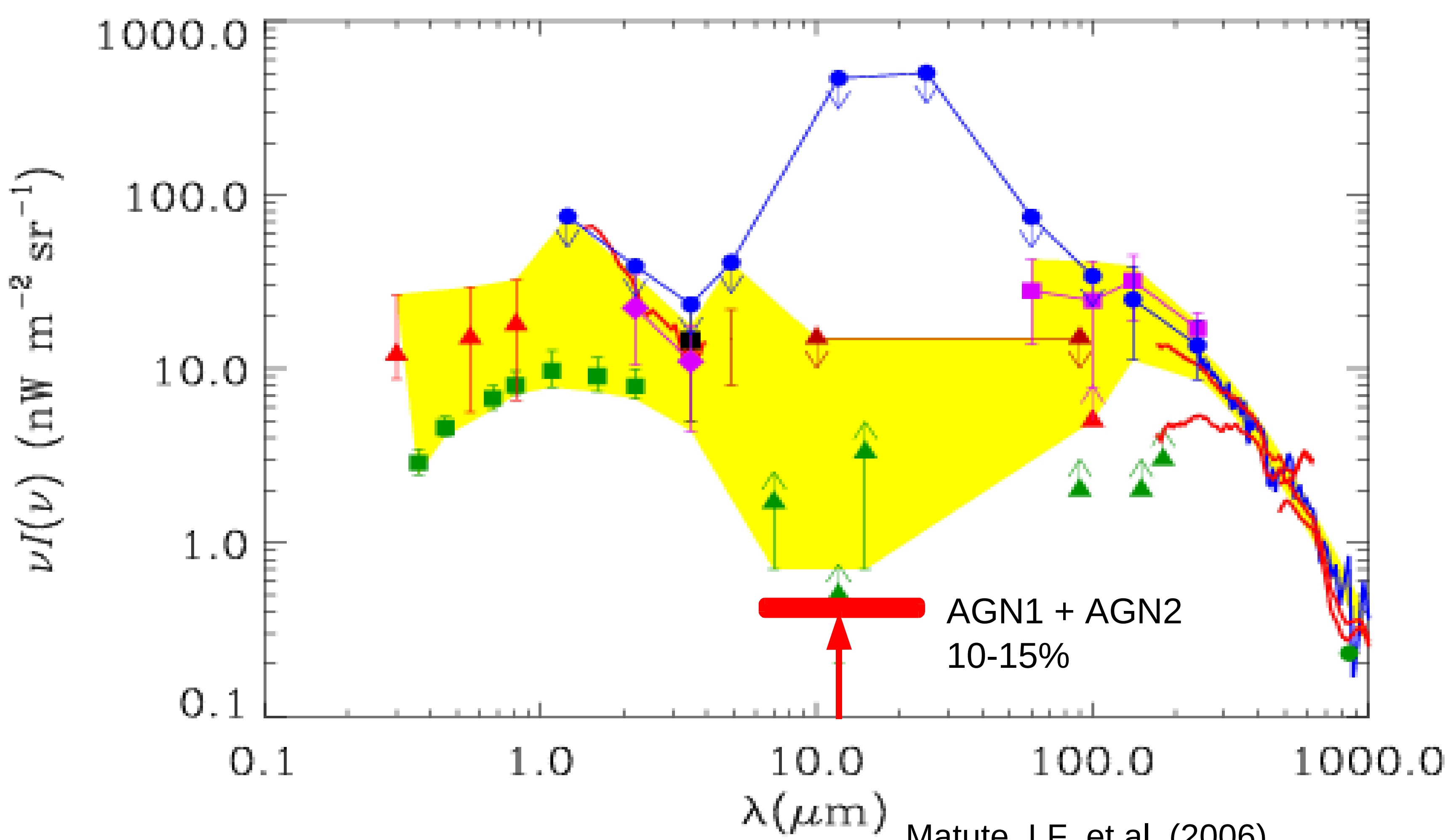

Matute, LF, et al. (2006)

Conclusions(2)

- The ELAIS-S1 Infrared (15 μm) final Catalog has been completed. It includes 406 sources with $0.5 < f_{15\mu m} < 100$ mJy.

Lari et al. 2001, MNRAS, 325, 1173

- 293/406 objects have been classified and the AGN and starburst counts derived

La Franca et al., 2004, AJ, 127, 3075
Gruppioni et al. 2002, MNRAS, 335, 831

- A strong luminosity plus density evolution for starburst galaxies has been found.

Pozzi et al. 2004, ApJ, 609, 122

- For the first time we have measured the evolution of AGN at 15 μm.
- **The predicted contribution of AGN to the MIR CIB is >5-10%**

Matute, La Franca et al. 2002 ,
Matute, La Franca et al., 2006

www.fis.uniroma3.it/ELAIS_S

The XMM/SWIRE/ELAIS-S1 field

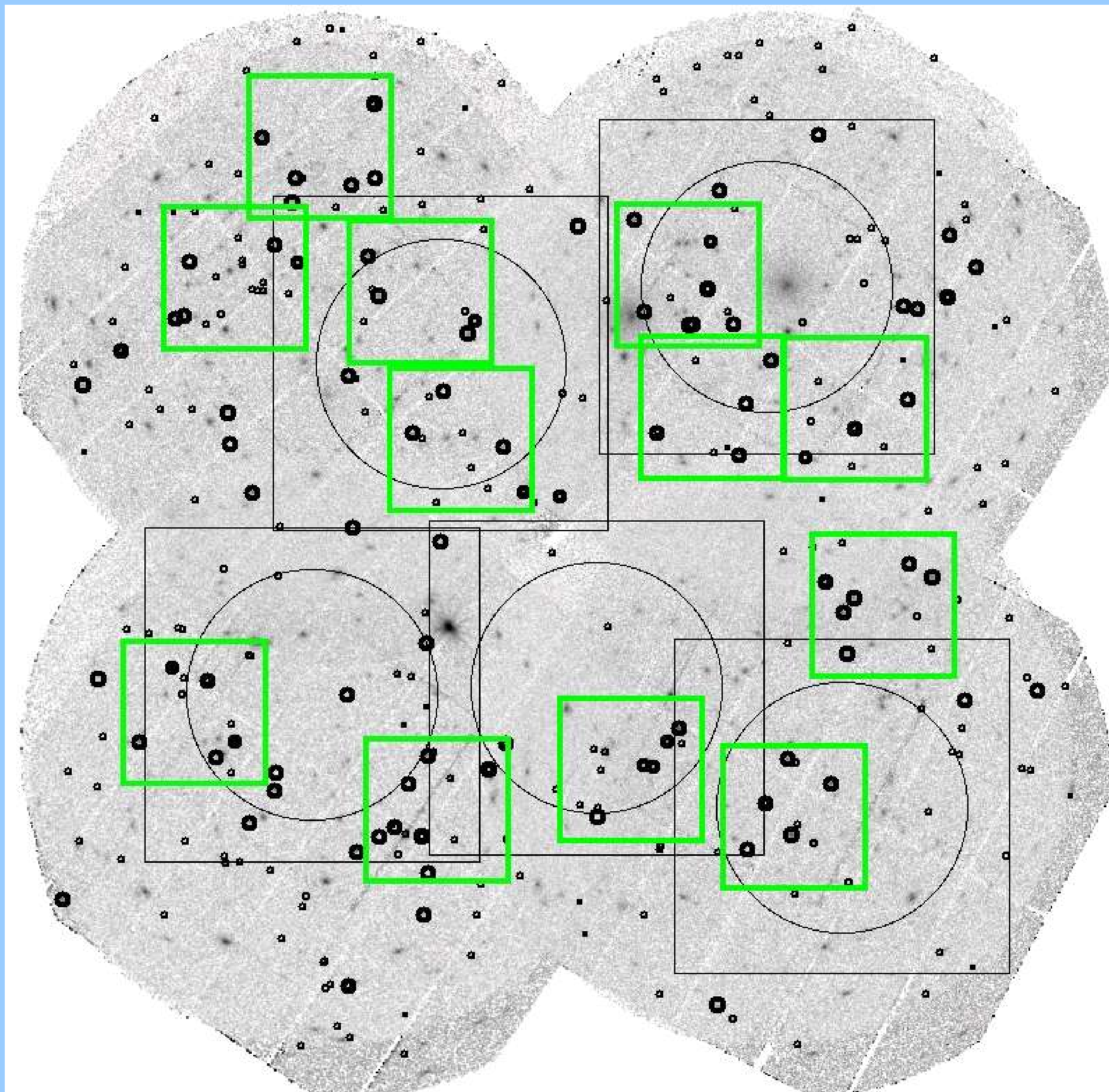

~100 hours with VIMOS and FORS2 @VLT during 2004/2005/2006

~1500 Zs (R<24.5)

LF, Sacchi et al. (in prep)

AGN and the CIRB

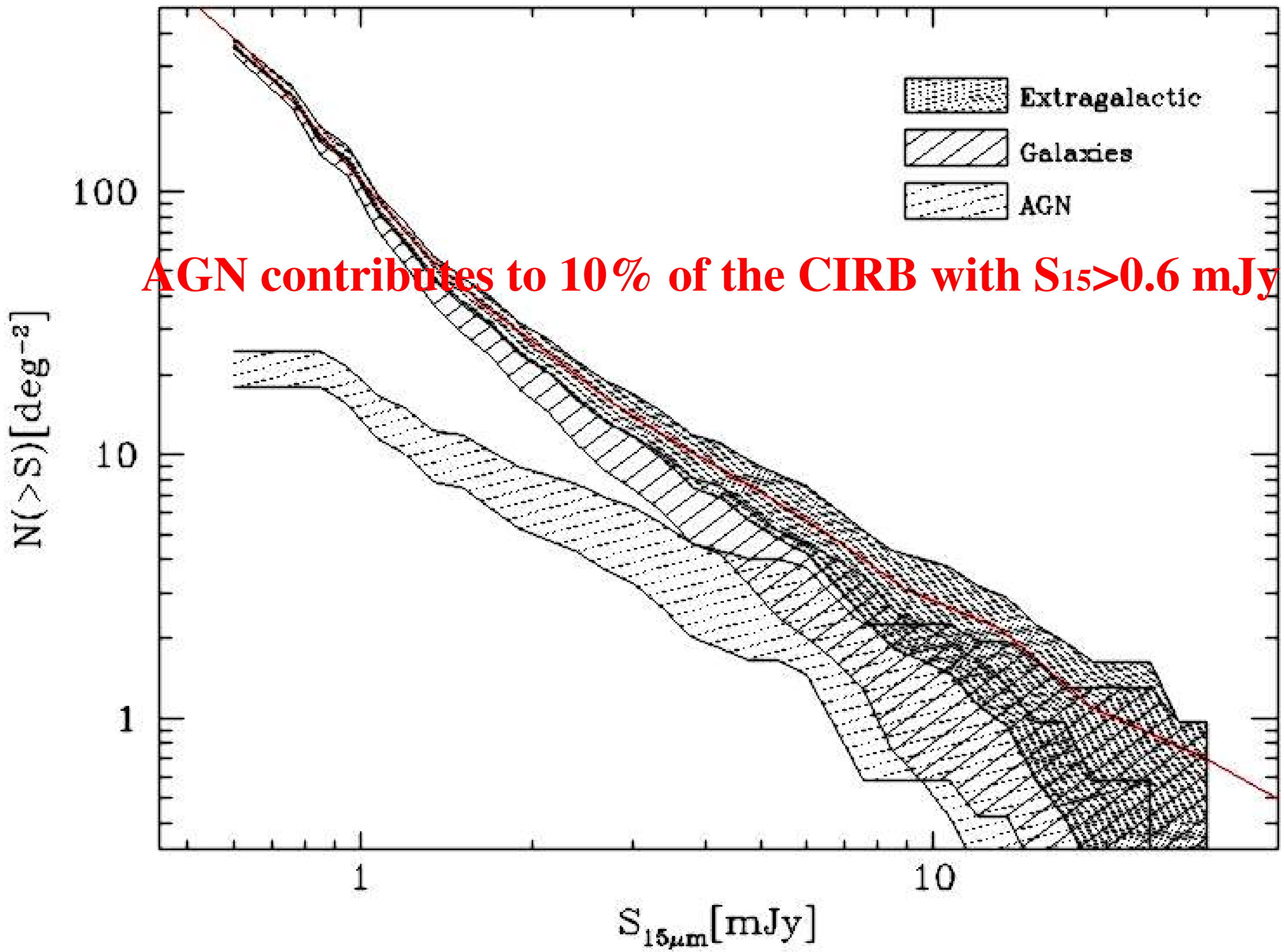

AGN contributes to 10% of the CIRB with S_{15}>0.6 mJy

LF, Gruppioni, Matute et al., AJ, (2004)

XMM detections of new MIR AGN

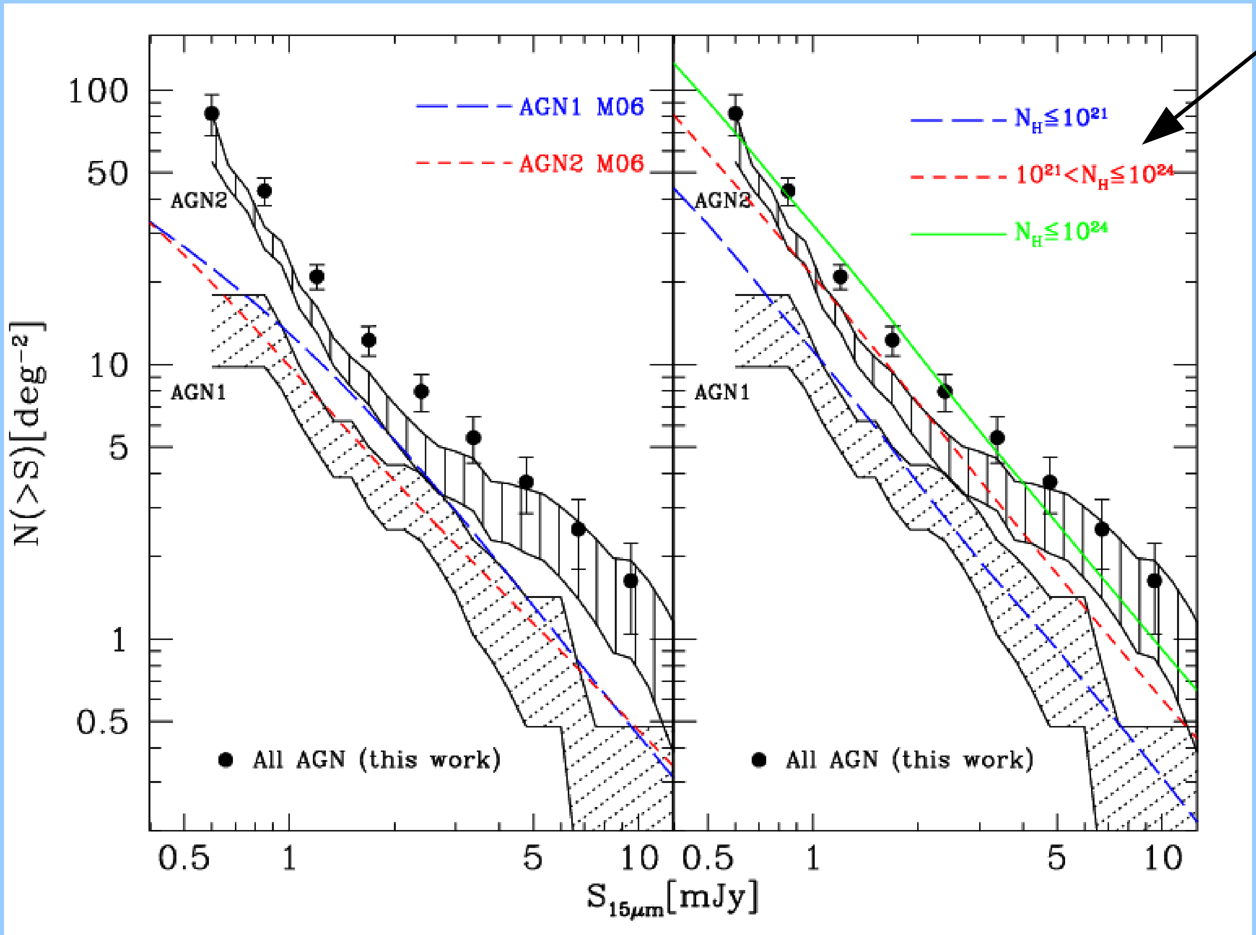

Silva et al. (2004)

-F(2-10 keV) > 2x10^{-15} cgs

-About 14% of the previously classified starburst galaxies harbor an AGN

-The fraction of AGN at ~1 mJy is about 20% at 15um and 25% at 24um.

La Franca, et al. , in prep

The XMM/SWIRE/ELAIS-S1 field

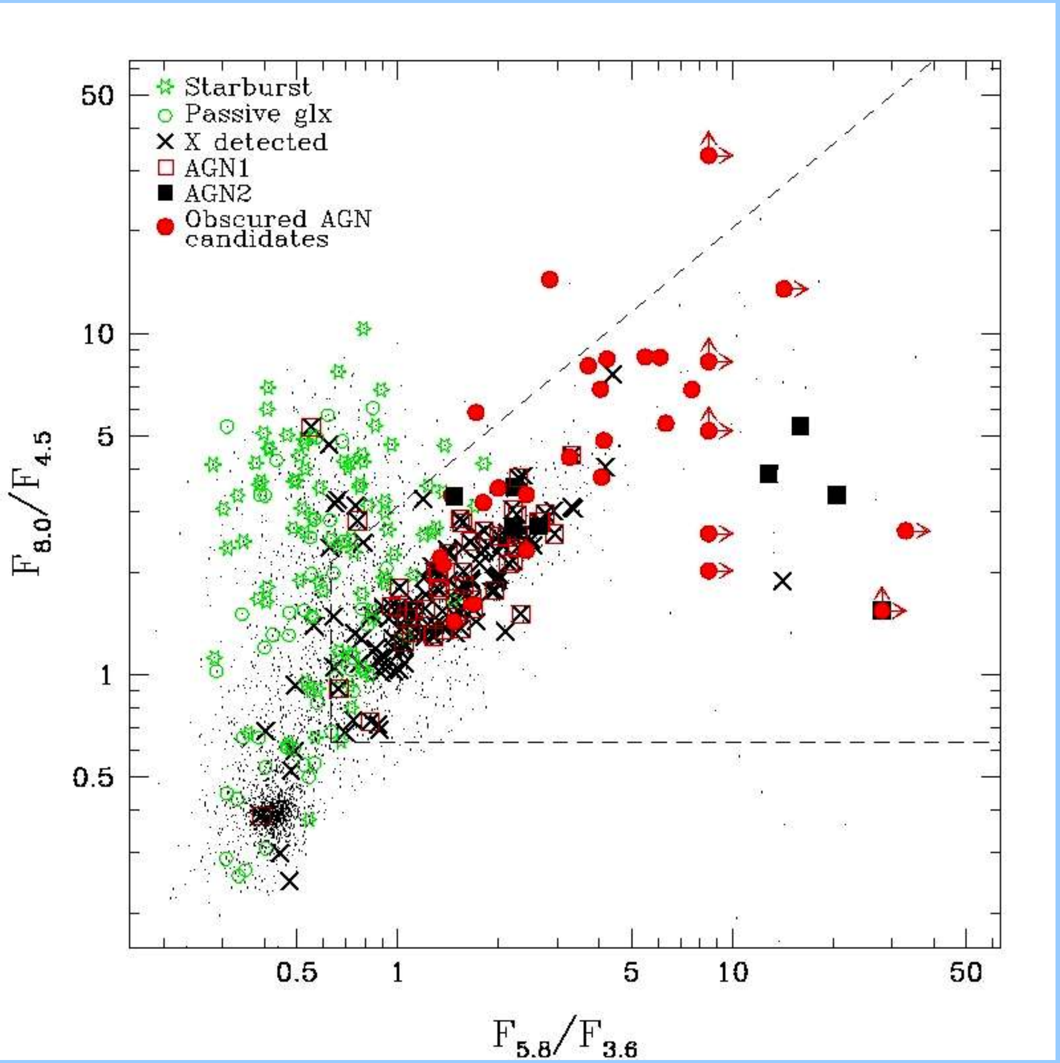

Counts and Fraction of AGN as a function of 24um flux

AGN and Galaxy SEDs from Polletta et al. (in prep)

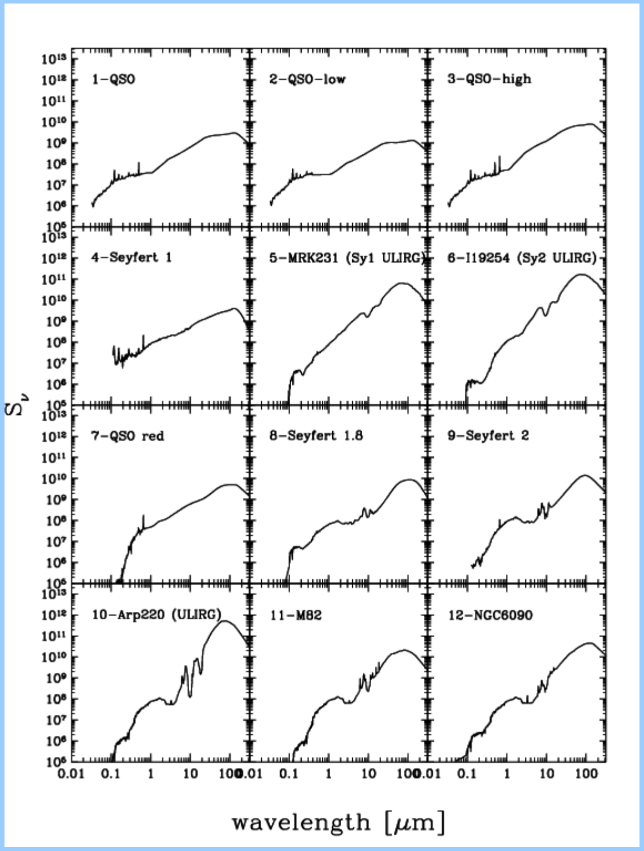

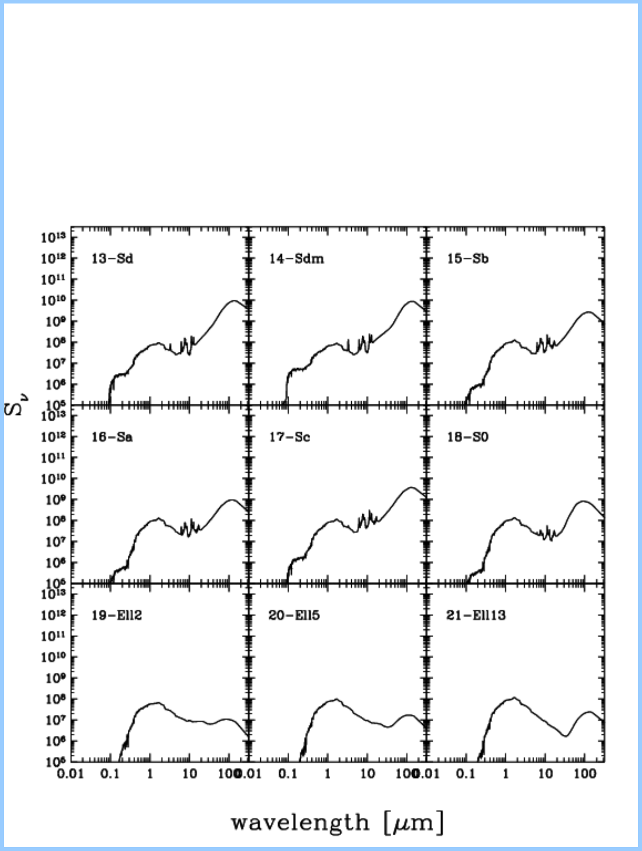

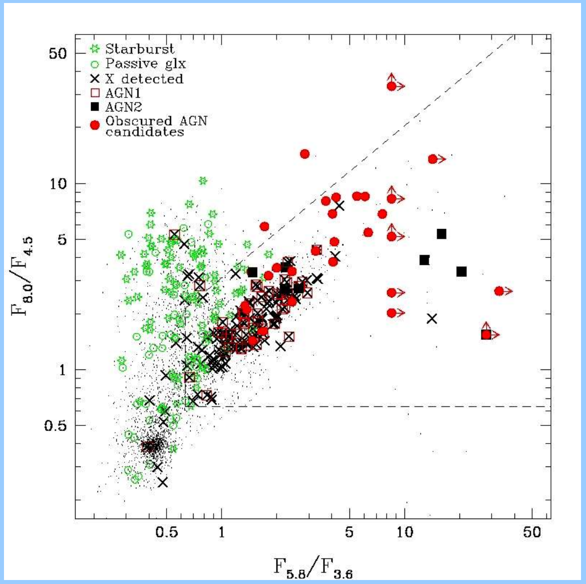

Counts and Fraction of AGN as a function of 24um flux

Optically and X-ray classified AGN

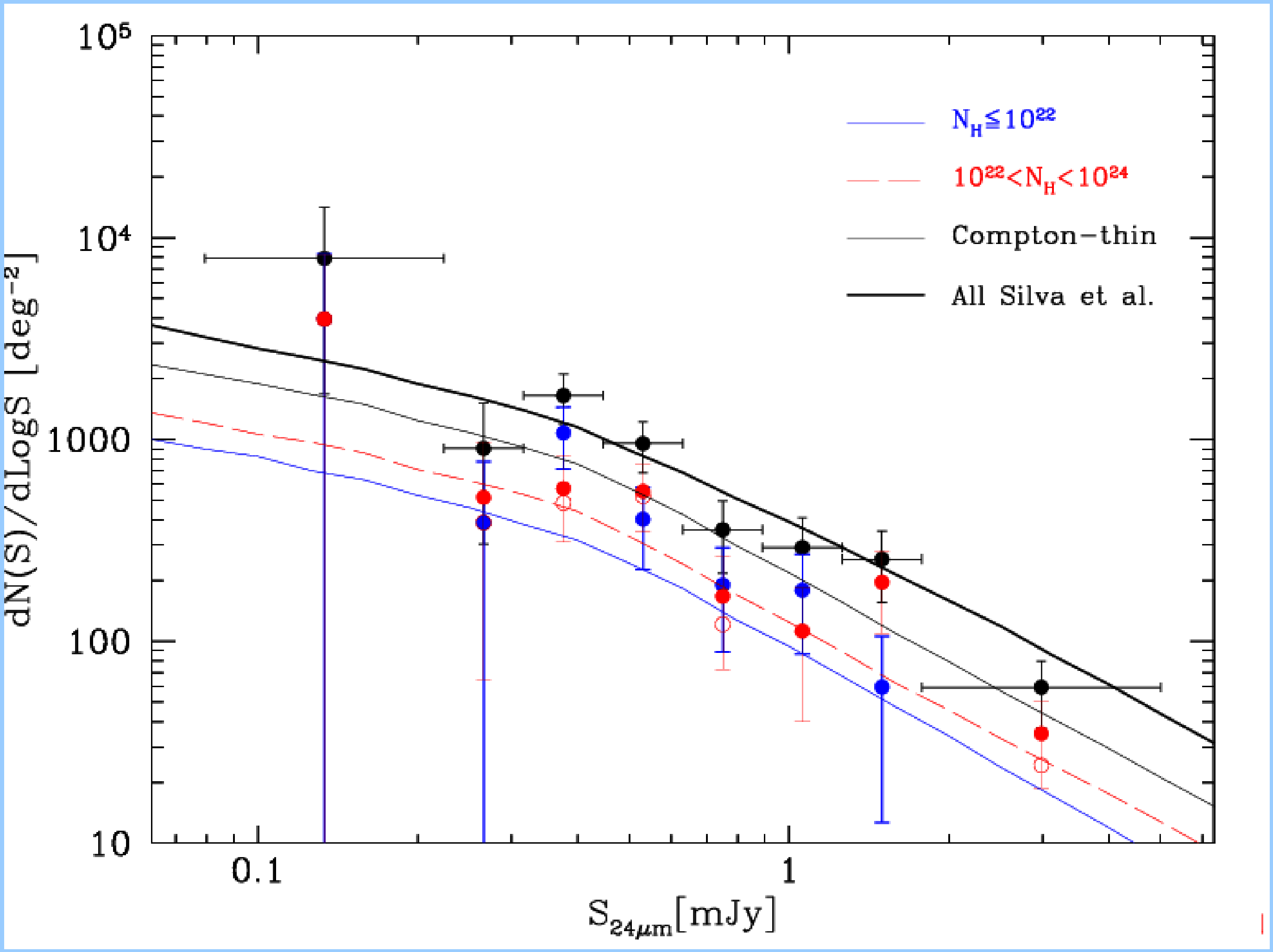

Counts and Fraction of AGN as a function of 24um flux

Optically and X-ray class. AGN

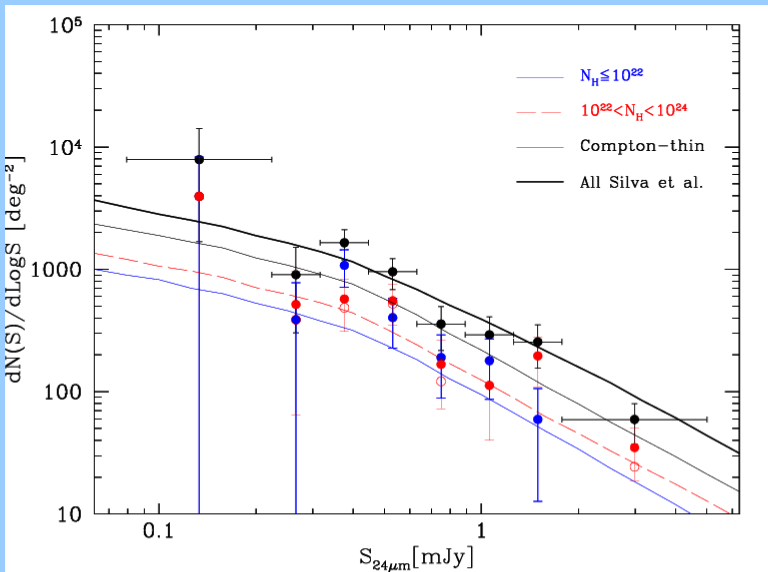

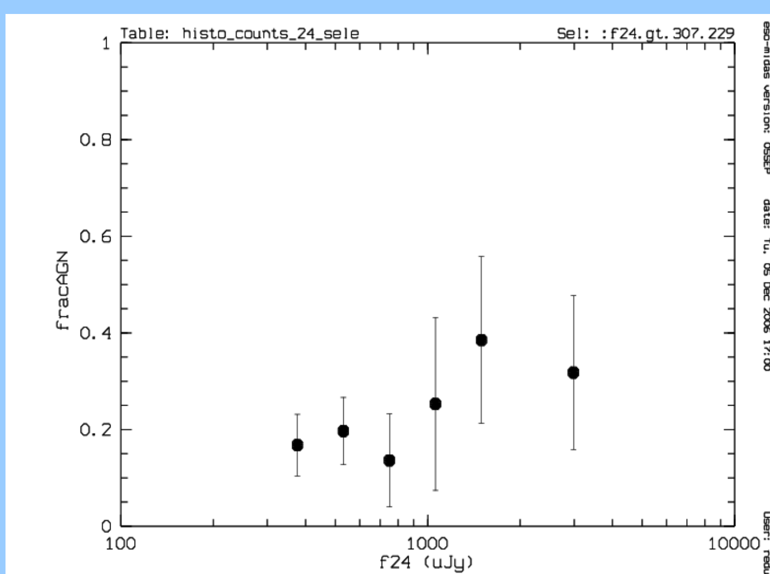

MIR-SED classified AGN

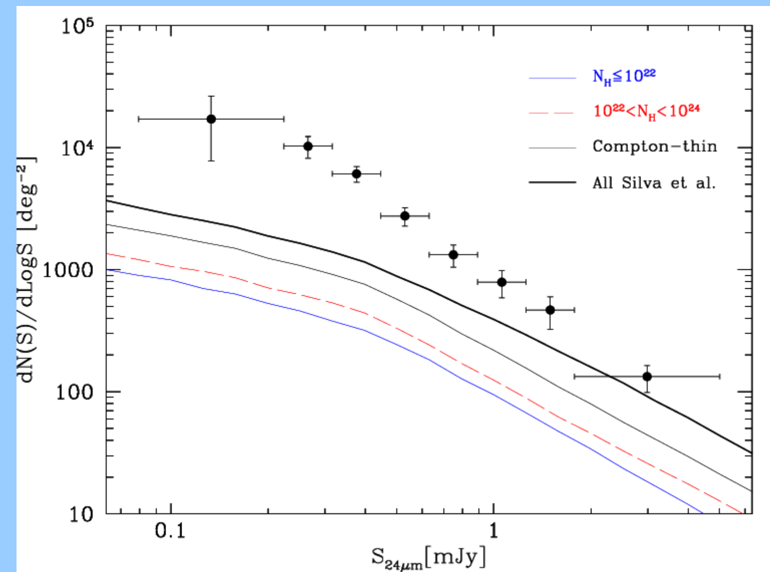

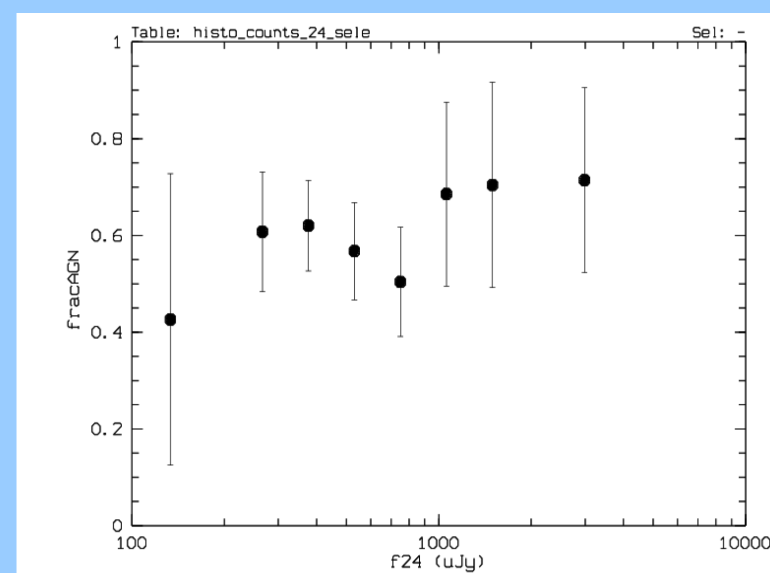

All X-ray detected sources have an AGN MIR SED

Fraction of AGN as a function of MIR flux

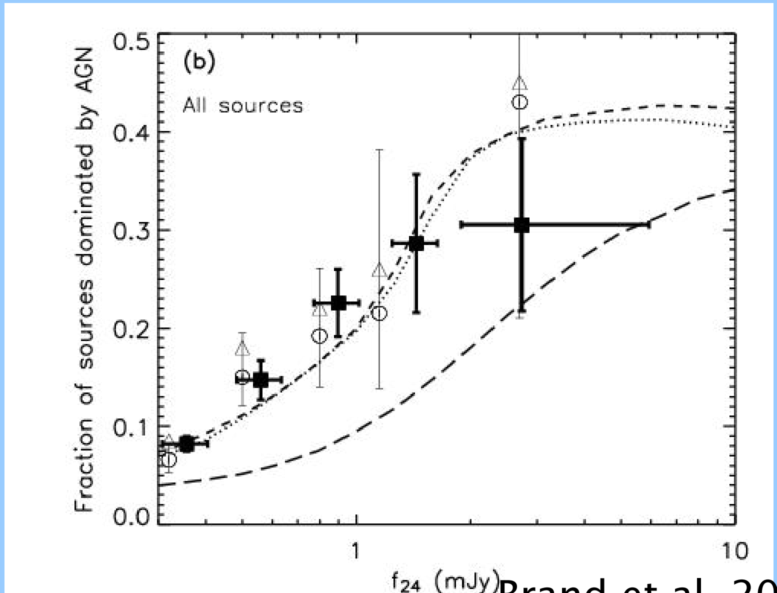

Brand et al. 2006

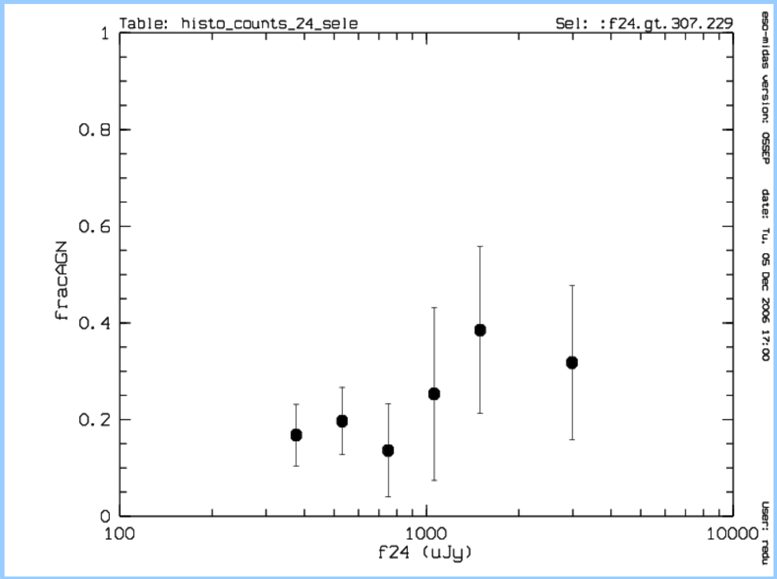

Optically and X-ray class. AGN

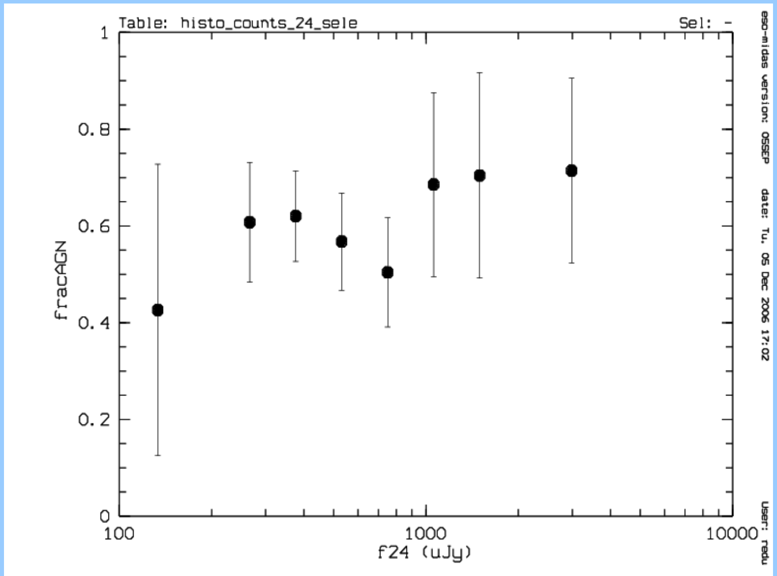

MIR-SED classified AGN

CONCLUSIONS

-The optical spectroscopic classification is not able to identify all the AGN2 population

-The best way to select Compton thin AGN2 is via deep X-ray observations

-There are promising results that demonstrate that it is possible to select (Compton thick) AGN2 with SED fitting in the mid-infrared, but the completeness and contamination from starburst galaxies need to be properly quantified